Astronomical signal and image processing

Seppo Mattila (sepmat@utu.fi)
Department of Physics and Astronomy, University of Turku

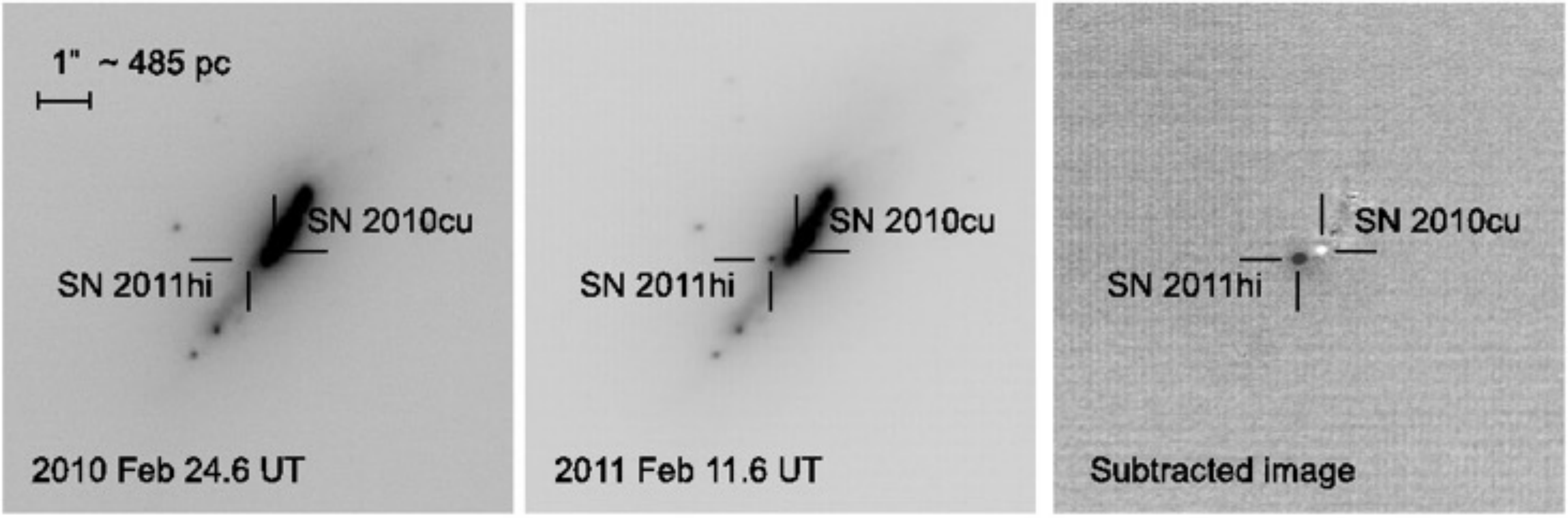

Course report

- The minimum length is 9 pages (12 pt font) of text (2 pages based on each of the four practical sessions + 0.5 page introduction + 0.5 page summary) + figures, tables, references
- For reporting the work done in each of the sessions please follow the advice of the teachers
- Keep in mind the learning outcomes (slide 4) when preparing your report
- For writing the report you can use any word processing software that you are familiar with. Please, save the report as PDF
- **Deadline for handing-in the reports on 15th August**
    - For late submission we will deduct 5% per (working) day !!

Learning outcomes

After completing the course the students should be able to:

(1) Describe the principles behind some advanced astronomical imaging techniques and identify suitable topics in astrophysics that can be studies with them;

(2) Understand the physics behind some of the most important medical imaging modalities and describe their value in clinical applications;

(3) Identify and discuss the differences and similarities in the challenges faced when analyzing data in these two different disciplines;

(4) Describe the theoretical basis and suitability of several image/signal processing and analysis methods commonly used in astronomy and medical imaging;

(5) Identify suitable algorithms and apply them to astronomical and/or medical imaging datasets to enhance their scientific and/or clinical value;

(6) Produce a written course report

Practical session IV

Thursday 14.6. Astronomical signal and image processing

10:00 - 11:30 Astronomical imaging: PSF, alignment, convolution, deconvolution, subtraction

11:45 - 12:30 Tutorial on astronomical imaging

12:30 - 13:30 Lunch

13:30 - 15:00 Astronomical spectroscopy: spatial and spectral resolution, classification

15:00 - 16:00 Tutorial on astronomical spectroscopy and independent work

Astronomical imaging

Telescopes

Nordic Optical Telescope, La Palma, Canary Islands

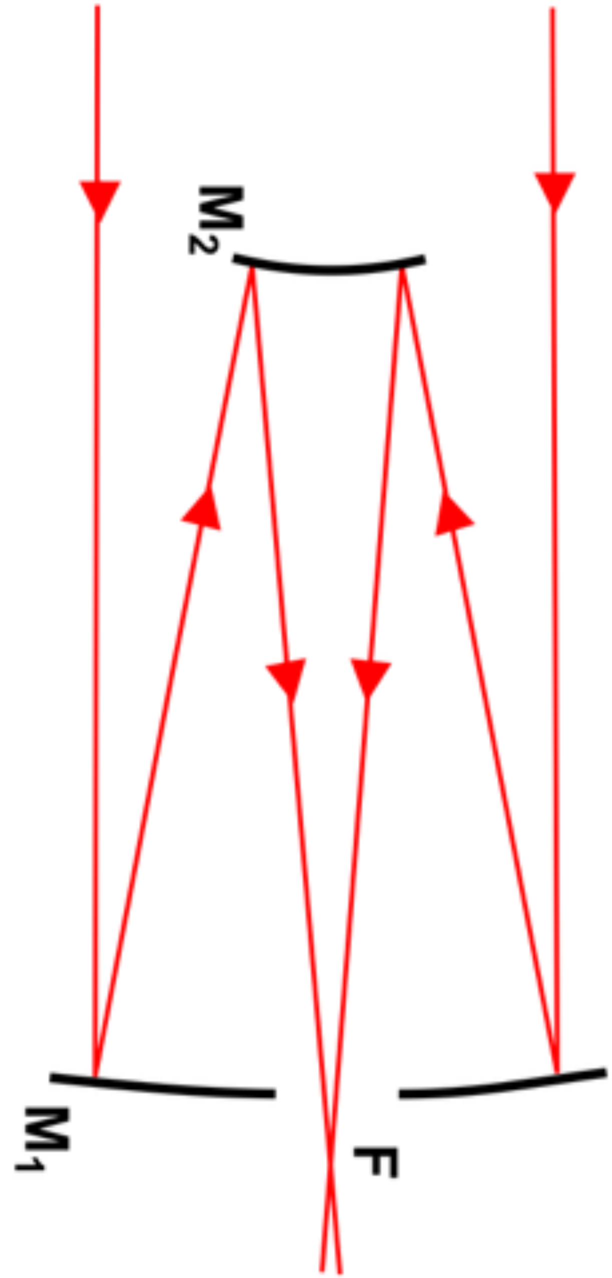

THE HAZARDS OF A PHOTON'S LIFE

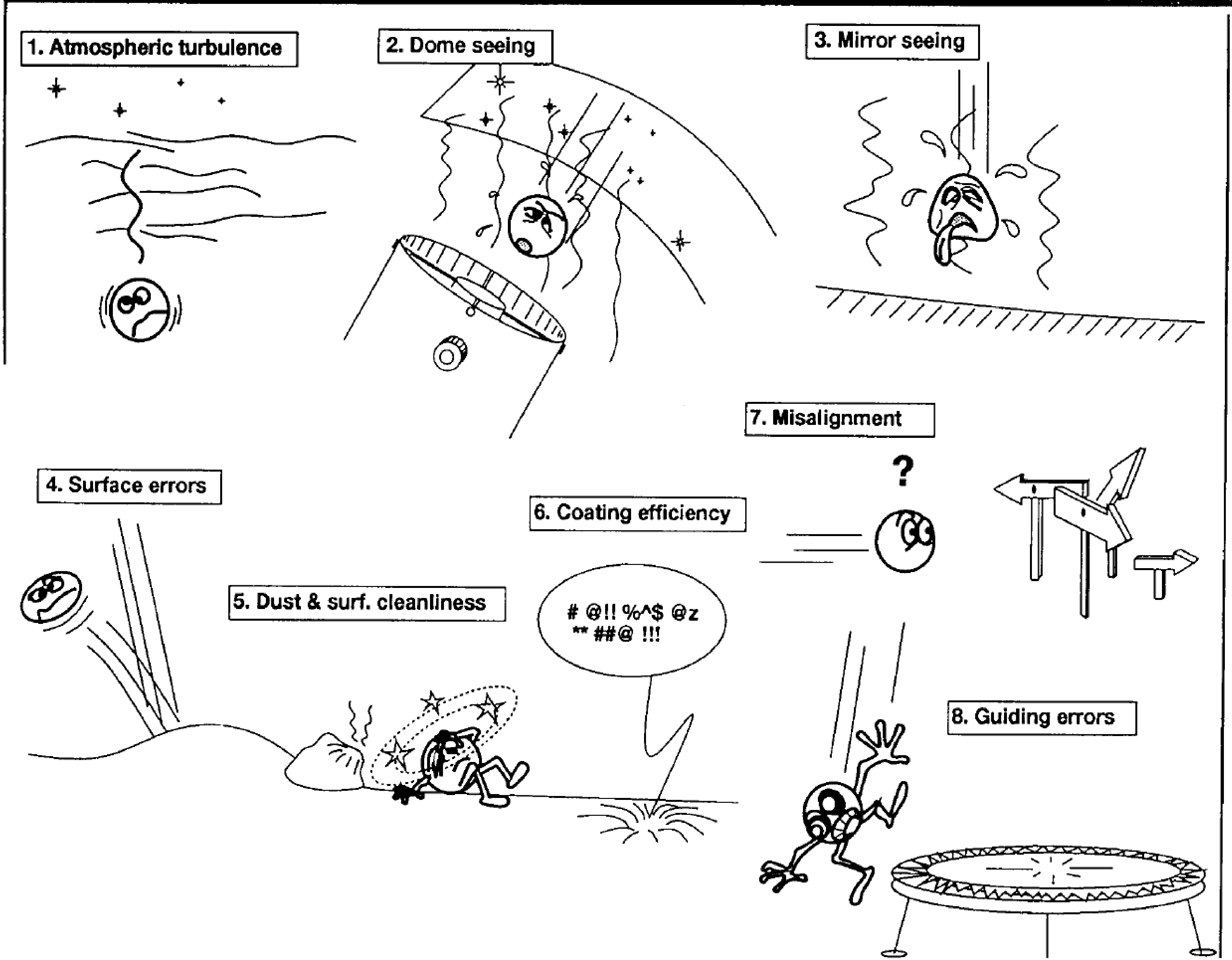

Point spread function (PSF)

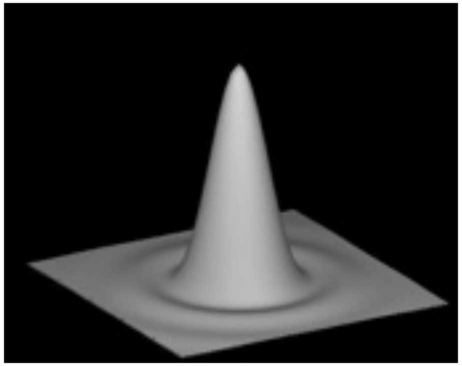

Ideal (diffraction limited) PSF if no atmosphere

$\theta \sim 1.22 \times \lambda / D$

(where λ is wavelength, D the diameter of the telescope and θ is in radians)

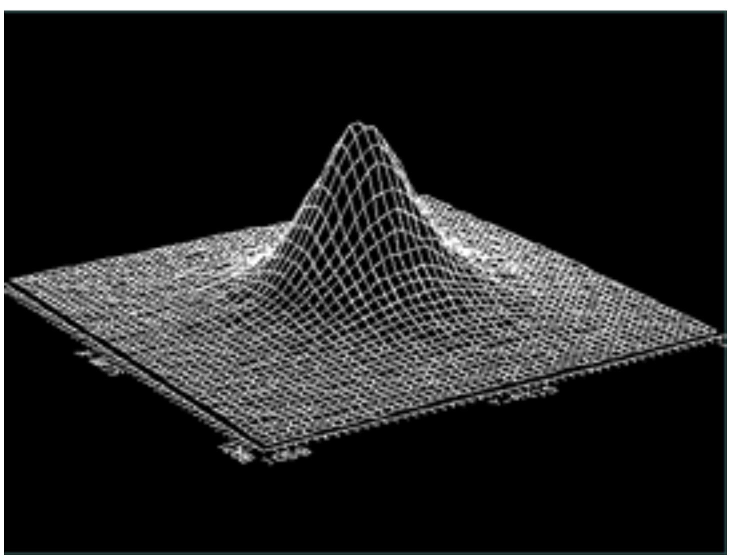

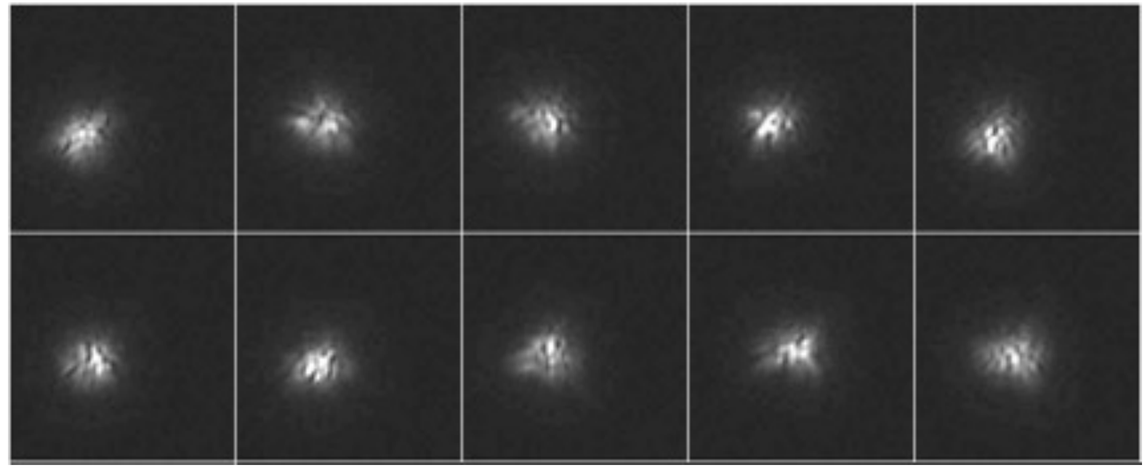

Atmospheric turbulence broadens the PSF resulting in a Gaussian PSF

$$I(r) = I(0)\exp(-r^2/2\sigma^2)$$

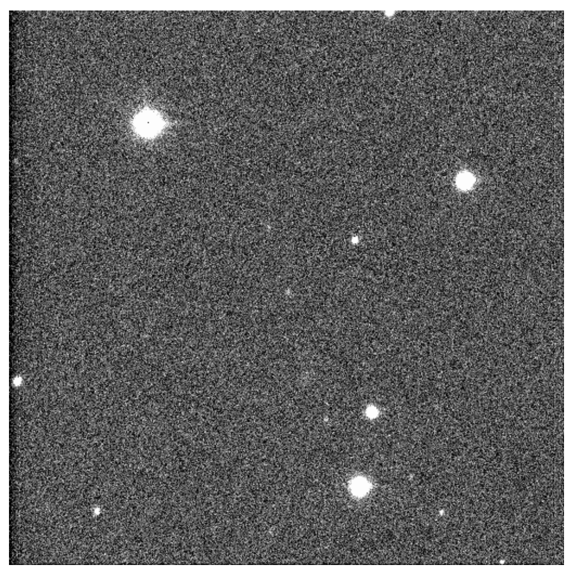

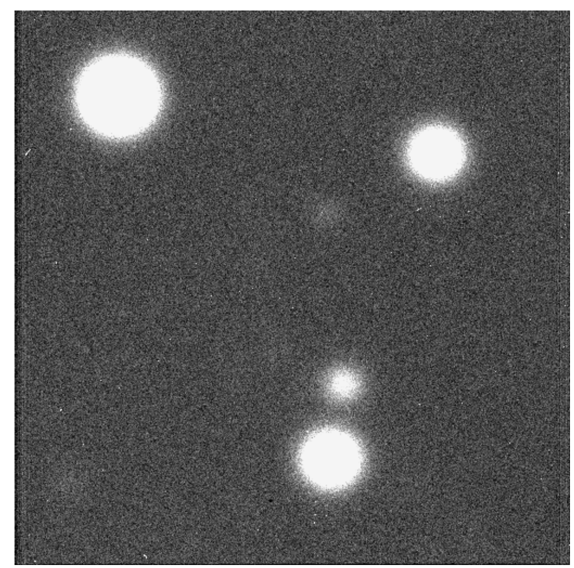

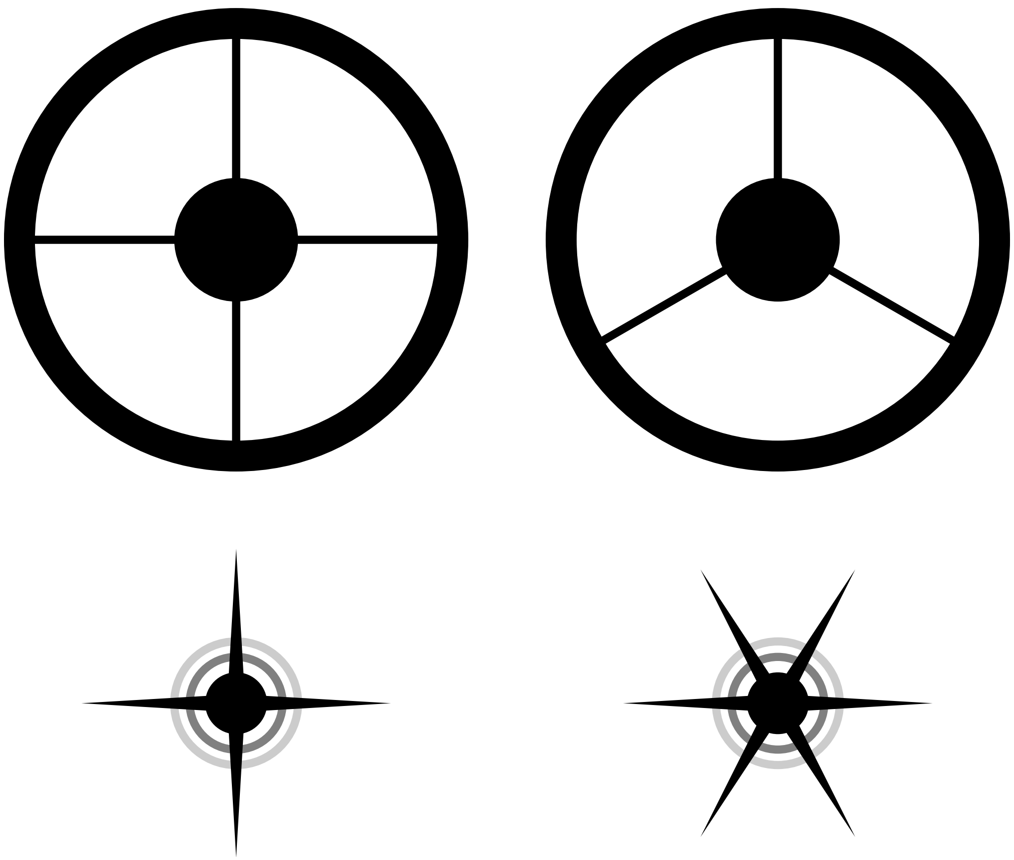

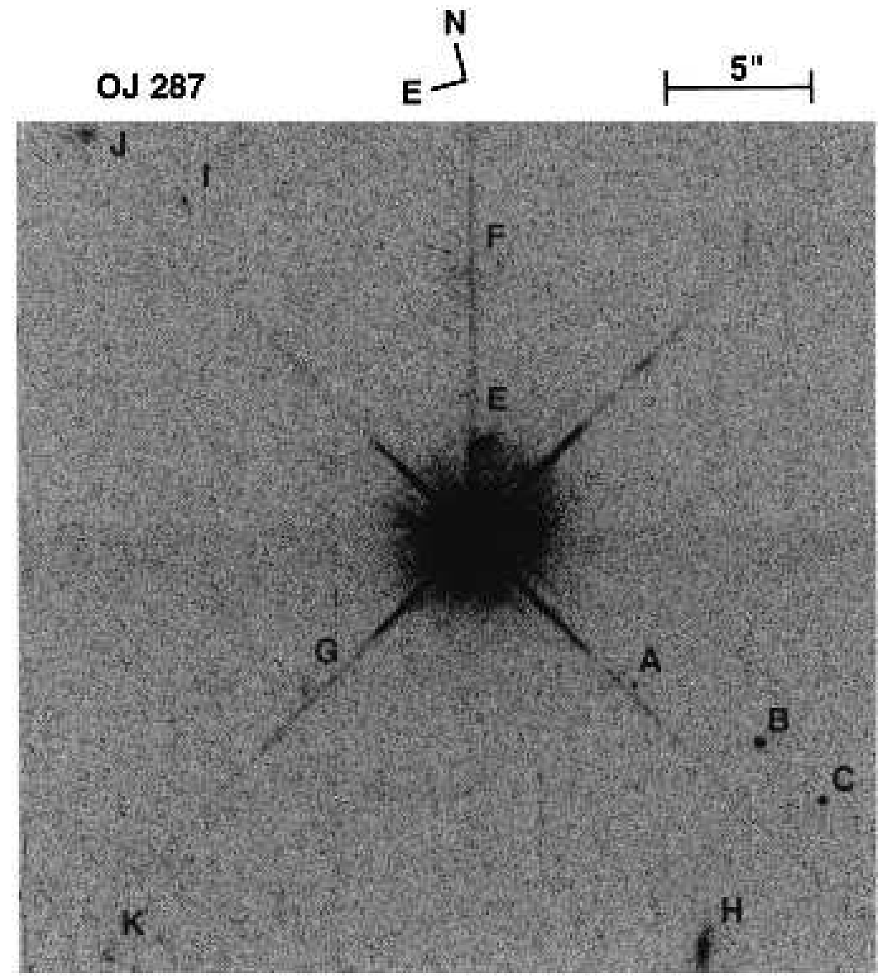
OJ 287
N
E
5"
J
I
F
E
G
A
B
C
H
K

Convolution

“real” signal   additive noise

$$b(\vec{x}) = f(\vec{x}) * p(\vec{x}) + n(\vec{x})$$

observed signal   PSF

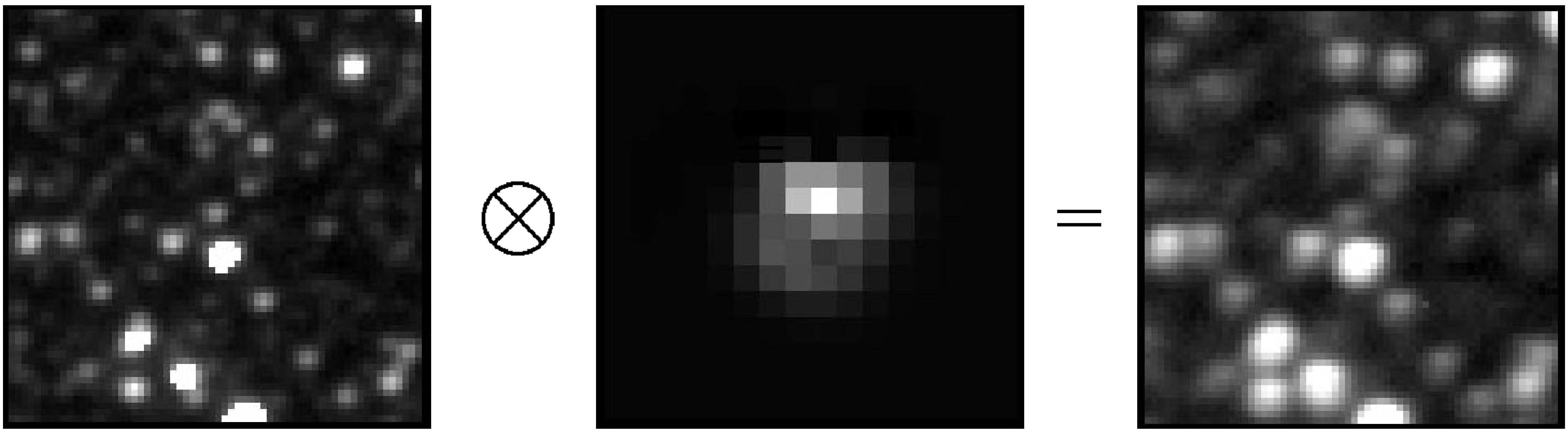

$$ref(x,y) \otimes kernel(x,y,u,v) = im(x,y)$$

Aland & Lupton 1998: A method for optimal image subtraction, arXiv:astro-ph/9712287

Convolution

“real” signal additive noise

$$b(\vec{x}) = f(\vec{x}) * p(\vec{x}) + n(\vec{x})$$

observed signal PSF

In the case of 1-D functions

$$(f * g)(x) = \int_{-\infty}^{\infty} f(\tau)g(x-\tau) \quad d\tau$$

In the case of discrete 1-D functions

$$(f * g)_j = \sum_{k=-m/2+1}^{m/2} f_k g_{j-k}$$

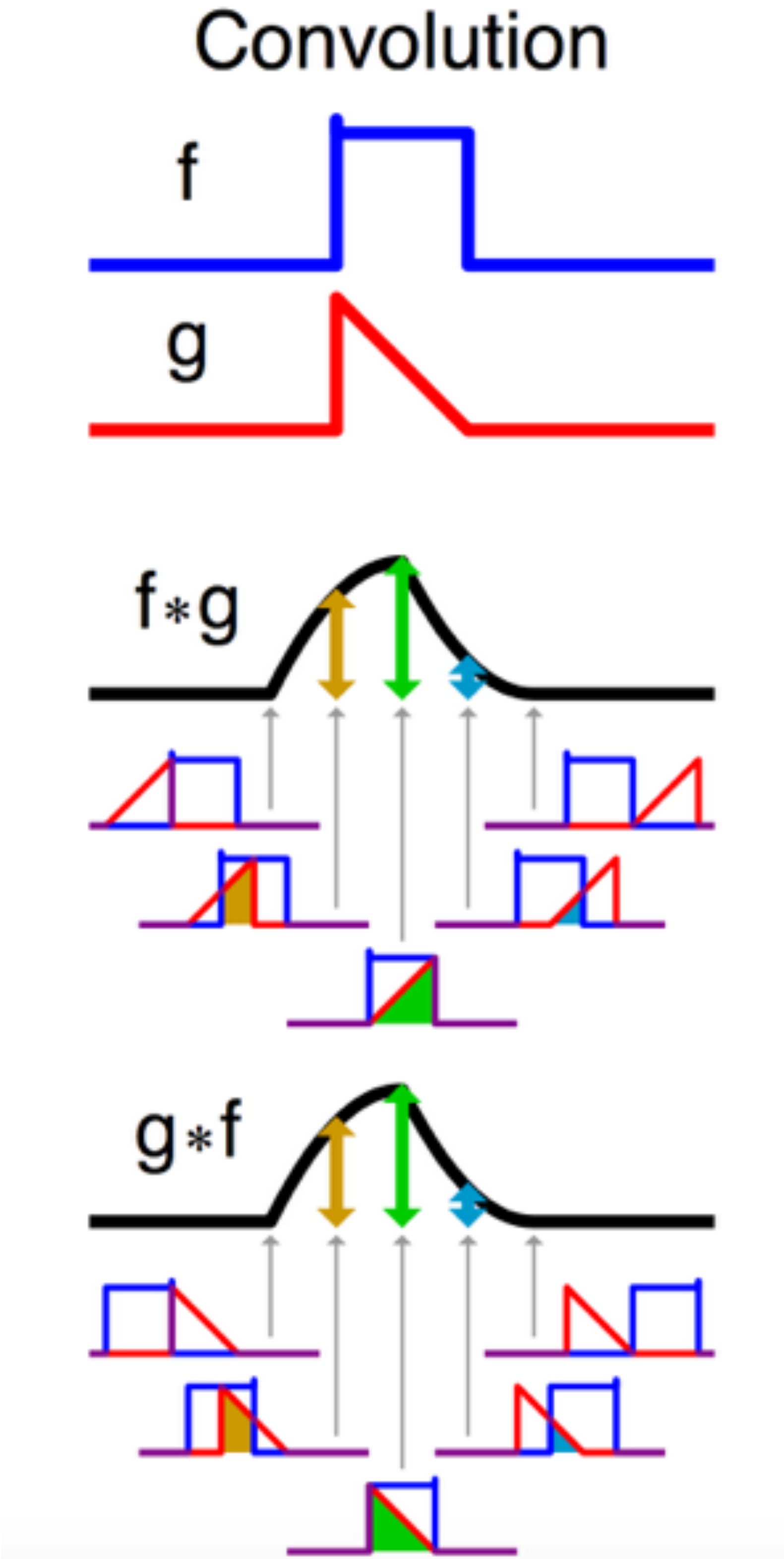

$$(f * g)(x) = \int_{-\infty}^{\infty} f(\tau) g(x - \tau) \quad d\tau$$

$$(f * g)_j = \sum_{k=-m/2+1}^{m/2} f_k g_{j-k}$$

Signal-to-Noise Ratio

- Most important measure of the level of 'goodness' of your observation

$$\frac{S}{N} = \frac{signal}{\sqrt{noise_1^2 + noise_2^2 + \ldots + noise_n^2}}$$

where $noise_1$, $noise_2$, ... are different sources of noise

- With convolution can reduce the noise and therefore increase the S/N

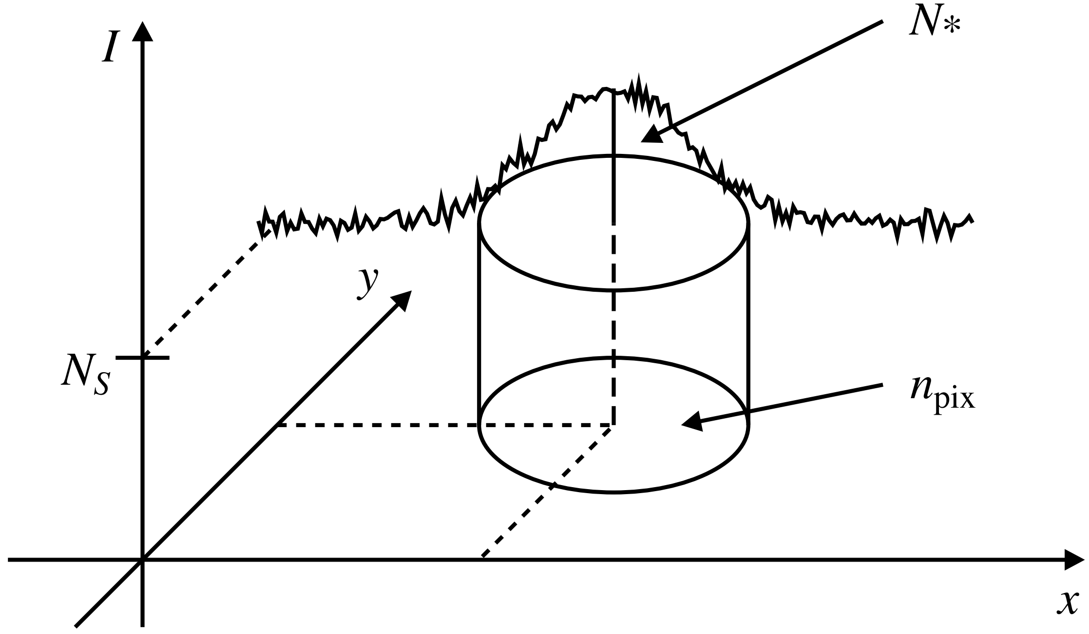

Signal-to-Noise Ratio

- Most important measure of the level of 'goodness' of your observation

$$\frac{S}{N} = \frac{signal}{\sqrt{noise_1^2 + noise_2^2 + \ldots + noise_n^2}}$$

where $noise_1$, $noise_2$, ... are different sources of noise

- With convolution can reduce the noise

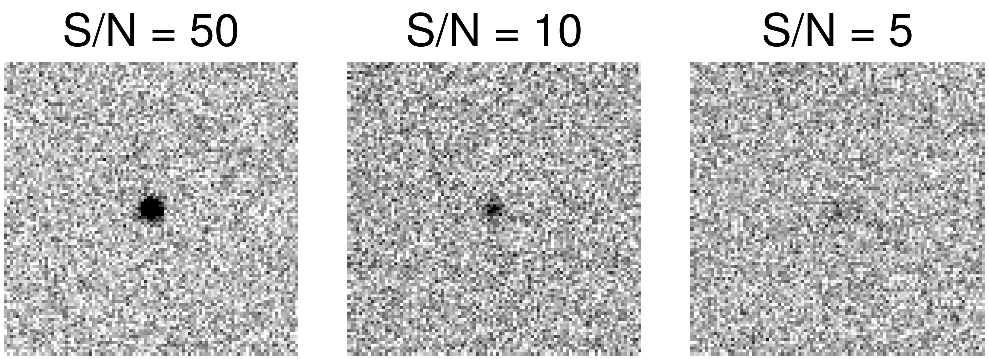

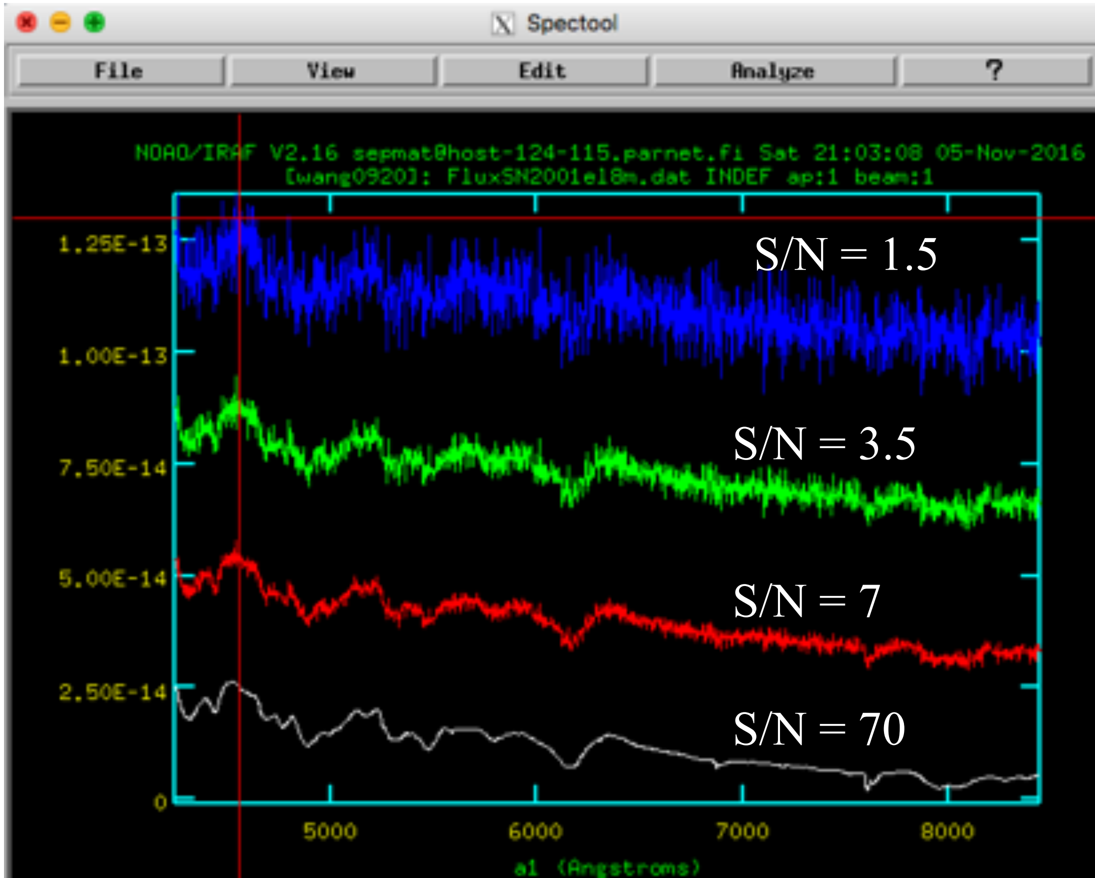

Discovery of supernovae by precise alignment, PSF matching and subtraction of images

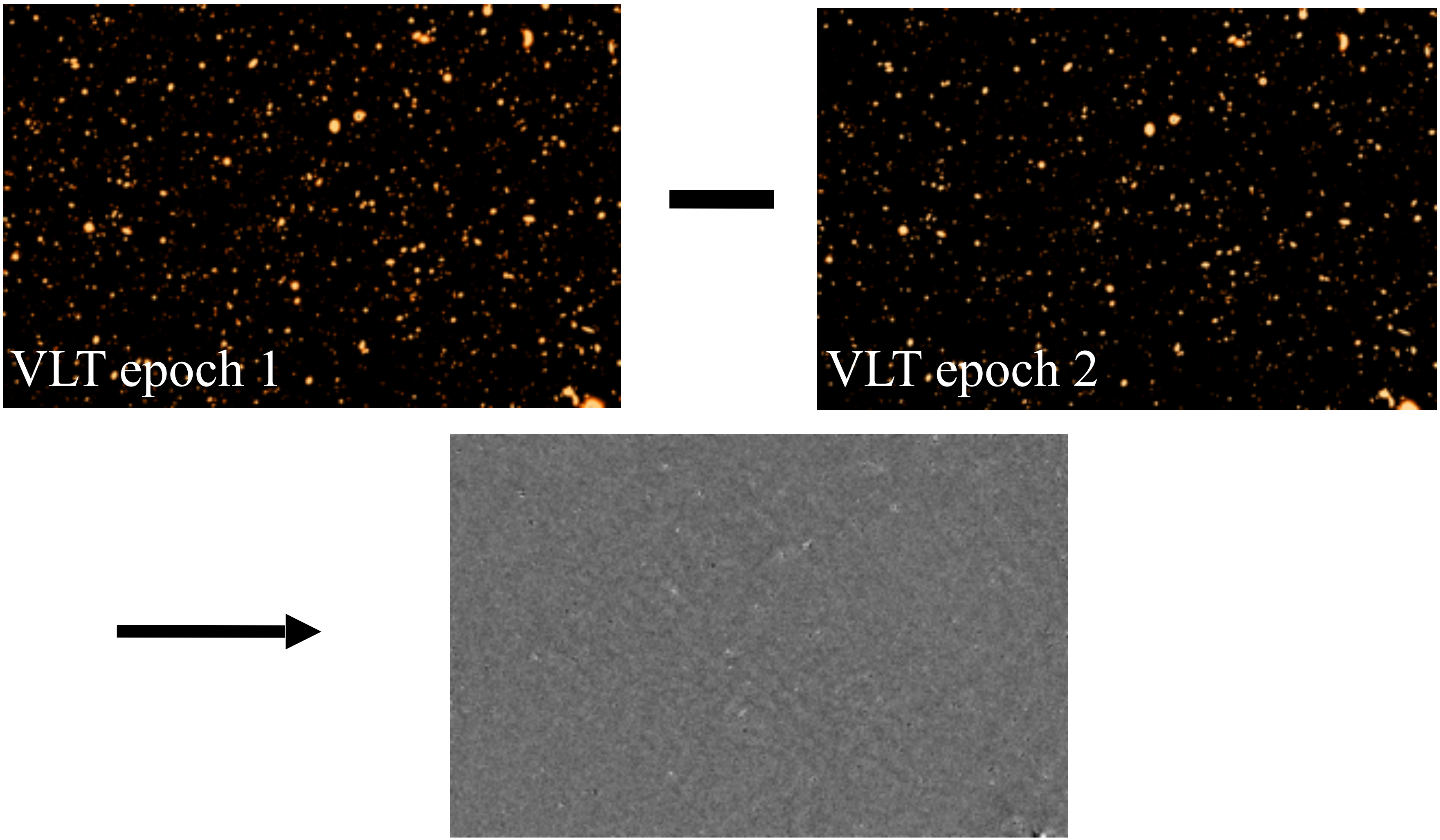


VLT/VIMOS
B 10 hours
V 5 hours
R 15 hours
I 30 hours
Melinder et al. 2011, 2012


Melinder et al. 2011, 2012

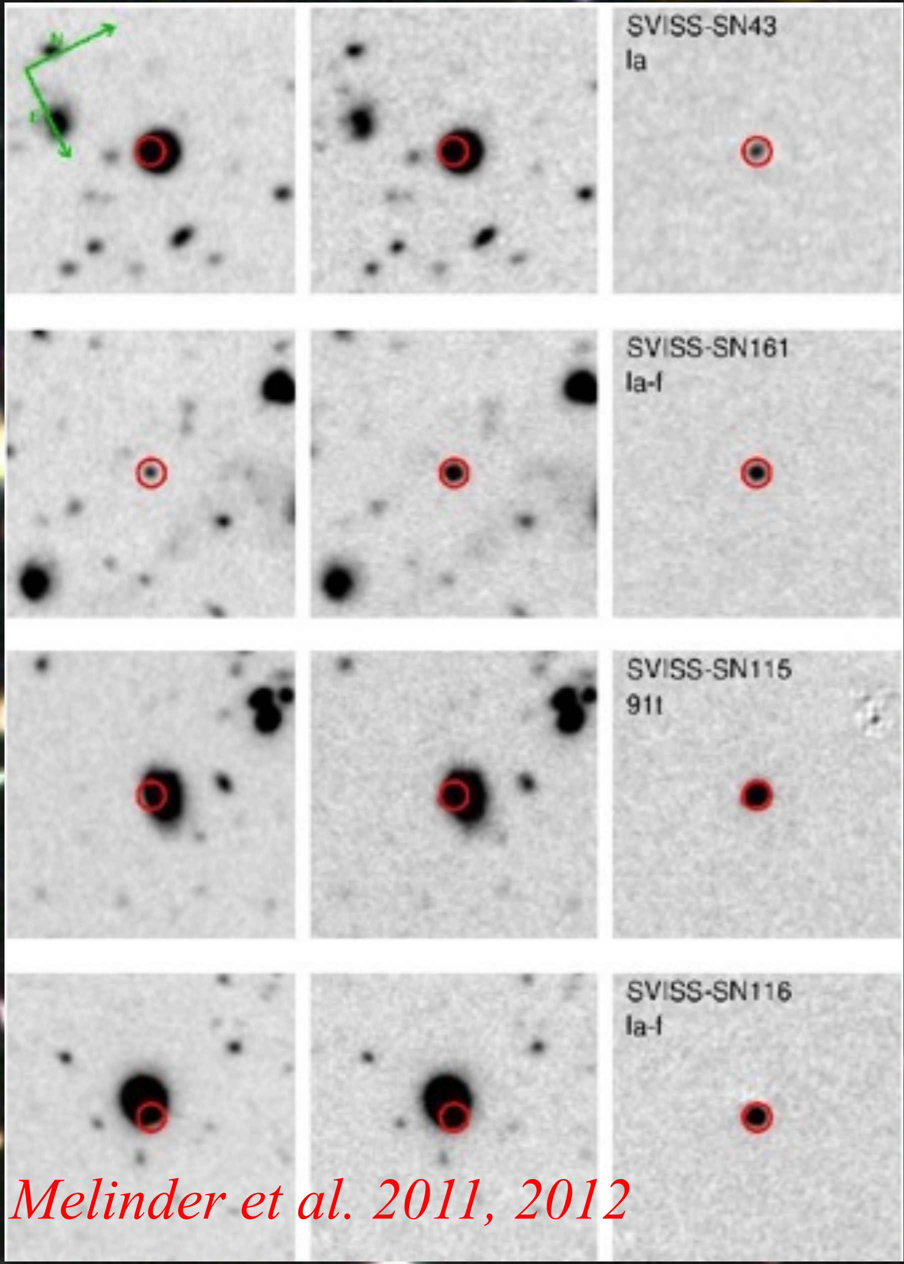

Melinder et al. 2011, 2012

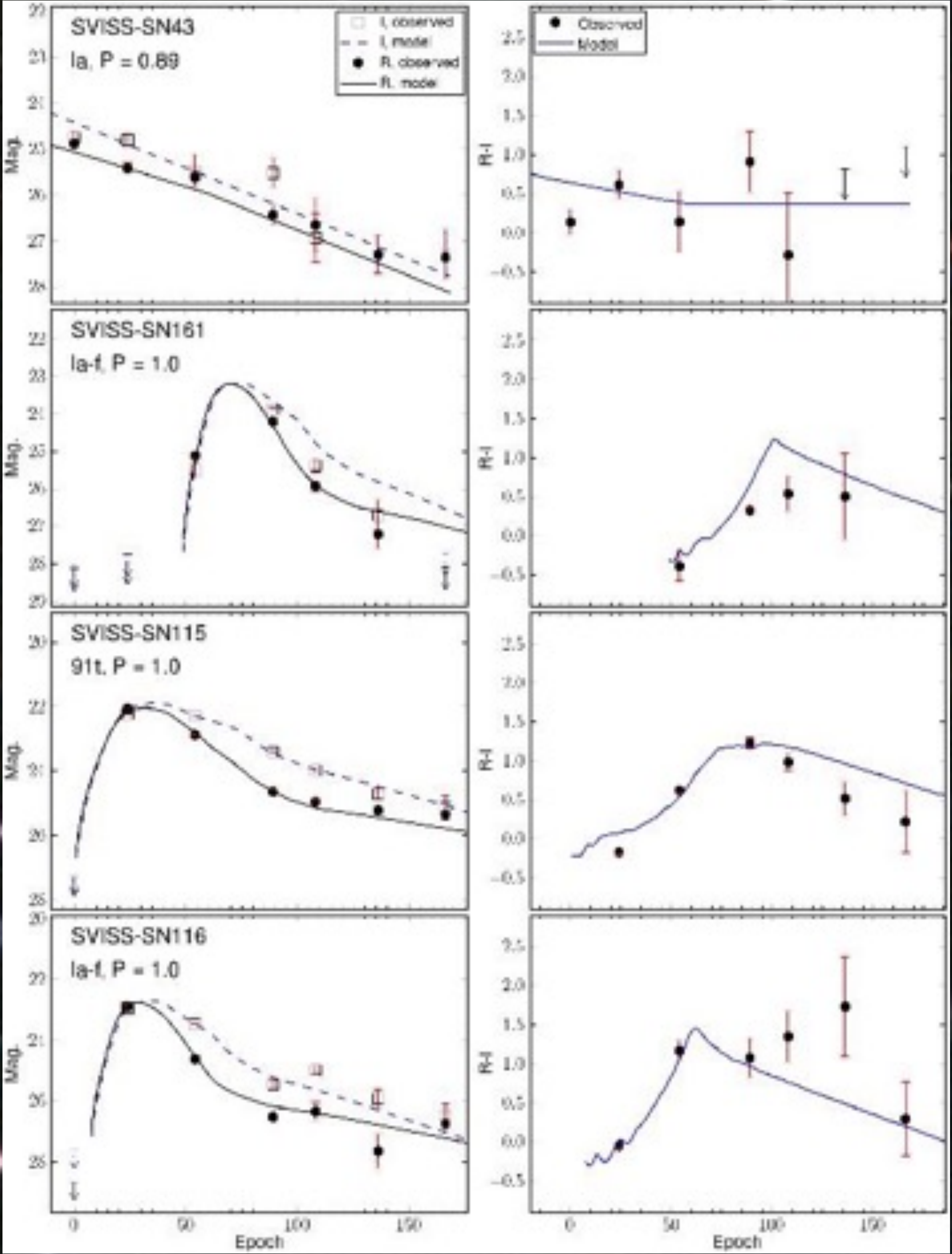

Discovery of supernovae by precise alignment, PSF matching and subtraction of images

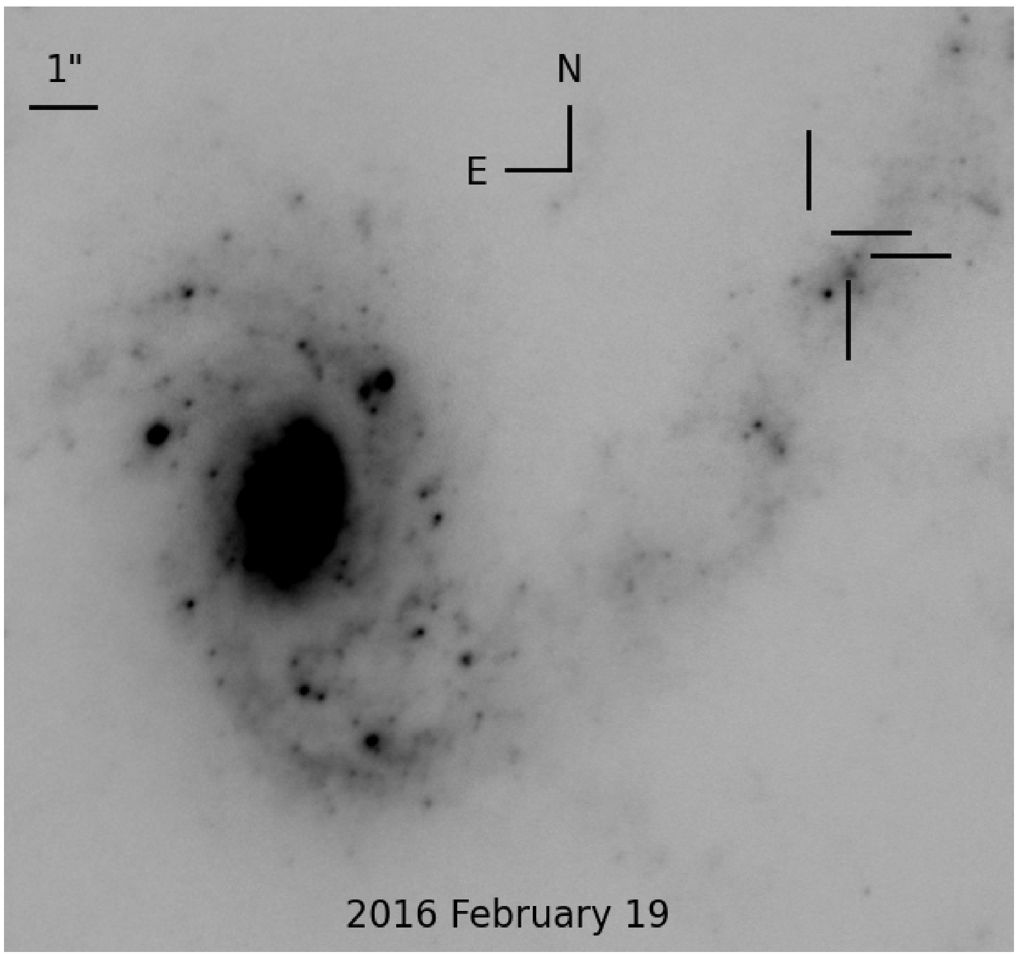

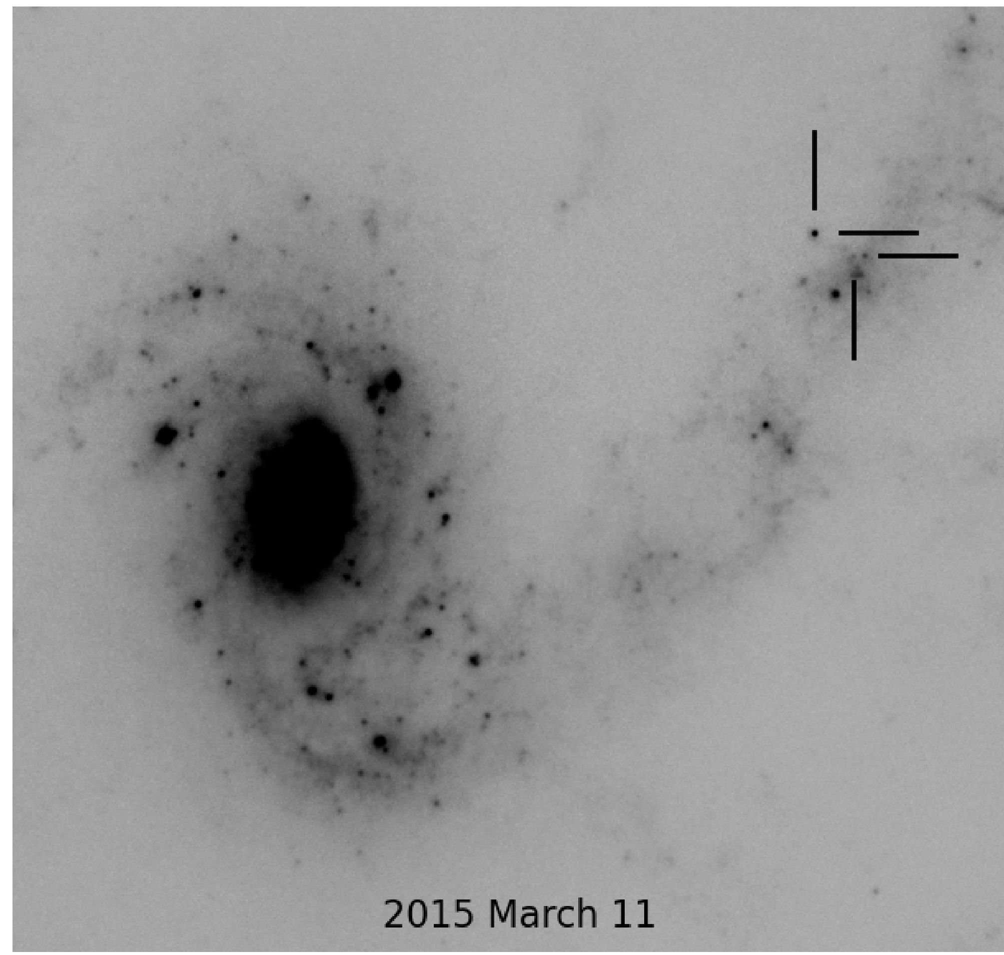

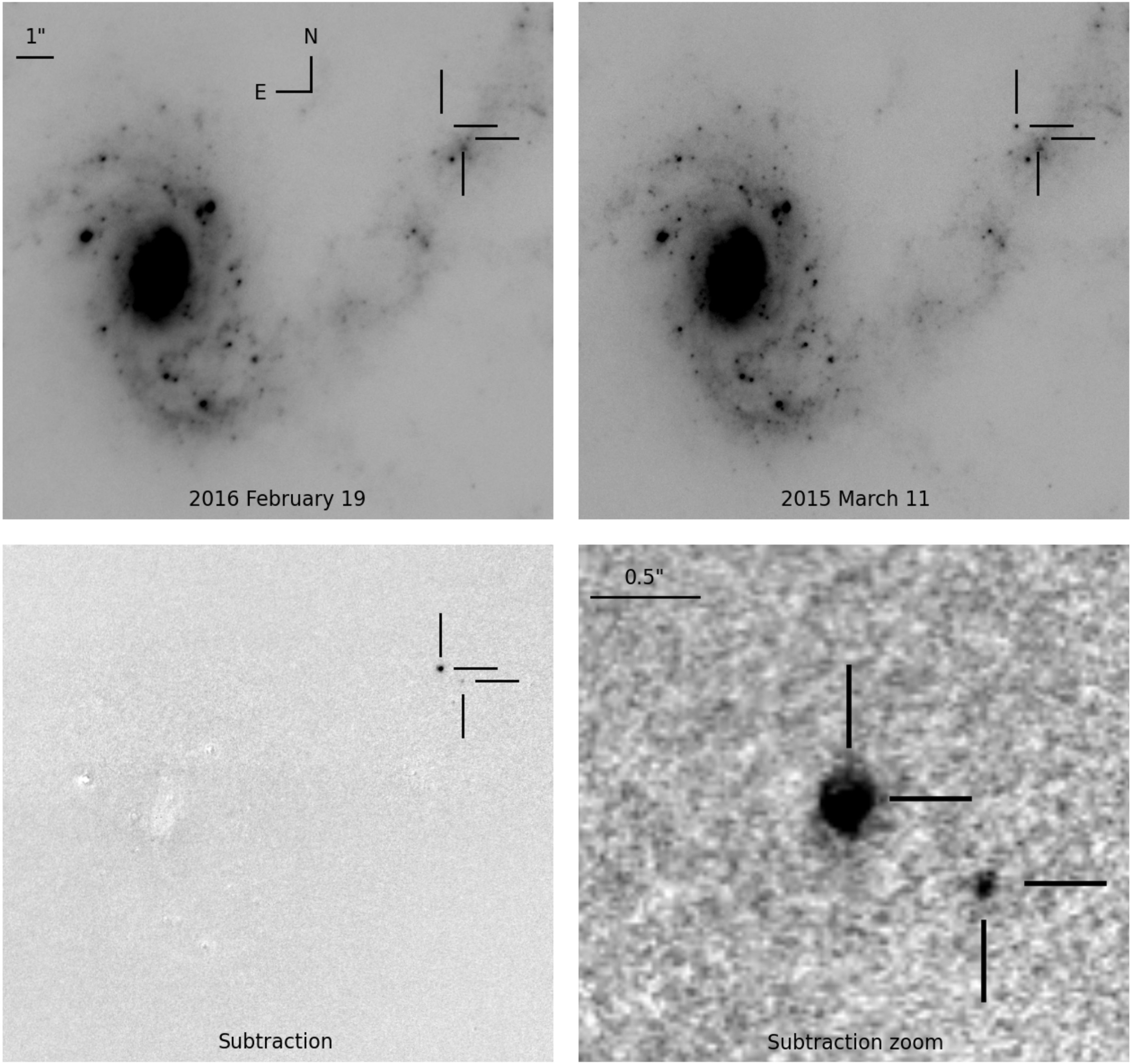
1"
N
E
2016 February 19
2015 March 11
Subtraction
0.5"
Subtraction zoom

Dust obscured SNe characterised at radio wavelengths

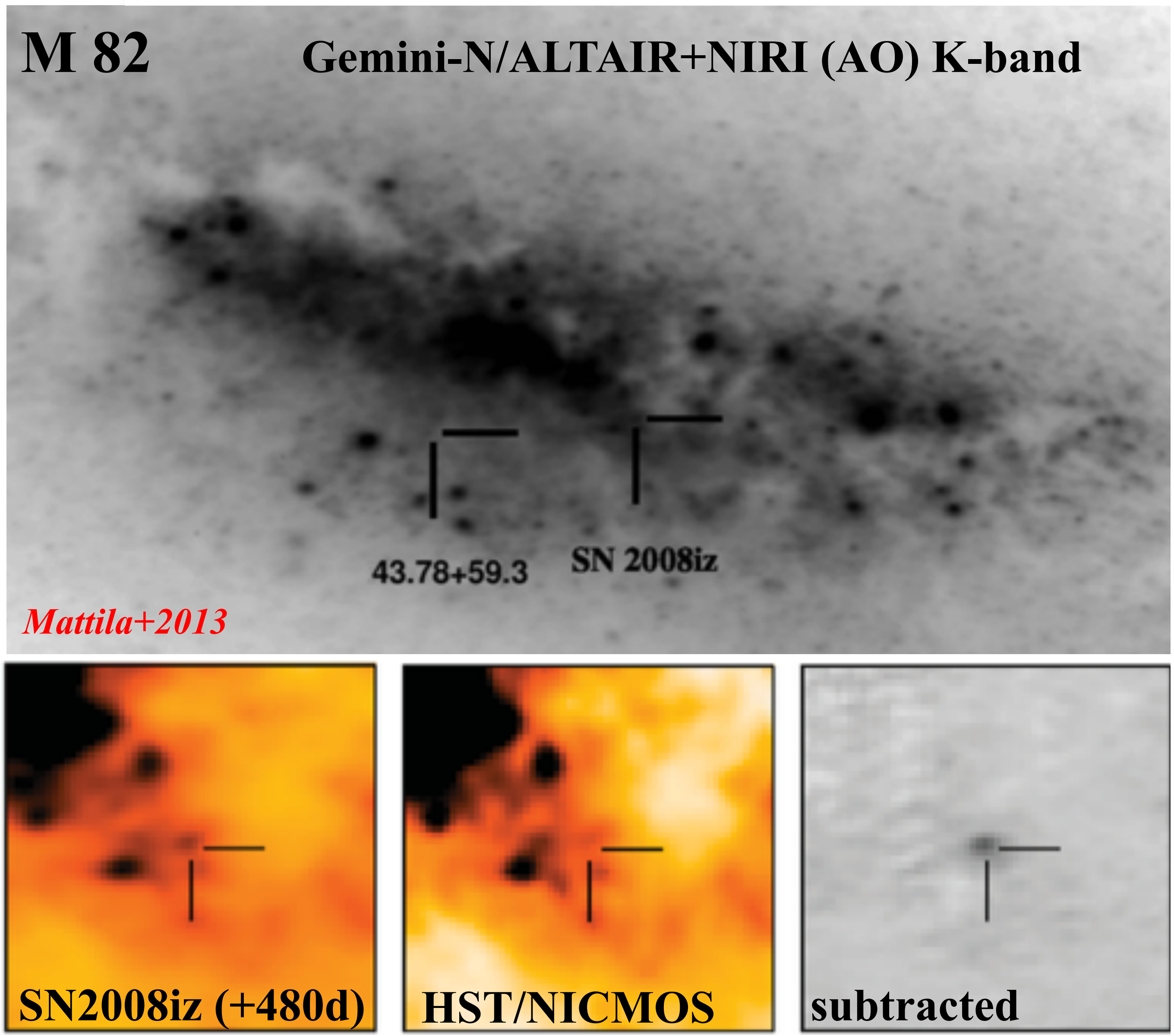

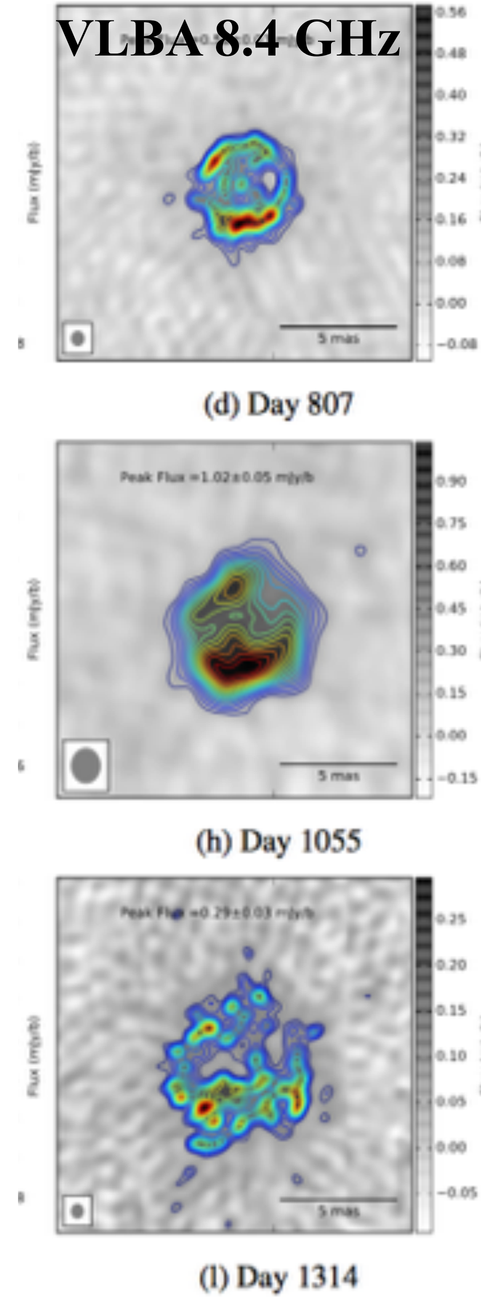

Kimani+2016

Dust obscured SNe characterised at IR wavelengths

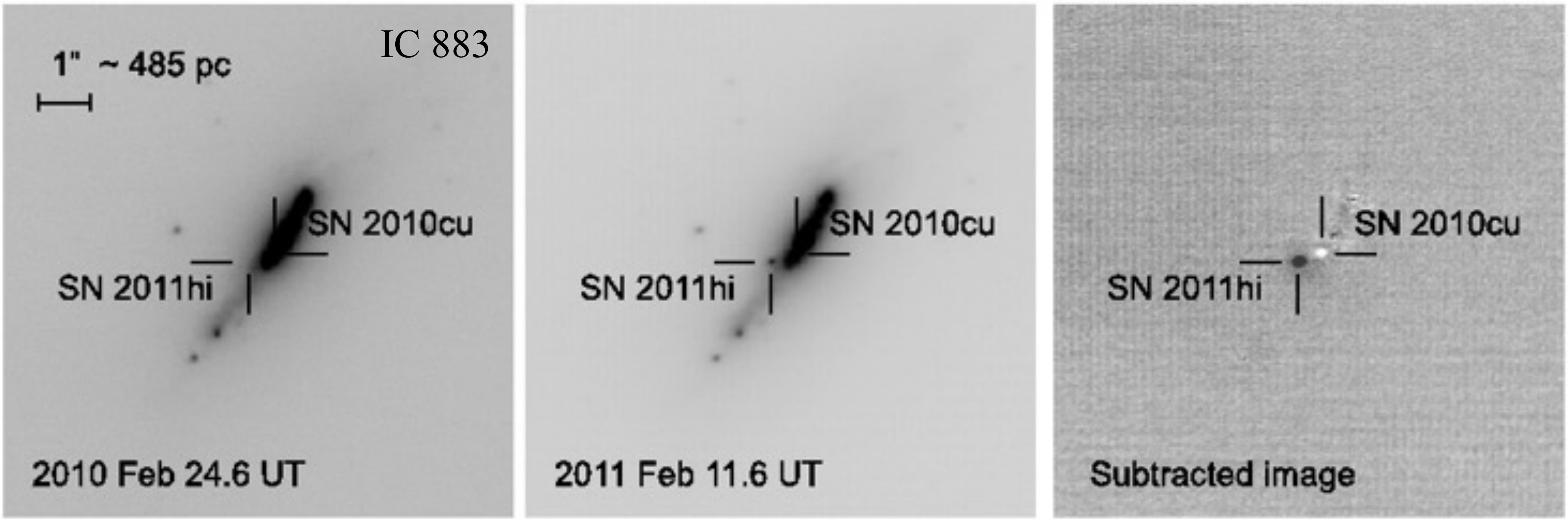

Kankare,SM+2012

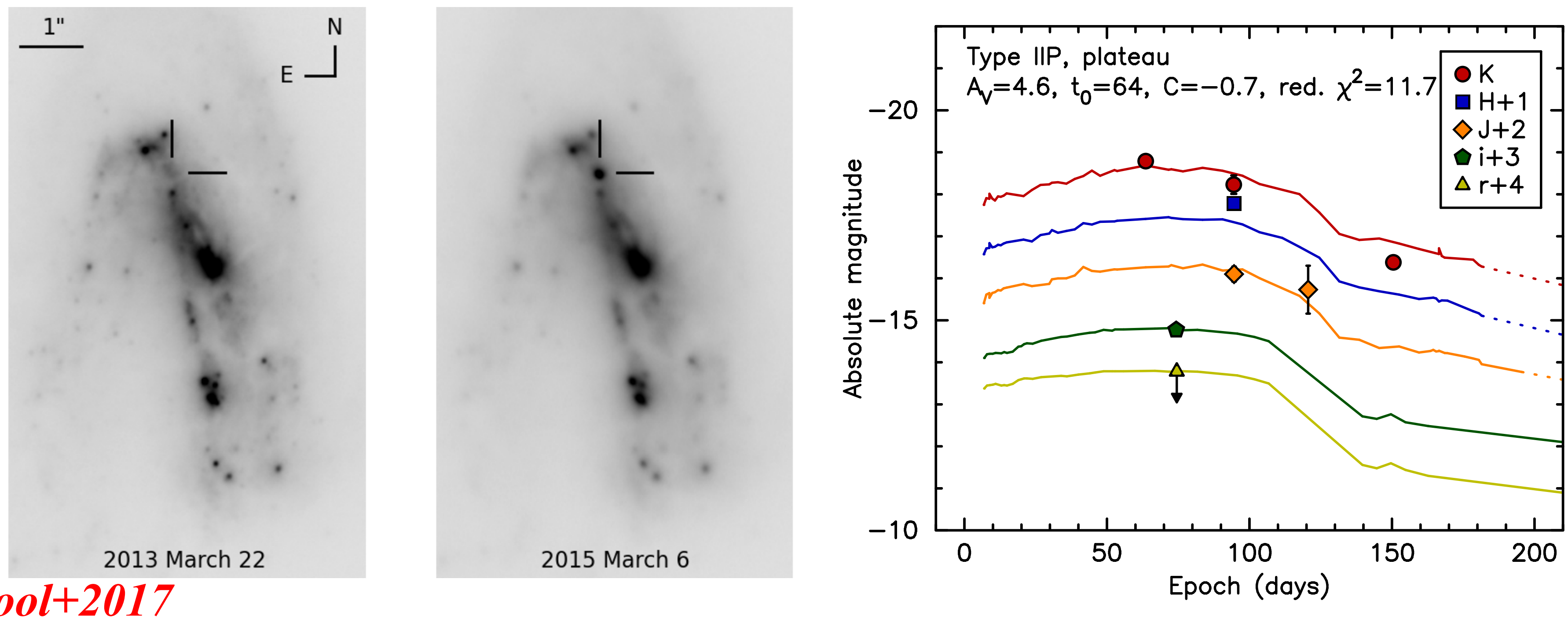

Kool+2017

“Dark” SNe in U/LIRGs

- Detailed comparison between CCSN rates and cosmic SF history can provide a useful consistency check and information on the mass range for CCSN progenitors
- CCSN rates need to be corrected for the fraction of CCSNe “missed” in the nuclear regions of U/LIRGs

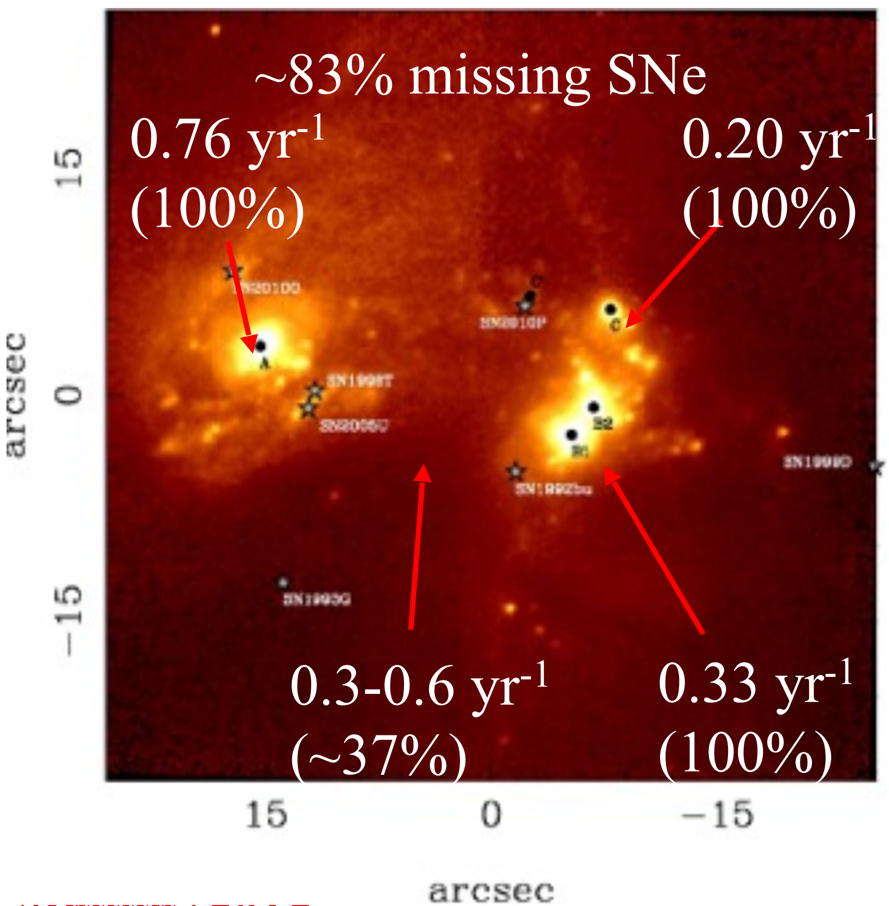

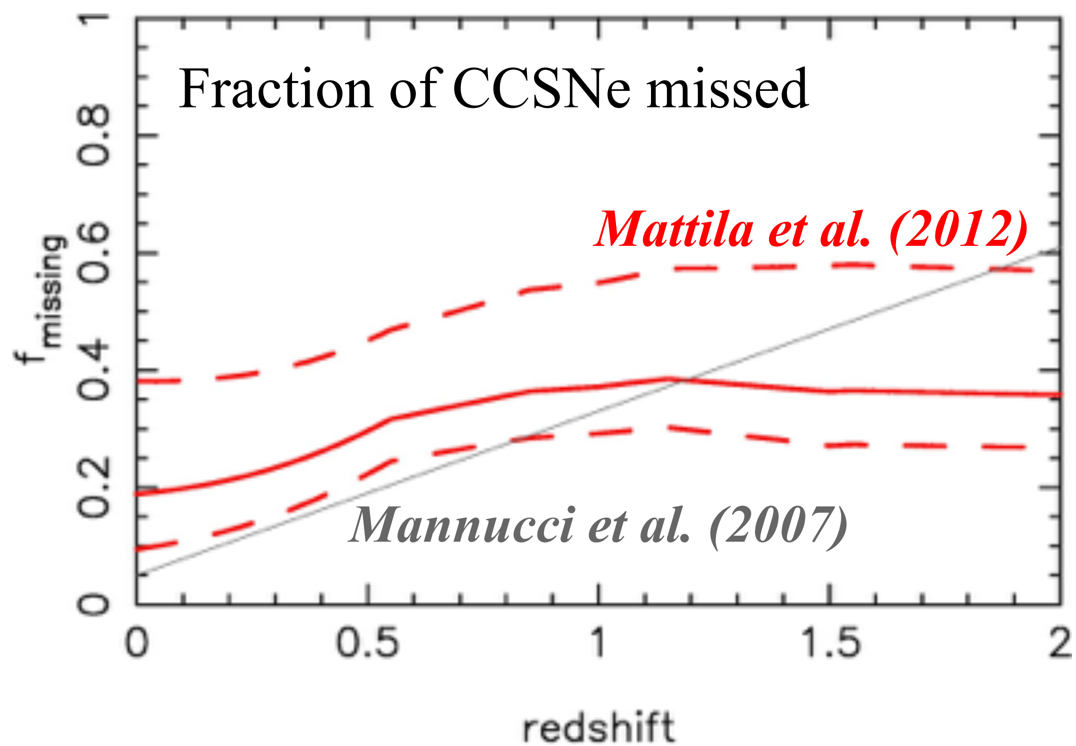

“Dark” SNe in U/LIRGs

- Detailed comparison between CCSN rates and cosmic SF history can provide a useful consistency check and information on the mass range for CCSN progenitors
- CCSN rates need to be corrected for the fraction of CCSNe “missed” in the nuclear regions of U/LIRGs

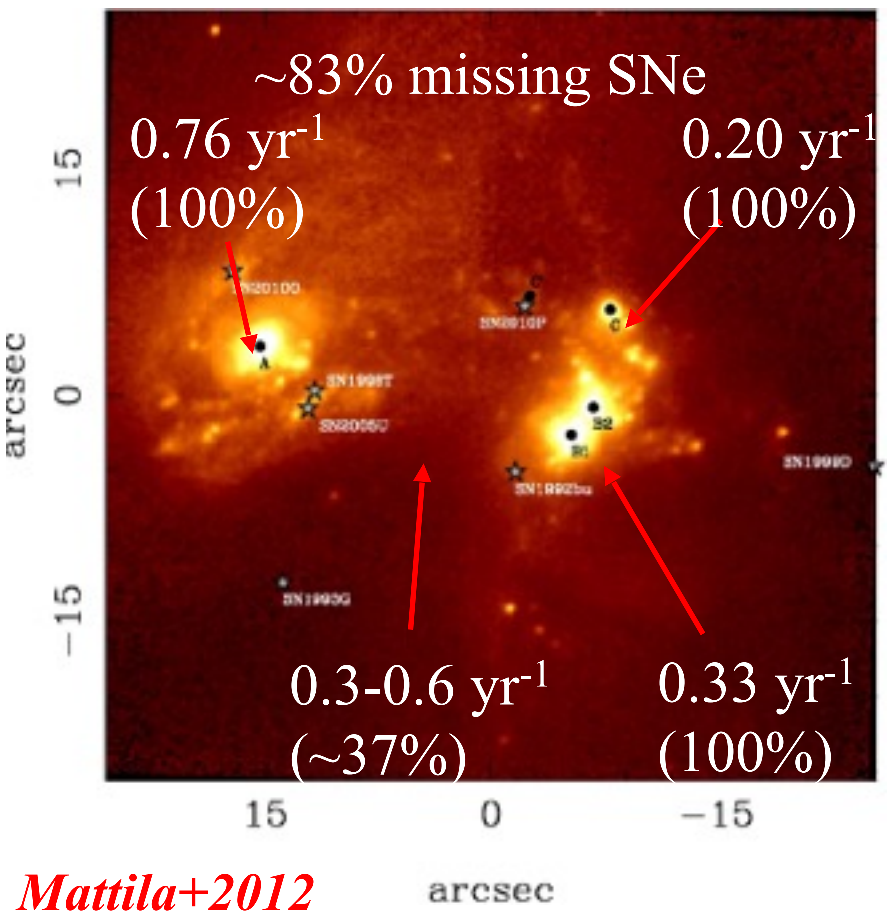

Mattila+2012

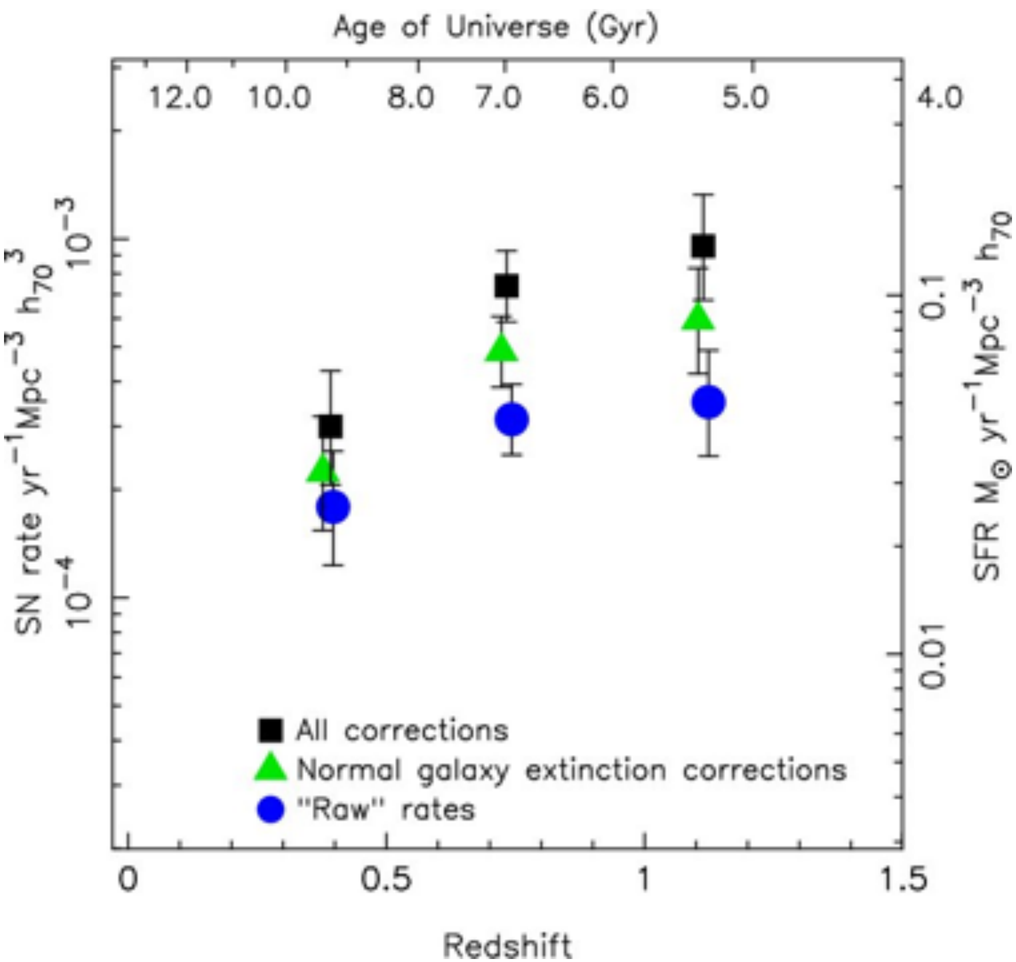

Dahlen...Mattila+2012

Supernova progenitors

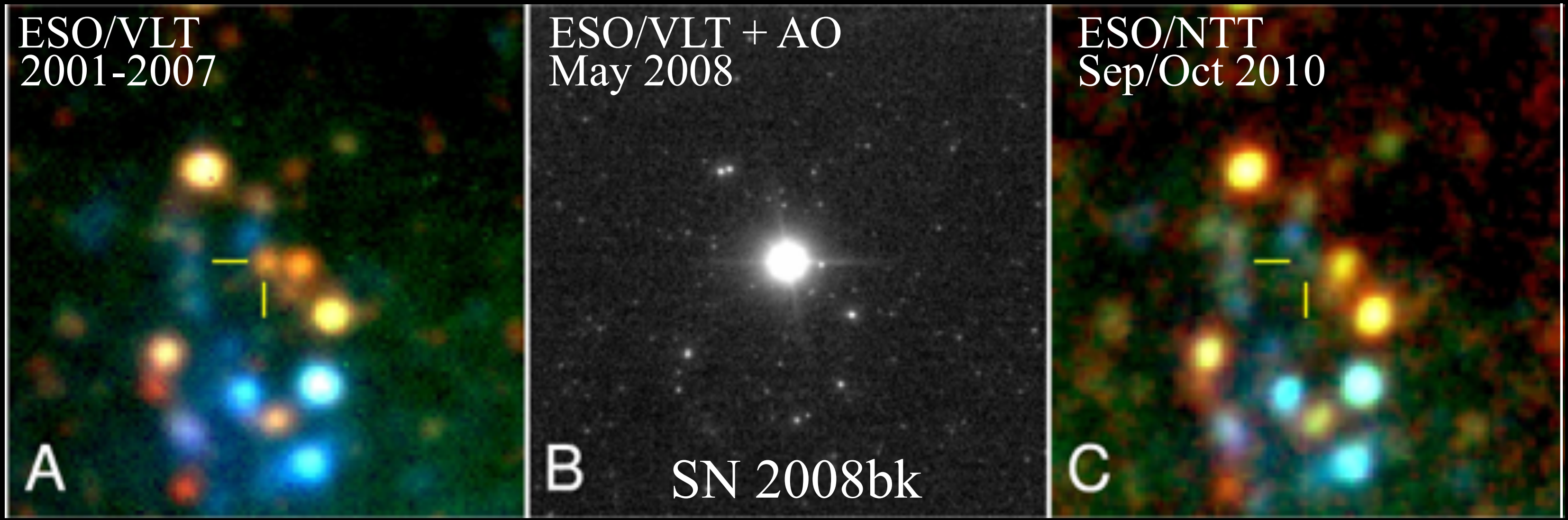

Mattila+ 2008, 2010; Maund+ 2014

Supergiants

Core-collapse

Supernova progenitors

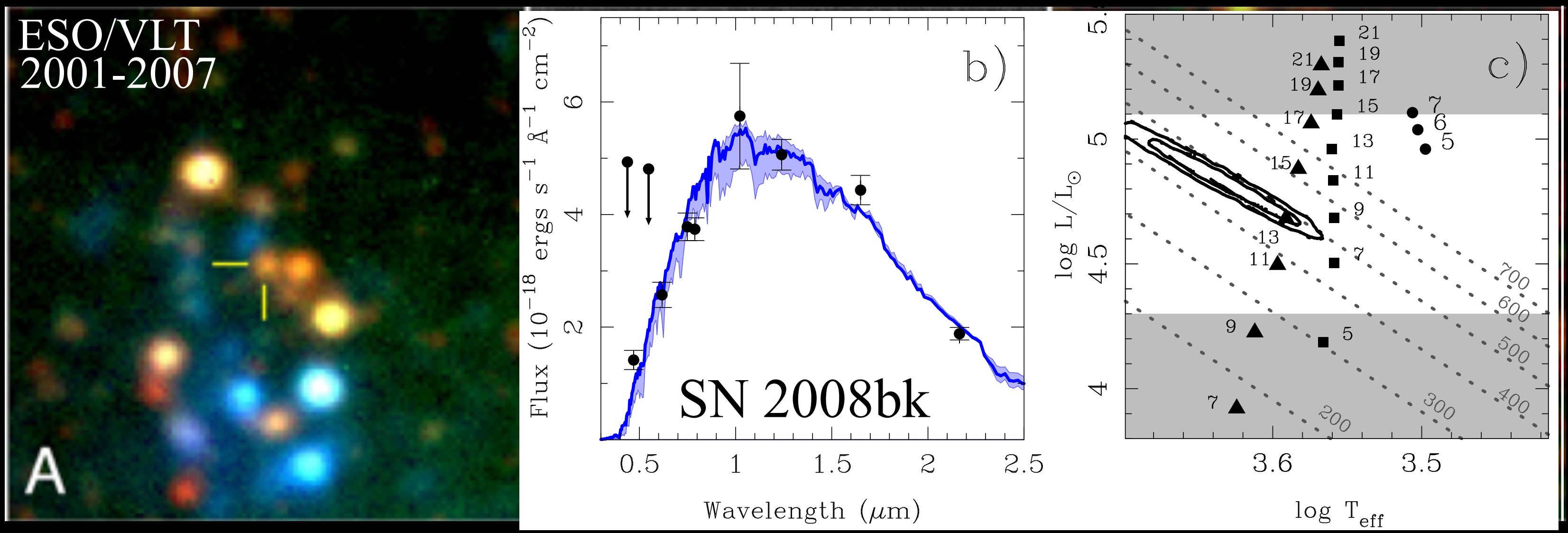

Mattila+ 2008, 2010; Maund+ 2014

Supergiants

Core-collapse

Optimal Image Subtraction

$$ref(x,y) \otimes kernel(x,y,u,v) = im(x,y) + bg(x,y)$$

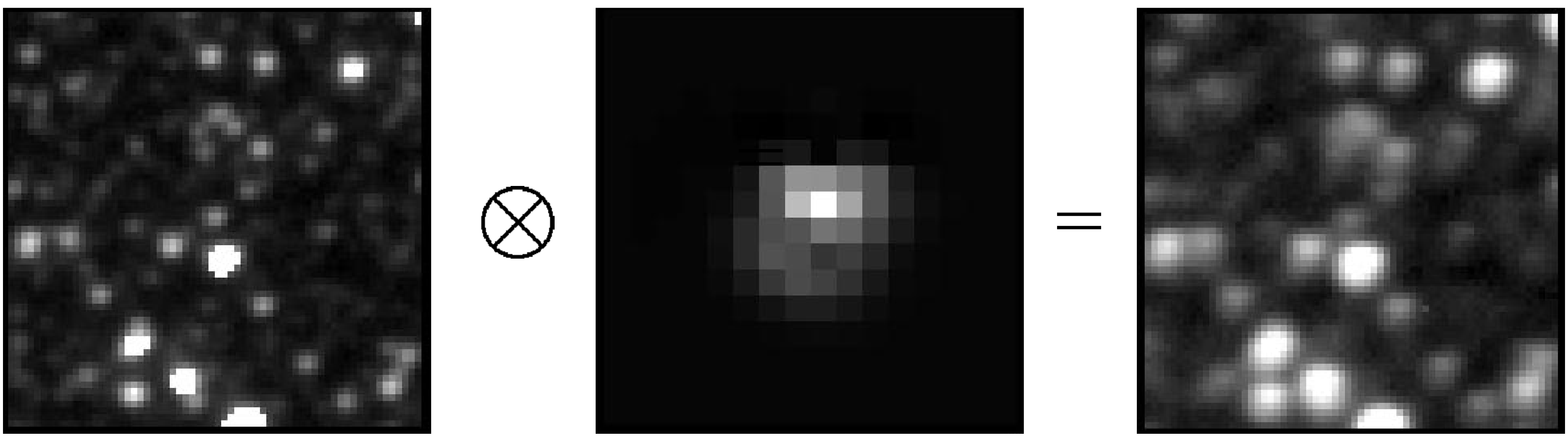

Aland & Lupton 1998: A method for optimal image subtraction, arXiv:astro-ph/9712287

Optimal Image Subtraction

$$ref(x,y) \otimes kernel(x,y,u,v) = im(x,y) + bg(x,y)$$

$$kernel(x,y,u,v) = \sum_{n}\sum_{d_n^x}\sum_{d_n^y}\sum_{\delta^x}\sum_{\delta^y}[a_n \underbrace{x^{\delta^x} y^{\delta^y}}_{3} \underbrace{e^{-(u^2+v^2)/2\sigma_n^2}}_{1} \underbrace{u^{d_n^x} v^{d_n^y}}_{2}]$$

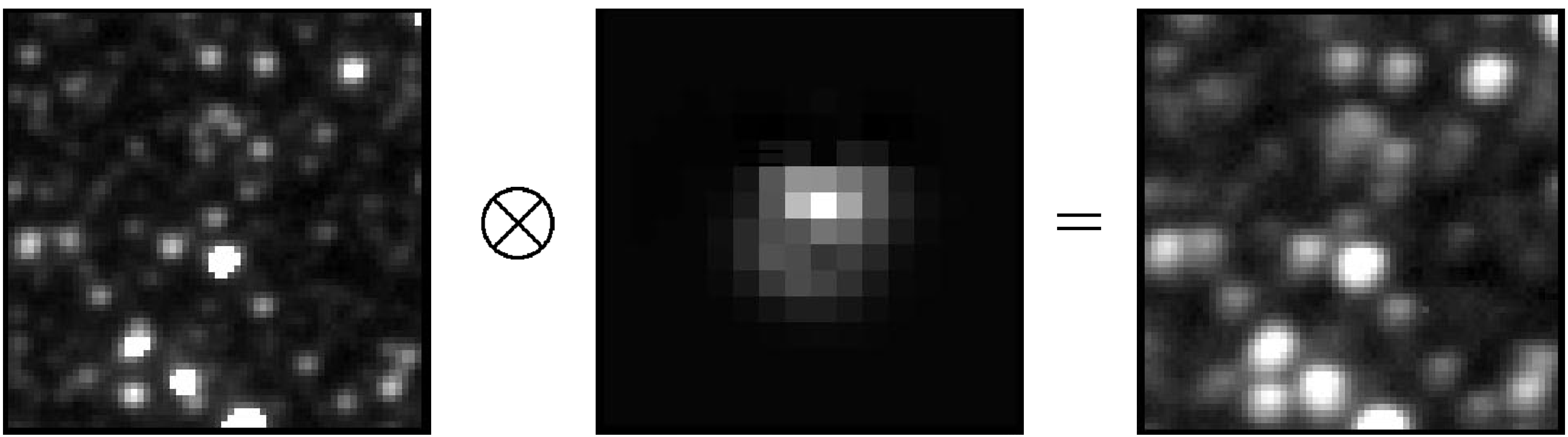

Aland & Lupton 1998: A method for optimal image subtraction, arXiv:astro-ph/9712287

Optimal Image Subtraction

$$ref(x,y) \otimes kernel(x,y,u,v) = im(x,y) + bg(x,y)$$

$$kernel(x,y,u,v) = \sum_{n}\sum_{d_n^x}\sum_{d_n^y}\sum_{\delta^x}\sum_{\delta^y}[a_n \underbrace{x^{\delta^x} y^{\delta^y}}_{3} \underbrace{e^{-(u^2+v^2)/2\sigma_n^2}}_{1} \underbrace{u^{d_n^x} v^{d_n^y}}_{2}]$$

The convolution kernel consists of a set of Gaussian functions (1) which are modified by polynomials (2) and a model for the spatial variations of the kernel (3) where $0 < d_n^y + d_n^x \leq D_n$, and $0 < \delta^y + \delta^x \leq D^k$.

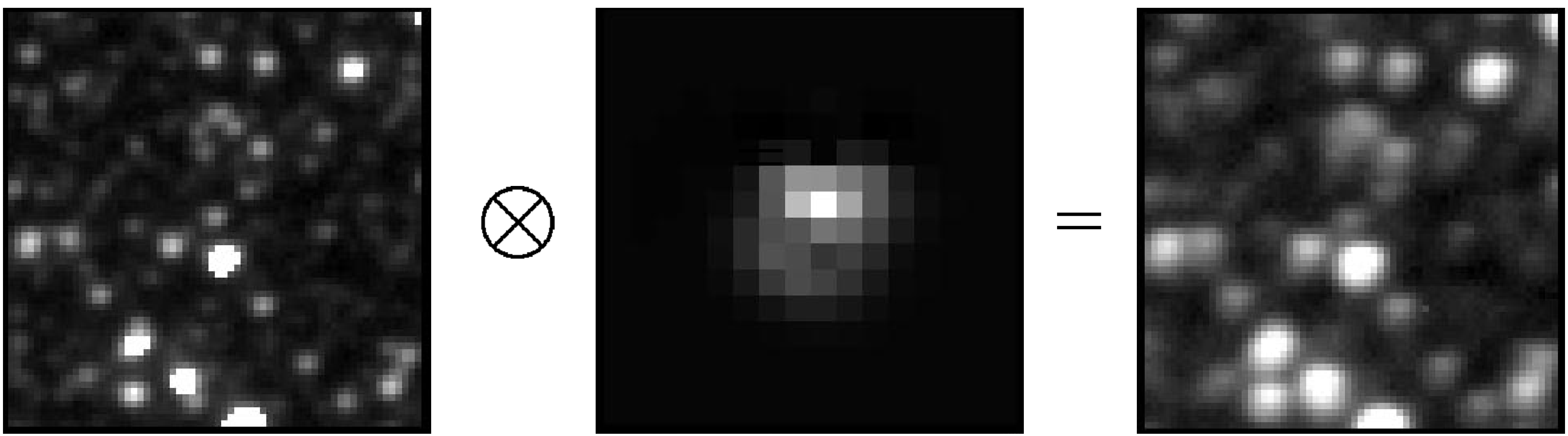

Aland & Lupton 1998: A method for optimal image subtraction, arXiv:astro-ph/9712287

Optimal Image Subtraction

$$ref(x,y) \otimes kernel(x,y,u,v) = im(x,y) + bg(x,y)$$

$$kernel(x,y,u,v) = \sum_{n} \sum_{d_n^x} \sum_{d_n^y} \sum_{\delta^x} \sum_{\delta^y} [a_n \underbrace{x^{\delta^x} y^{\delta^y}}_{3} \underbrace{e^{-(u^2+v^2)/2\sigma_n^2}}_{1} \underbrace{u^{d_n^x} v^{d_n^y}}_{2}]$$

$$bg(x,y) = \sum_{i} \sum_{j} a_i x^i y^j$$

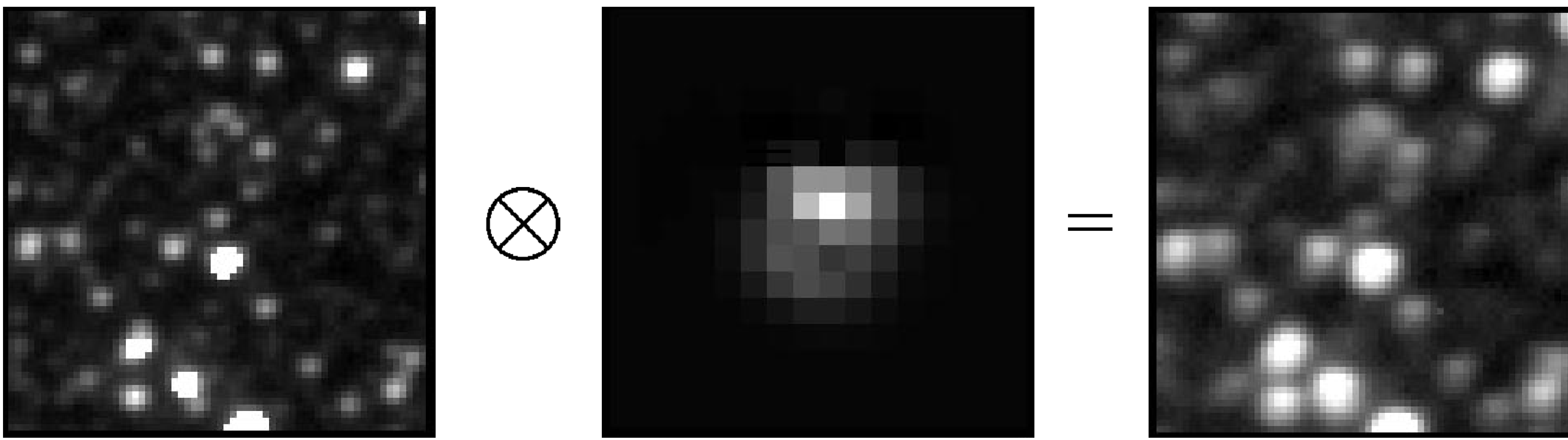

Aland & Lupton 1998: A method for optimal image subtraction, arXiv:astro-ph/9712287

Convolution: Optimal Image Subtraction

$$kernel(x,y,u,v) = \sum_n \sum_{d_n^x} \sum_{d_n^y} \sum_{\delta^x} \sum_{\delta^y} [a_n \underbrace{x^{\delta^x} y^{\delta^y}}_{3} \underbrace{e^{-(u^2+v^2)/2\sigma_n^2}}_{1} \underbrace{u^{d_n^x} v^{d_n^y}}_{2}]$$

$$bg(x,y) = \sum_i \sum_j a_i x^i y^j$$

n	number of Gaussian functions in the kernel
σ_n	sigmas of the Gaussians
D_n	polynomial degrees associated with each of the n gaussians
D^k	degree of the polynomial transform for the spatial variations of the kernel
D^{bg}	degree of the polynomial used to model the background variations
N_x	number of stamps along x-axis
N_y	number of stamps along y-axis
S_k	width of the convolution kernel
S_s	width of the region used for fitting the background
N_c	minimum number of counts in the middle of a stamp
N_{min}	minimum value of a pixel to be included in the fit
N_{sat}	maximum value of a pixel to be included in the fit

Aland & Lupton 1998: A method for optimal image subtraction, arXiv:astro-ph/9712287

THE RESTORATION OF HST IMAGES AND SPECTRA

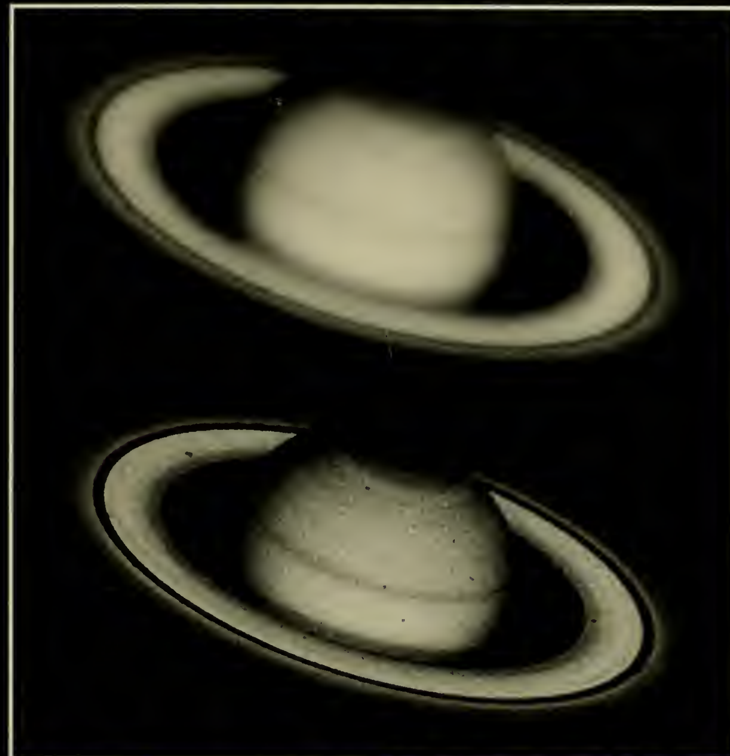

Proceedings of a Workshop held at the
Space Telescope Science Institute
Baltimore, Maryland
20-21 August 1990

Edited by R.L. White and R.J. Allen

SPACE TELESCOPE SCIENCE INSTITUTE

NASA
National Aeronautics and
Space Administration

Preface

This volume presents the proceedings of the workshop on *The Restoration of HST Images and Spectra*, held at the Space Telescope Science Institute in Baltimore on 1990 August 21–22. The workshop was organized on short notice and was held less than 2 months after the spherical aberration in the Hubble Space Telescope's mirror was discovered. Consequently, relatively little real HST data were available for restoration experiments, and only a few of the workshop participants had access even to that data. Nevertheless, the papers in this volume cover the issues, problems, and techniques quite well and give an indication of directions for future research. Many of the participants have subsequently obtained HST data and have been further studying the problem; we expect that this is only the first in a series of workshops on this topic and that future workshops will have more results of direct relevance to HST.

We have long expected that eventually sophisticated image processing techniques would be applied to HST data; the presence of spherical aberration in HST has pushed us into the restoration game with a vengeance! If there is a bright side to this problem, it is that it may lead astronomers to become more knowledgable about the uses and limits of image restoration methods for a wide range of astronomical data analysis problems.

The Problem

The HST primary mirror is too flat. The difference Δ between the designed mirror surface and the actual surface varies as $\Delta = 2.3\,\mu\mathrm{m}\,(r/R)^4$, where r is the radial distance from the center of the mirror and $R = 1.2$ m is the radius of the mirror. This error leads to an optical path length error twice as large; the minimum resulting wavefront RMS error is 0.5 waves at $\lambda = 5000$ Å. This error has been determined independently from measurements in orbit and from the flawed ground test equipment which was used to figure the mirror. The measurements currently differ by 10%, but the difference seems to be due to aberrations within the Wide Field/Planetary Camera used to make the measurments, so there is relatively little uncertainty about the nature of problem.

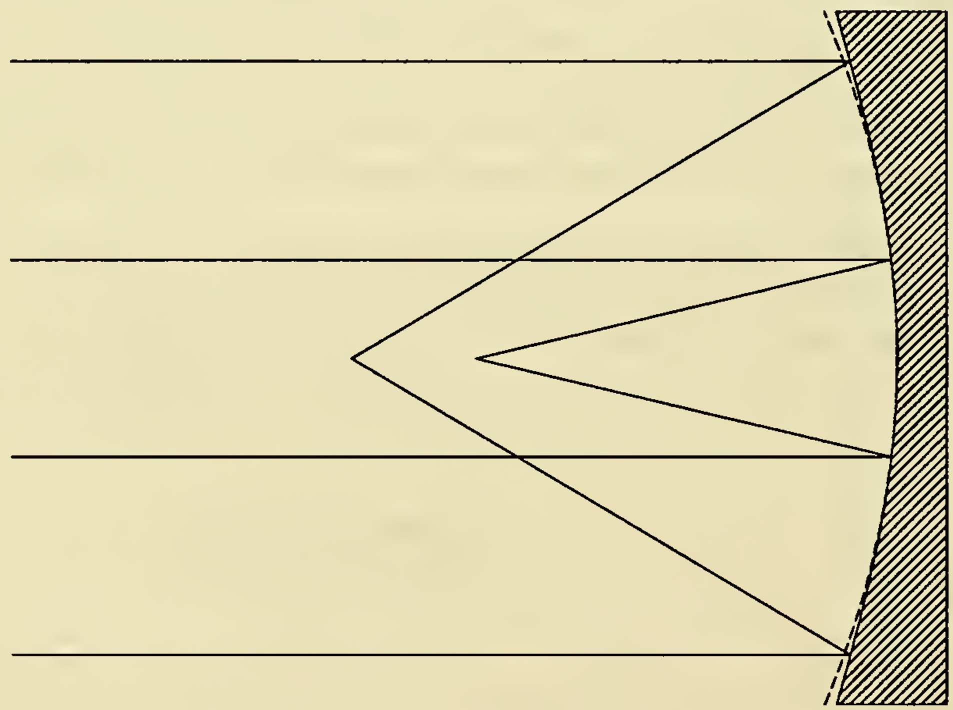

Figure 1. Schematic optical diagram showing effect of spherical aberration on paraxial and marginal rays. Desired surface shape is shown with dashed line.

As a consequence of this aberration, light reflected from the center of the HST primary mirror ("paraxial" rays) does not focus at the same point as light reflected from the edge of the mirror ("marginal" rays). The marginal focus is about 4 cm beyond the paraxial

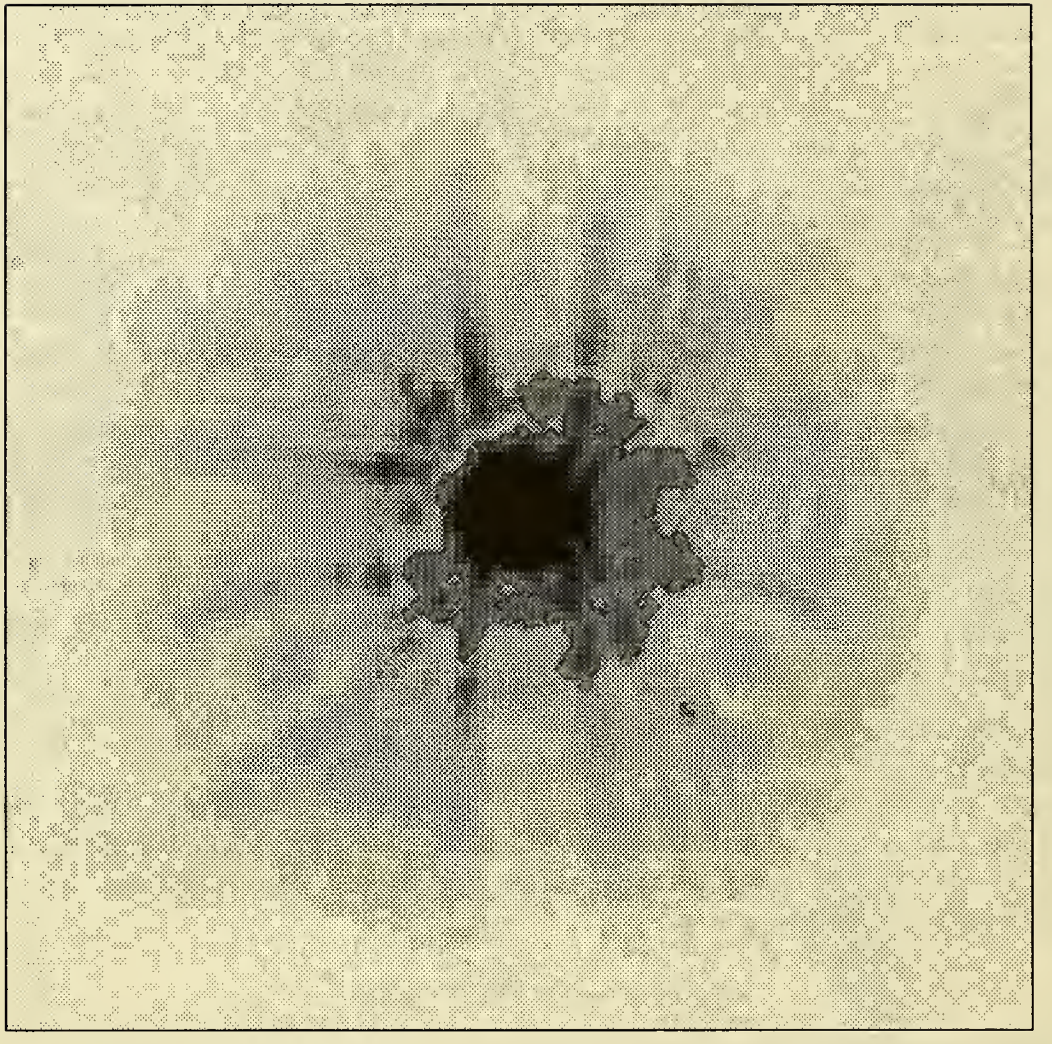

Figure 2. Grey scale representation of a bright star obtained on 15 July 1990 with the Planetary Camera. The field of view of this 200 pixels square sub-image is 8.6 × 8.6 arcsec.

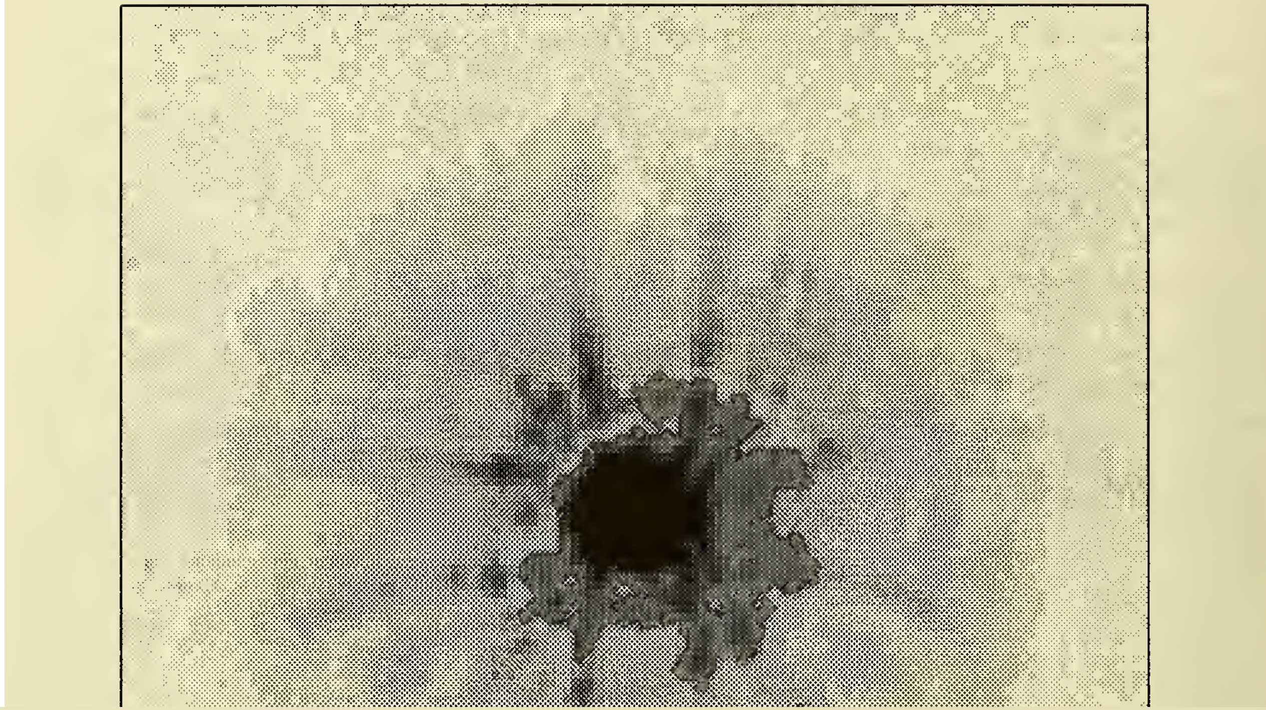

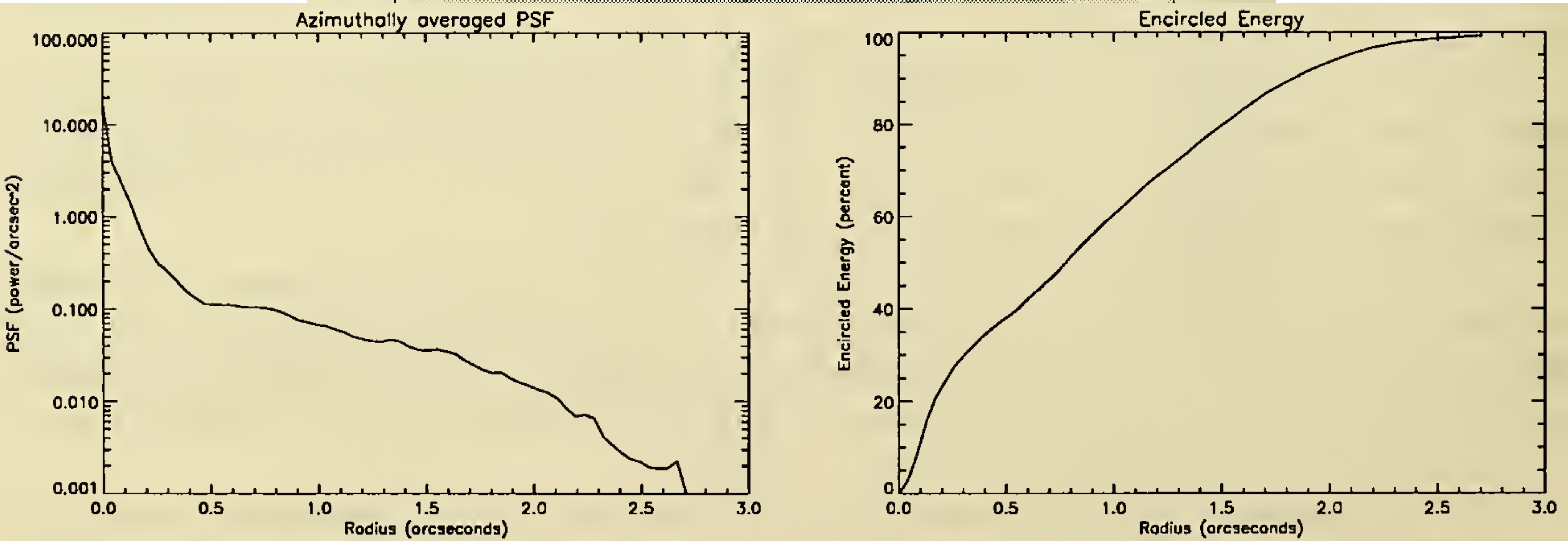

Figure 3. The encircled energy and intensity profile of the star in Figure 2 out to a radius of 4 arcsec.

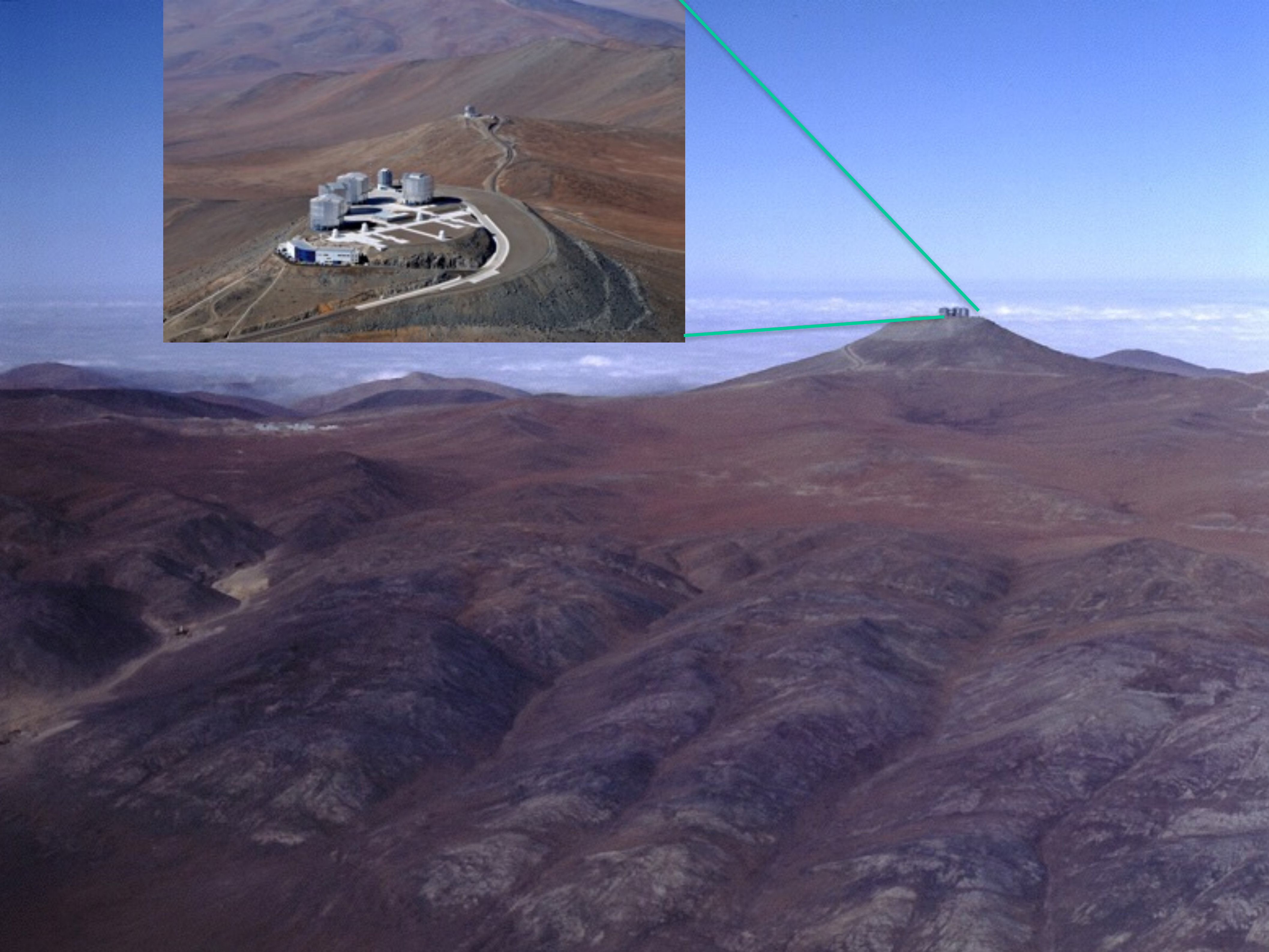

Adaptive Optics imaging

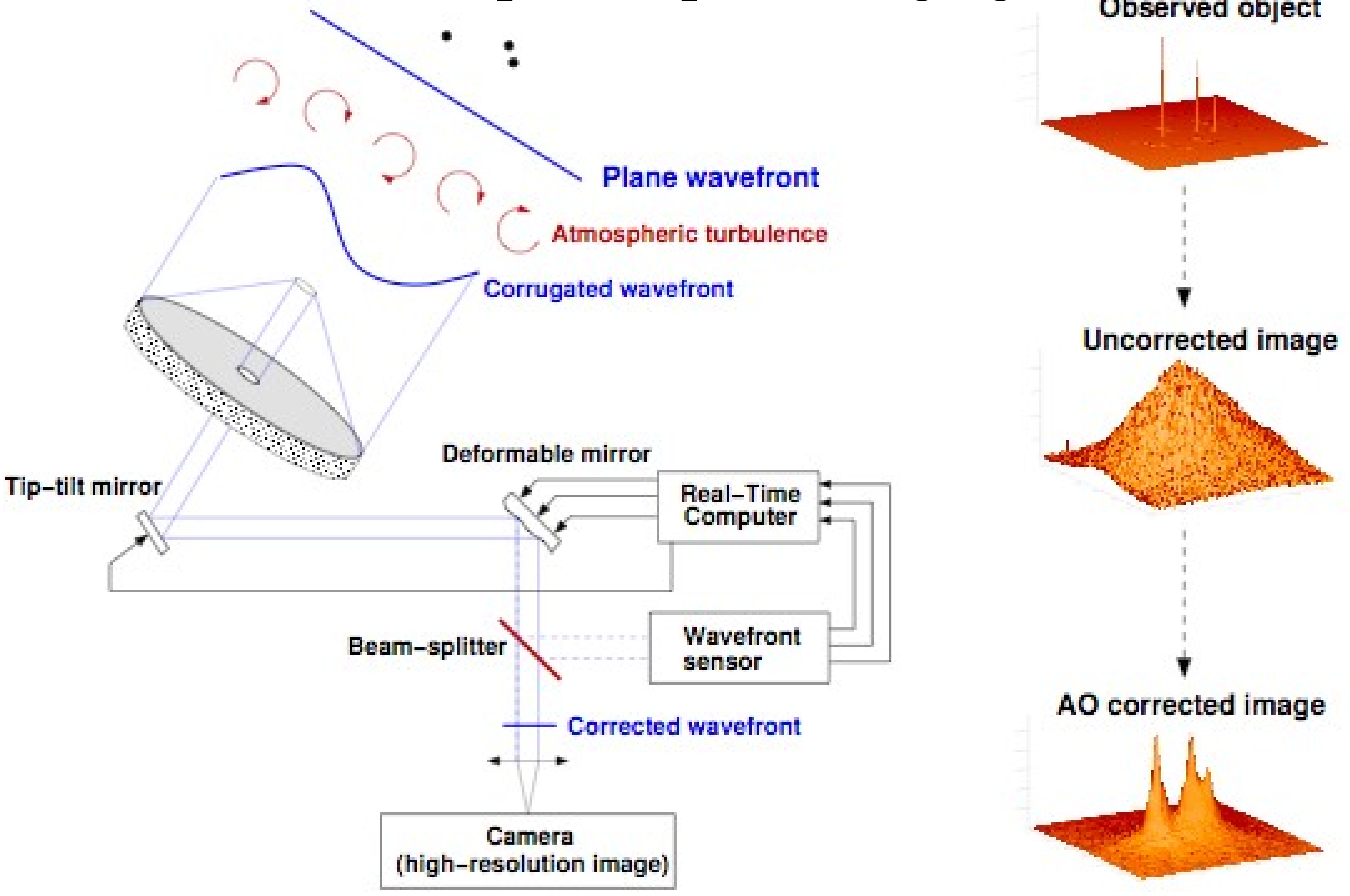

Figure 3-1: Principle of Adaptive Optics

VLT/NACO User manual

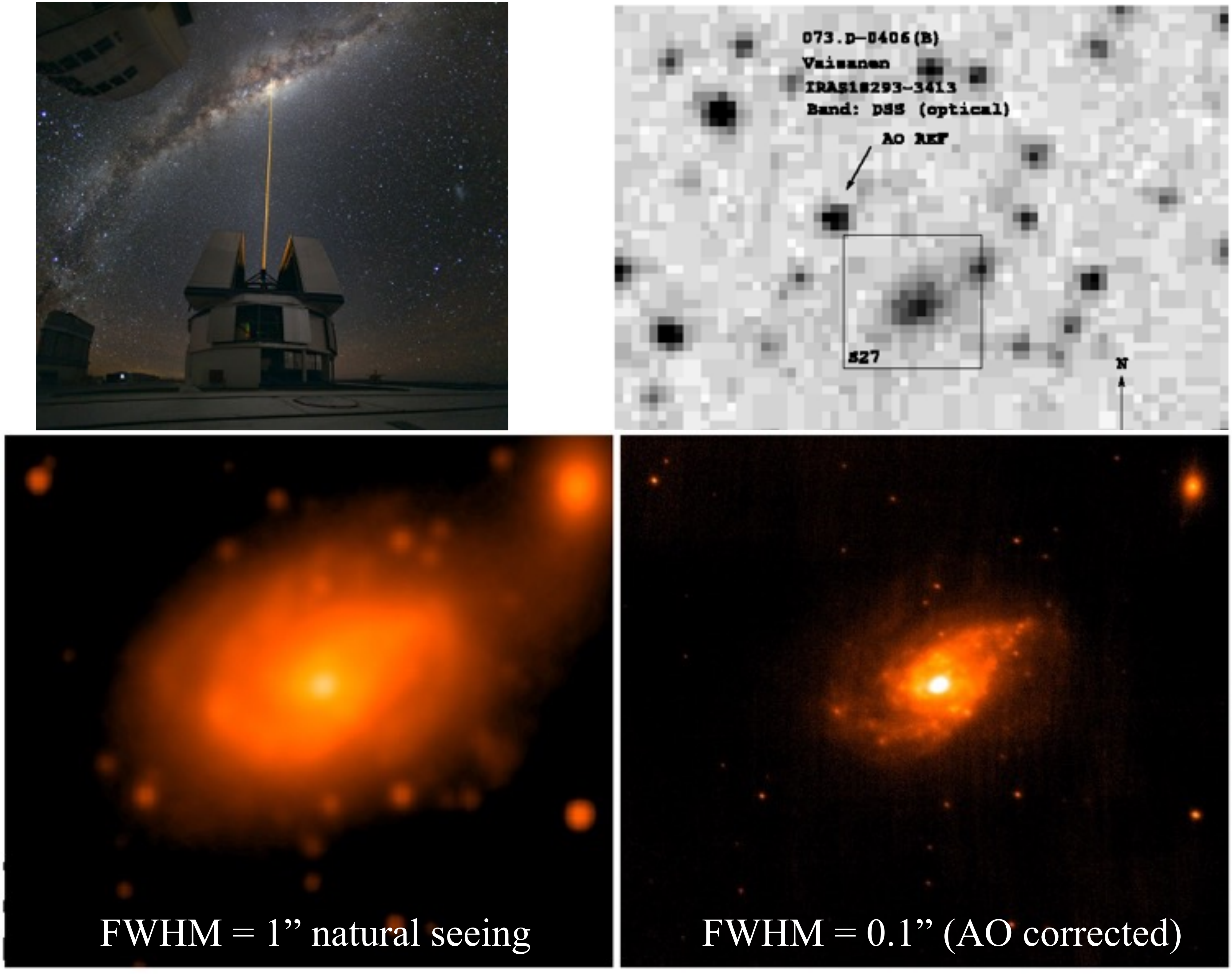
073.D-0406(B)
Vaisanen
IRAS18293-3413
Band: DSS (optical)
AO REF
S27
N
FWHM = 1” natural seeing
FWHM = 0.1” (AO corrected)

Deconvolution

We have observed data *I* (intensity distribution) corresponding to an observation of a "real image" O through an imaging system characterised by the PSF *P* and additive noise *N*.

$$I(x,y) = \int_{x_1=-\infty}^{+\infty}\int_{y_1=-\infty}^{+\infty} P(x-x_1, y-y_1)O(x_1,y_1)dx_1dy_1$$

$$+ \ N(x,\ y)$$

$$= (P * O)(x,\ y) + N(x,\ y),$$

The Convolution Theorem: Convolution in either domain is equivalent to multiplication in the other.

In Fourier space:

$$\hat{I}(u,\ v) = \hat{O}(u,\ v)\hat{P}(u,\ v) + \hat{N}(u,\ v).$$

Starck, Pantin & Murtagh 2002: Deconvolution in Astronomy

Deconvolution

In Fourier space:

$$\hat{I}(u, v) = \hat{O}(u, v)\hat{P}(u, v) + \hat{N}(u, v).$$

$$\frac{\hat{I}(u, v)}{\hat{P}(u, v)} = \hat{O}(u, v) + \frac{\hat{N}(u, v)}{\hat{P}(u, v)} .$$

This method, sometimes called the *Fourier-quotient method*, is very fast. We need to do only a Fourier transform and an inverse Fourier transform. However, in the presence of noise, this method cannot be used.

Starck, Pantin & Murtagh 2002: Deconvolution in Astronomy

THE ASTRONOMICAL JOURNAL VOLUME 79, NUMBER 6 JUNE 1974

An iterative technique for the rectification of observed distributions

L. B. Lucy*

Departments of Physics and Astronomy, The University of Pittsburgh, Pittsburgh, Pennsylvania 15213

(Received 15 January 1974; revised 26 March 1974)

An iterative technique is described for generating estimates to the solutions of rectification and deconvolution problems in statistical astronomy. The technique, which derives from Bayes' theorem on conditional probabilities, conserves the constraints on frequency distributions (i.e., normalization and non-negativeness) and, at each iteration, increases the likelihood of the observed sample. The behavior of the technique is explored by applying it to problems whose solutions are known in the limit of infinite sample size, and excellent results are obtained after a few iterations. The astronomical use of the technique is illustrated by applying it to the problem of rectifying distributions of $v \sin i$ for aspect effect; calculations are also reported illustrating the technique's possible use for correcting radio–astronomical observations for beam-smoothing. Application to the problem of obtaining unbiased, smoothed histograms is also suggested.

Application of the Richardson-Lucy algorithm in astronomy

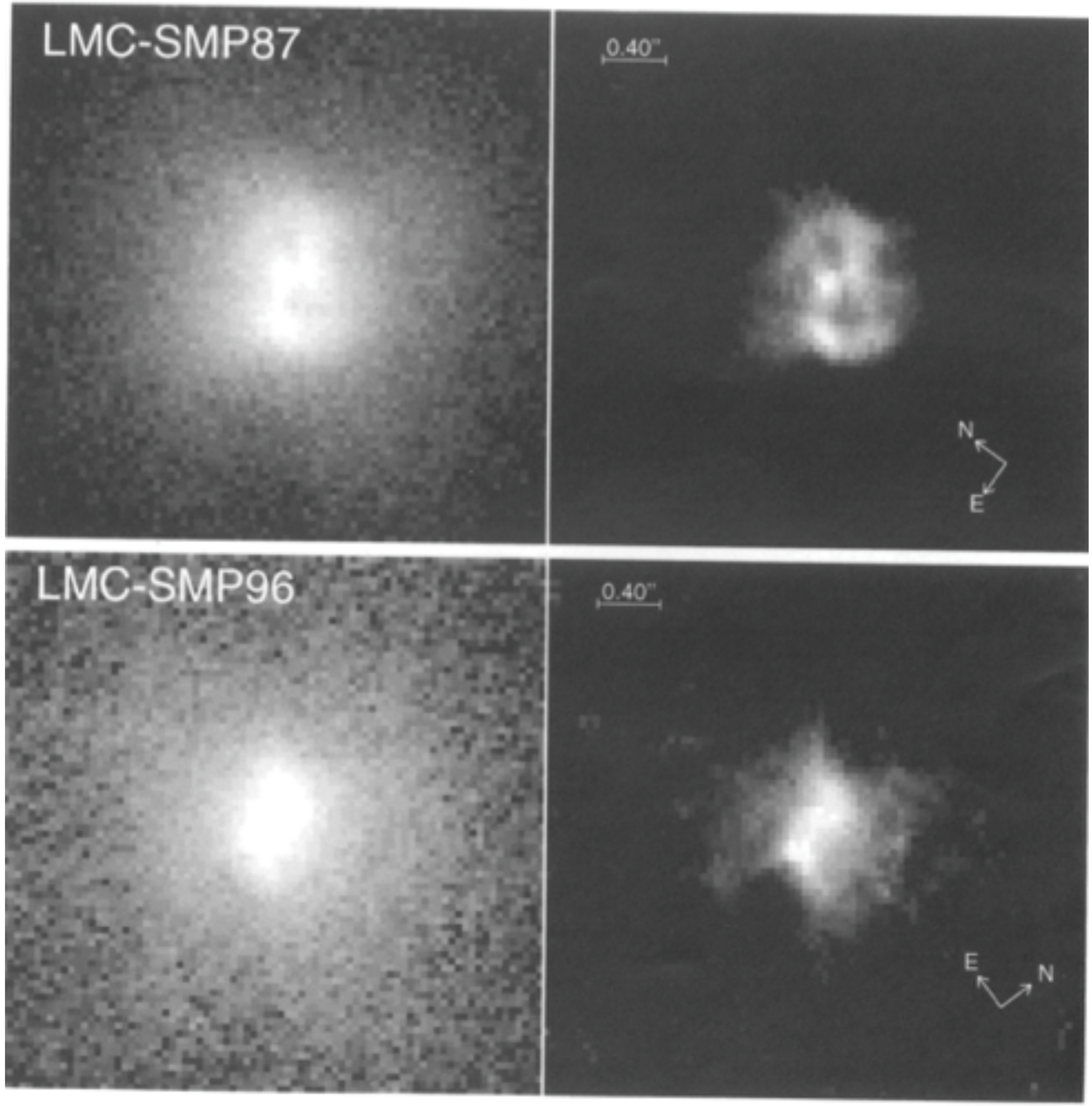

Dopita et al. 1996: Hubble Space Telescope Observations of Planetary Nebulaea

Application of the Richardson-Lucy algorithm to medical images

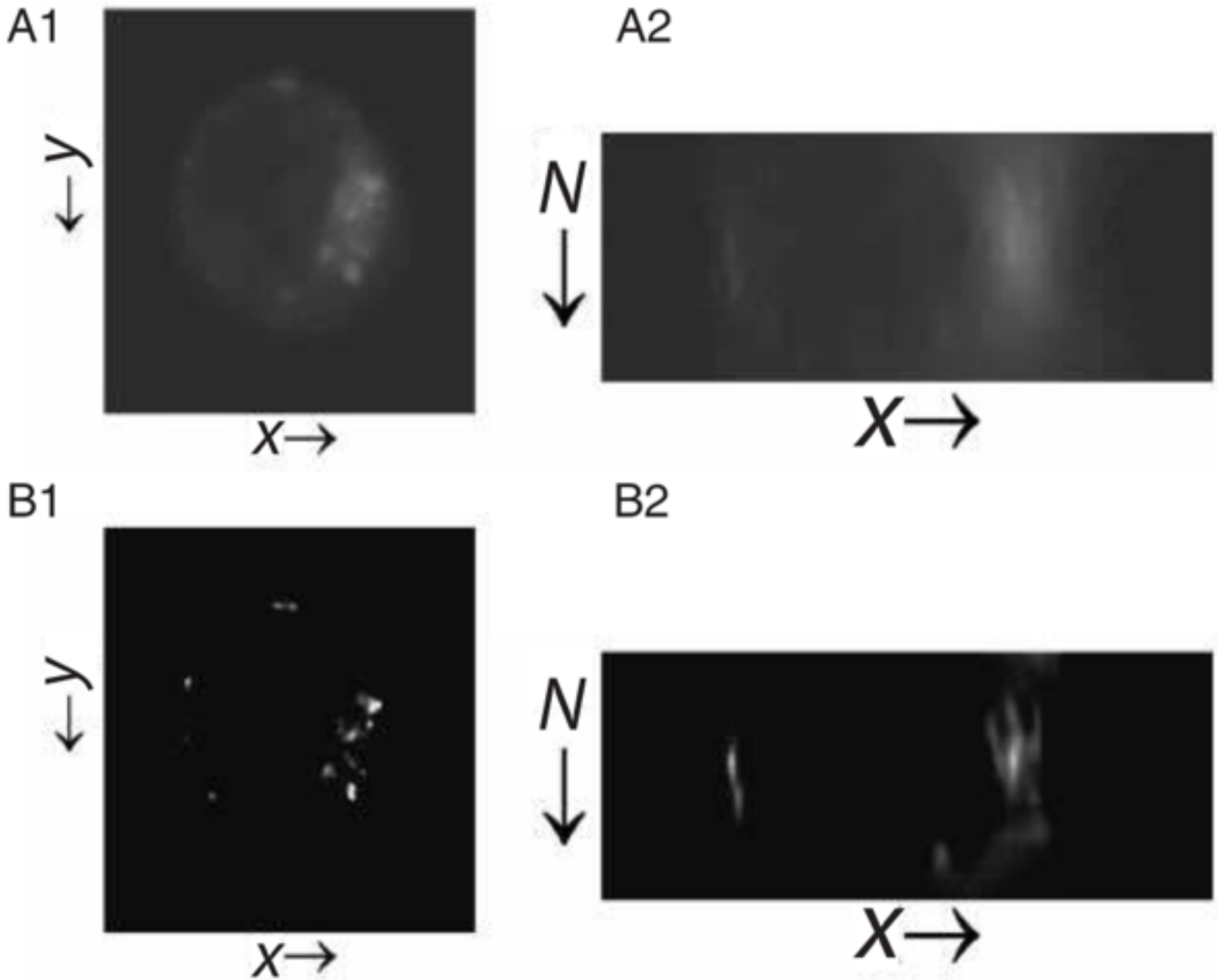

Lai et al. 2003, Journal of Microscopy

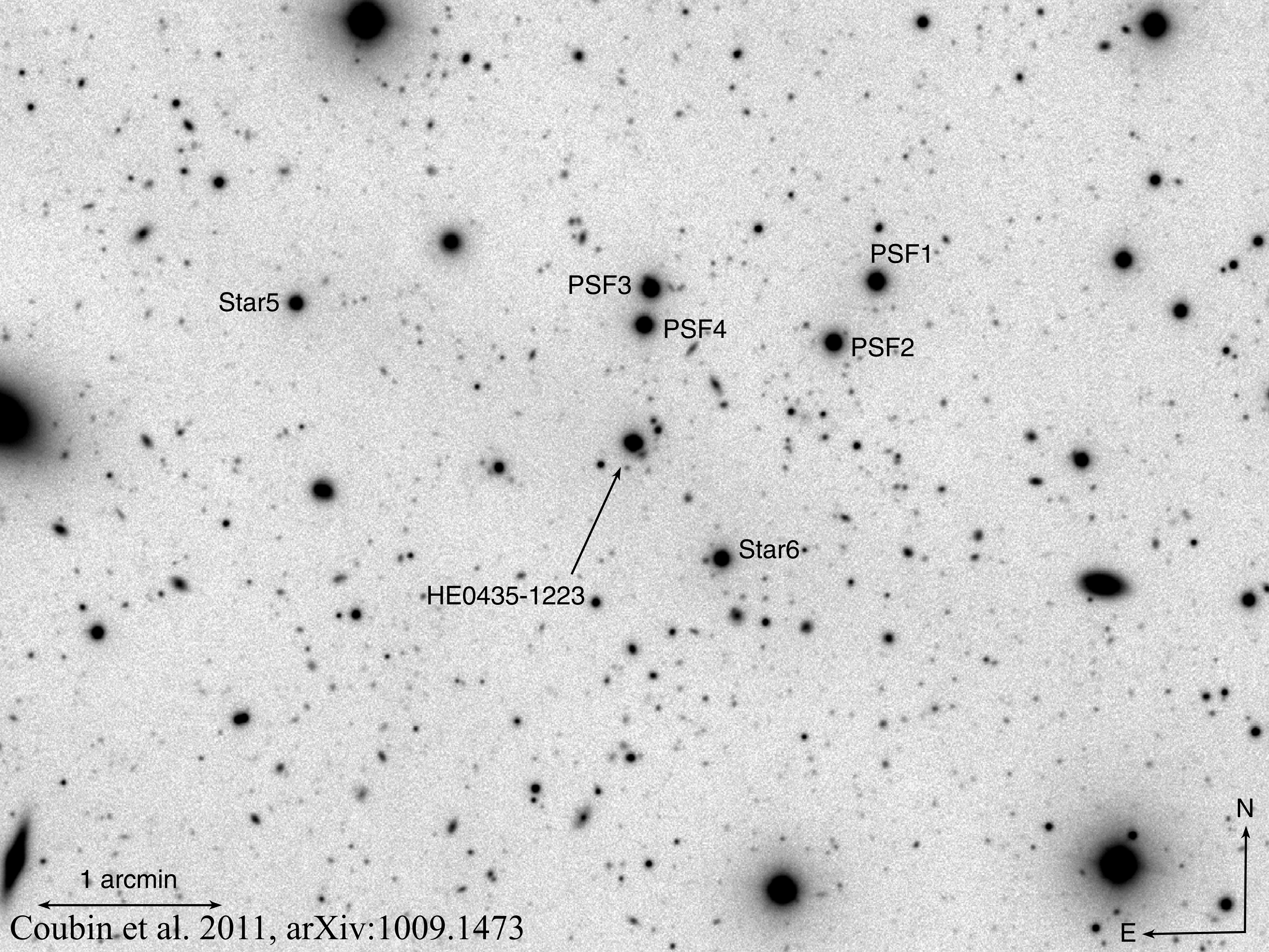

Coubin et al. 2011, arXiv:1009.1473

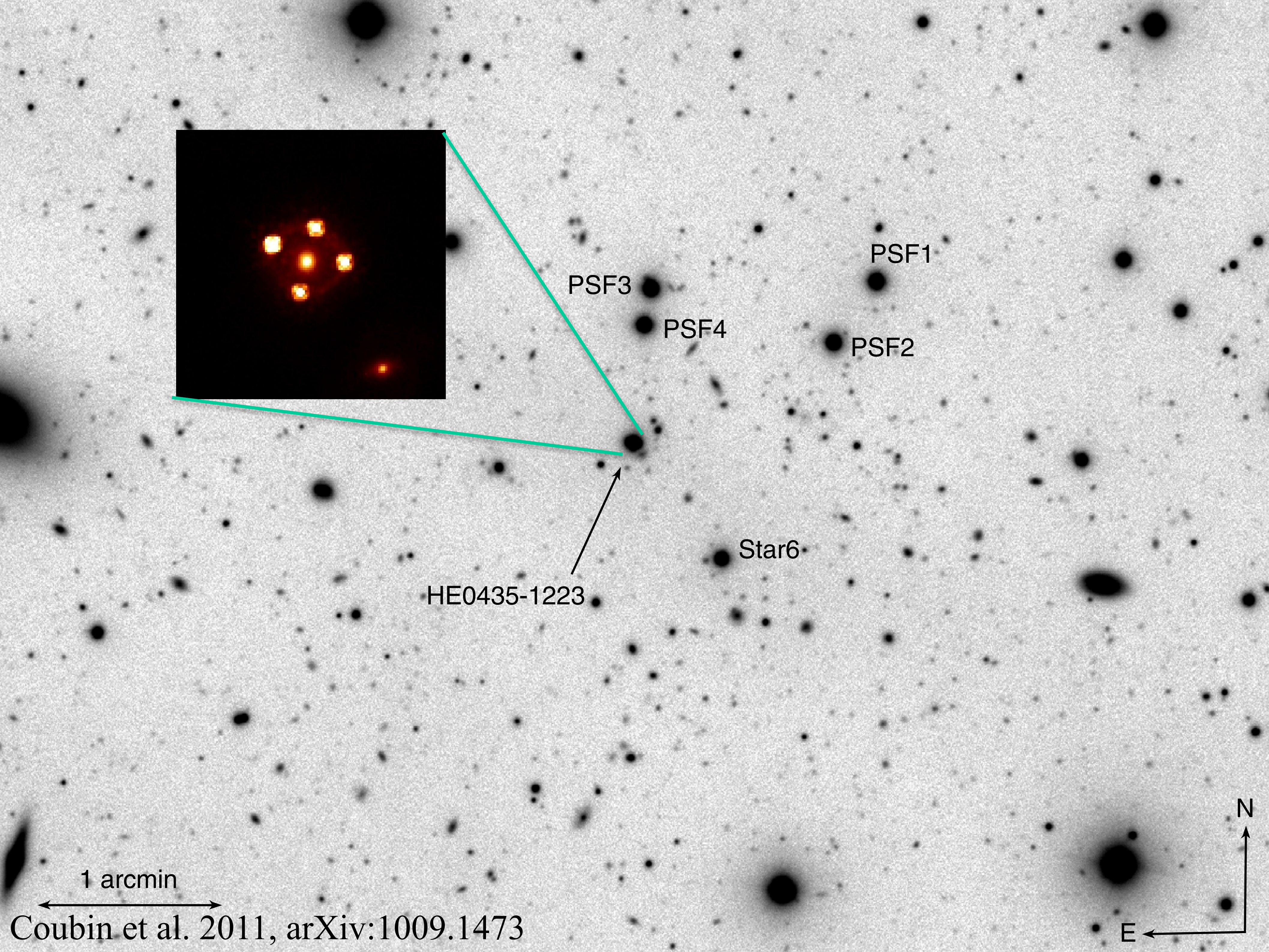
PSF1
PSF3
PSF4
PSF2
Star6
HE0435-1223
N
E
1 arcmin
Coubin et al. 2011, arXiv:1009.1473

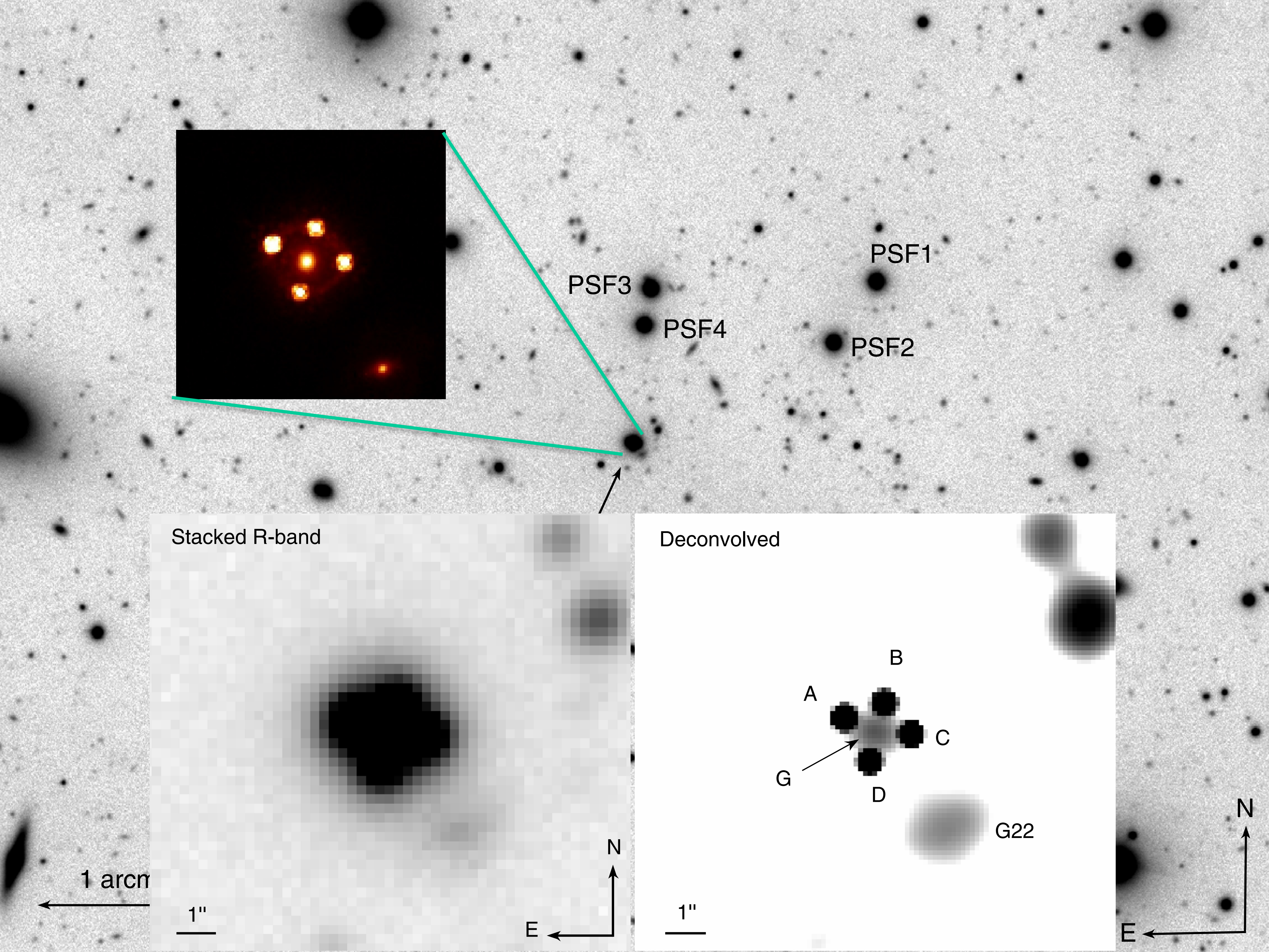
PSF1
PSF2
PSF3
PSF4
Stacked R-band
Deconvolved
A
B
C
D
G
G22
1"
1"
N
E
N
E
1 arcm

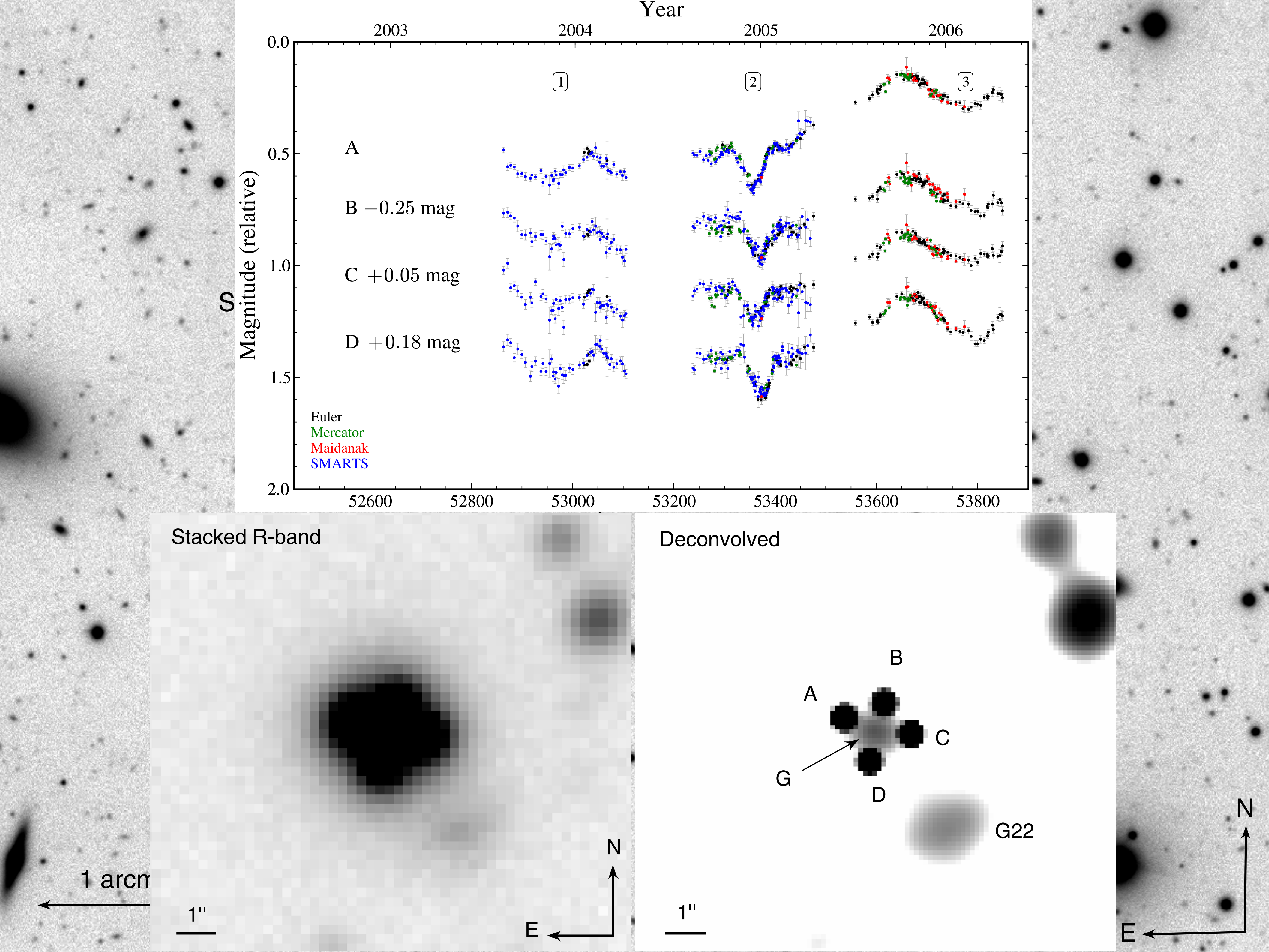
Year
2003
2004
2005
2006
Magnitude (relative)
1
2
3
A
B −0.25 mag
C +0.05 mag
D +0.18 mag
Euler
Mercator
Maidanak
SMARTS
0.0
0.5
1.0
1.5
2.0
52600
52800
53000
53200
53400
53600
53800
Stacked R-band
Deconvolved
A
B
C
D
G
G22
N
E
1"
1 arcm

Astronomical spectroscopy

Spectroscopic observations

- Determine the flux density as a function of wavelength (spectral energy distribution, spectral lines, physical conditions, velocities etc.)
- Use a mask with a narrow aperture (slit) to cut the 2D image to 1D
- Use a diffraction grating (or a grism) to disperse the incident light beam into spectrum
- Spectrographs use an imaging device (CCD) to record the dispersed light

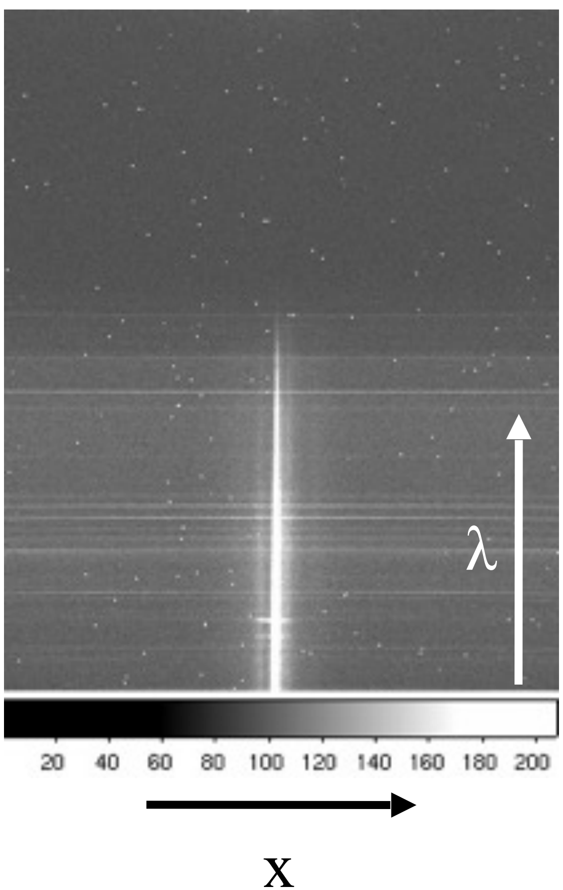

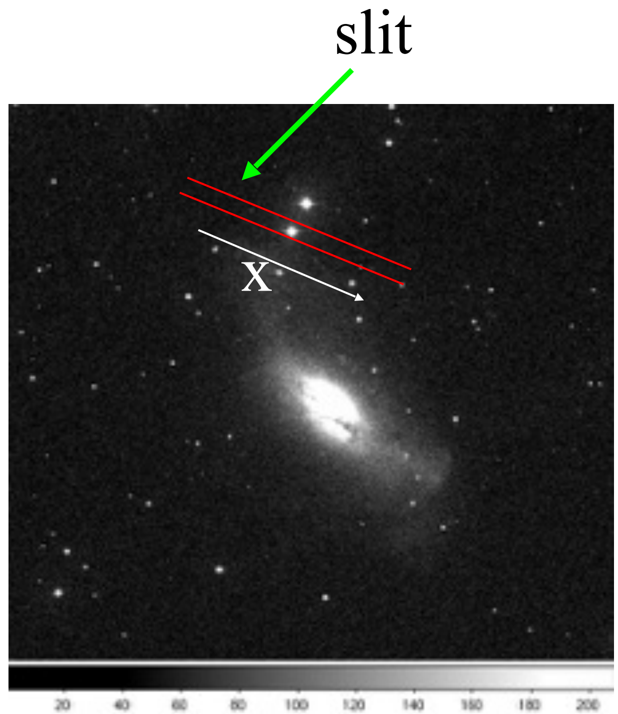

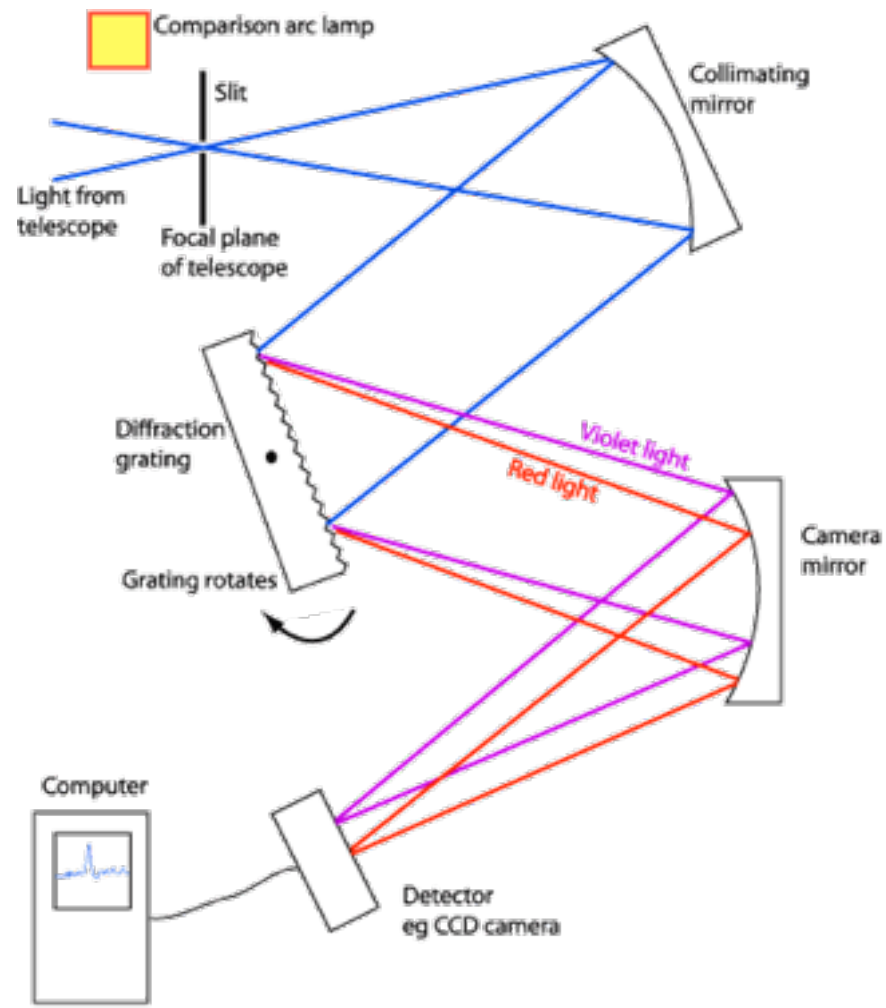

Spectroscopic observations

- Determine the flux density as a function of wavelength (spectral energy distribution, spectral lines, physical conditions, velocities etc.)
- Use a mask with a narrow aperture (slit) to cut the 2D image to 1D
- Use a diffraction grating (or a grism) to disperse the incident light beam into spectrum
- Spectrographs use an imaging device (CCD) to record the dispersed light

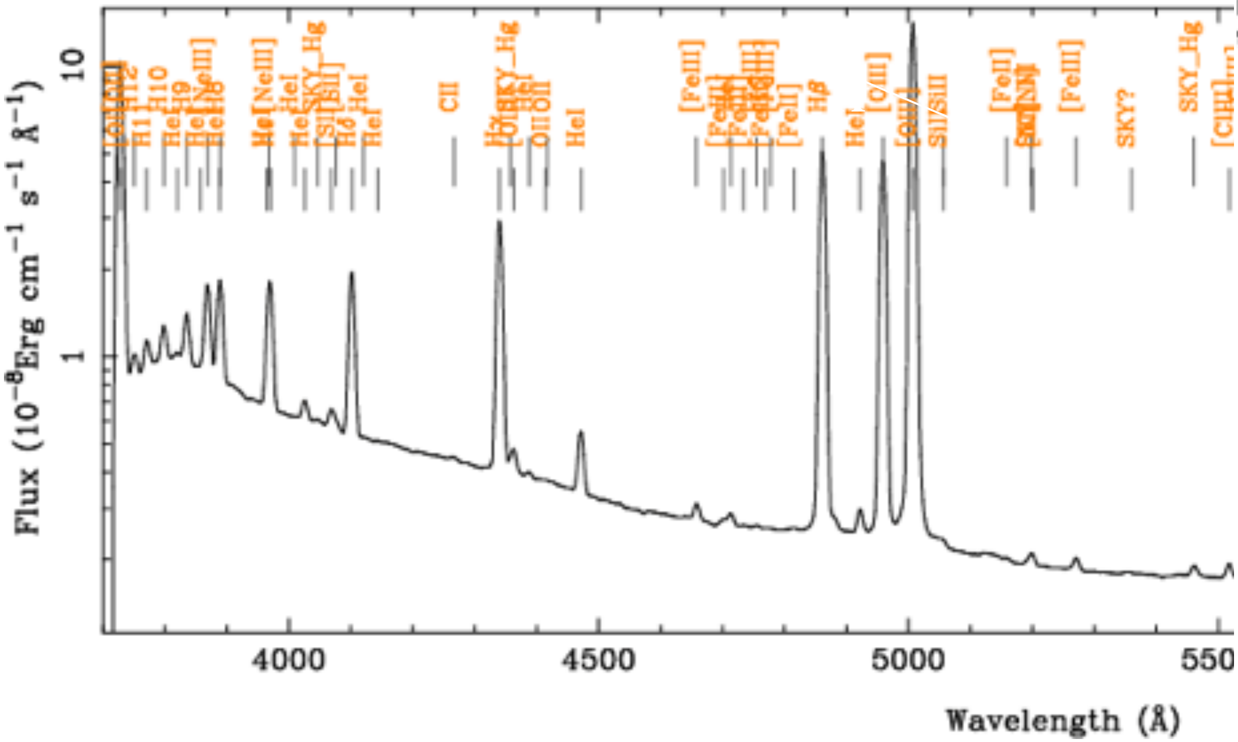

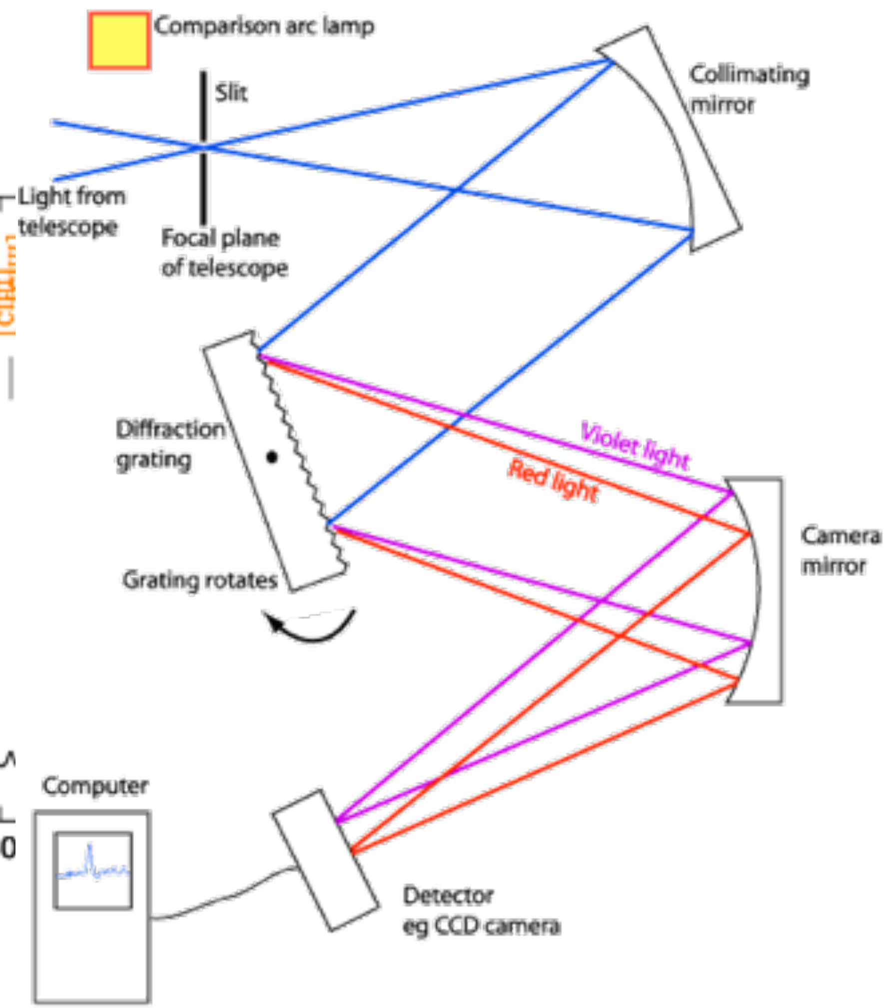

$$a(\sin\alpha - \sin\beta) = m\lambda \qquad m = \ldots, -1, 0, 1, \ldots$$

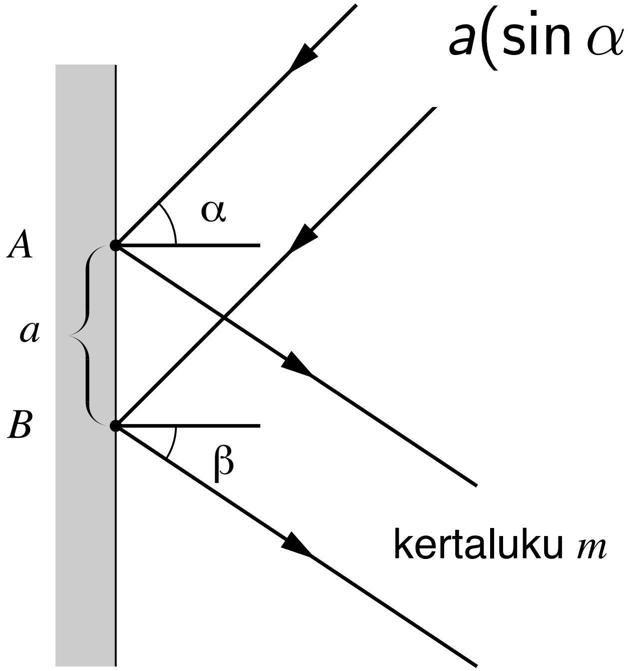

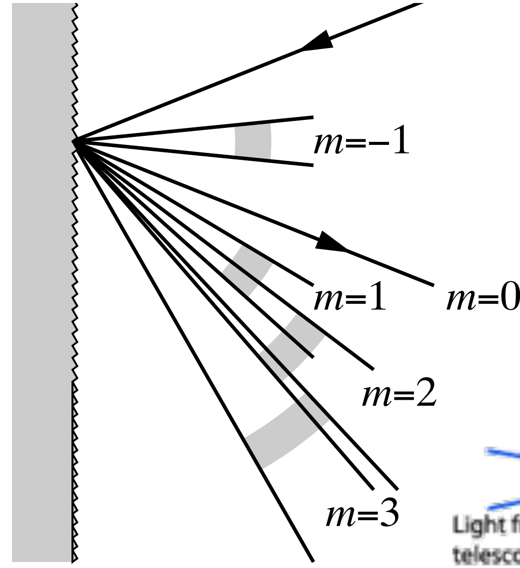

α = angle of incidence
β = angle of diffraction
m = order of diffraction
λ = wavelength
a = grating constant
(distance between successive grooves)

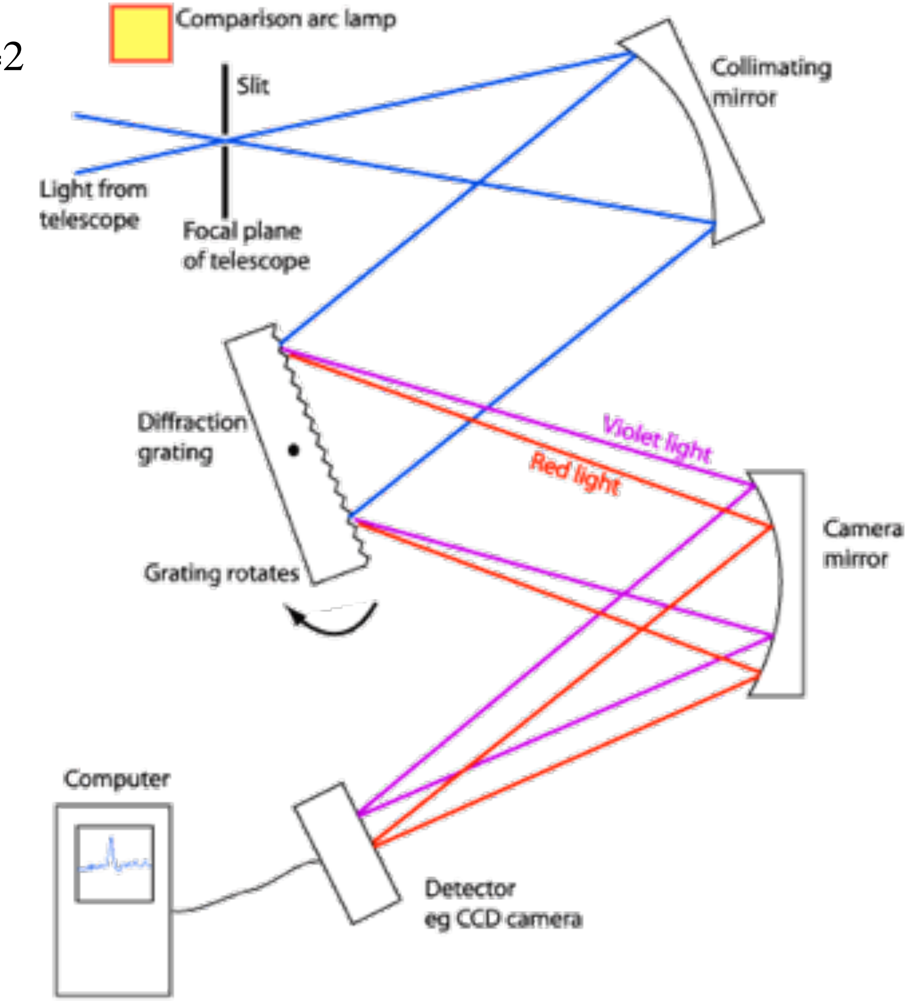

A Schematic Diagram of a Slit Spectrograph

$$a(\sin\alpha - \sin\beta) = m\lambda \qquad m = \dots, -1, 0, 1, \dots$$

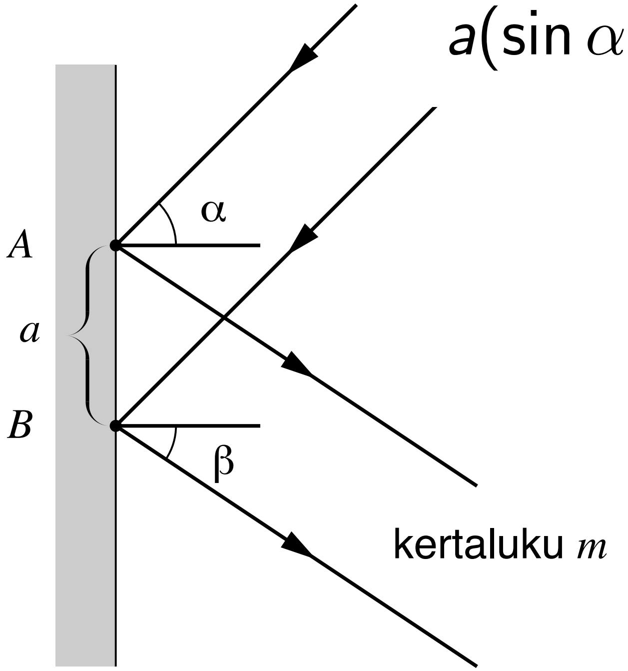

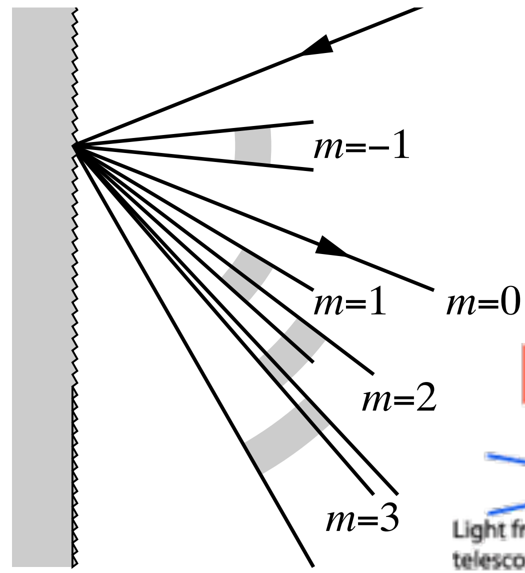

α = angle of incidence
β = angle of diffraction
m = order of diffraction
λ = wavelength
a = grating constant
(distance between successive grooves)

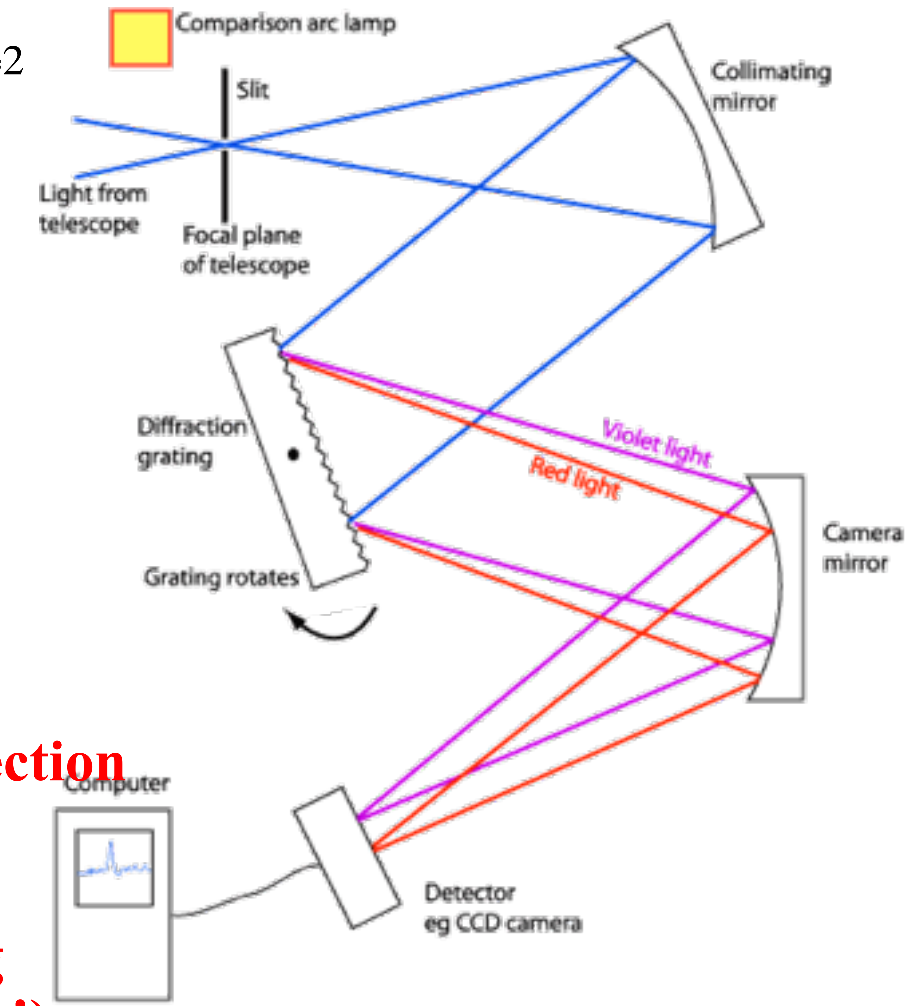

A Schematic Diagram of a Slit Spectrograph

Notes:

m = 0: all wavelengths diffract in the same direction (no spectrum formed!)

Spectra of different orders can overlap causing so called second order contamination (use filter!)

Spectroscopic observations

Spectral resolution $R = N\,m$
where m is the diffraction order and N the total number of grooves

- Resolving power of a spectrograph R = λ / Δλ = c / Δvelocity
- For example
  - Low-resolution R = 500 at 650nm gives Δλ = 1.3nm (600 km/s)
  - High-resolution T = 50 000 gives Δλ = 0.013nm (6 km/s)

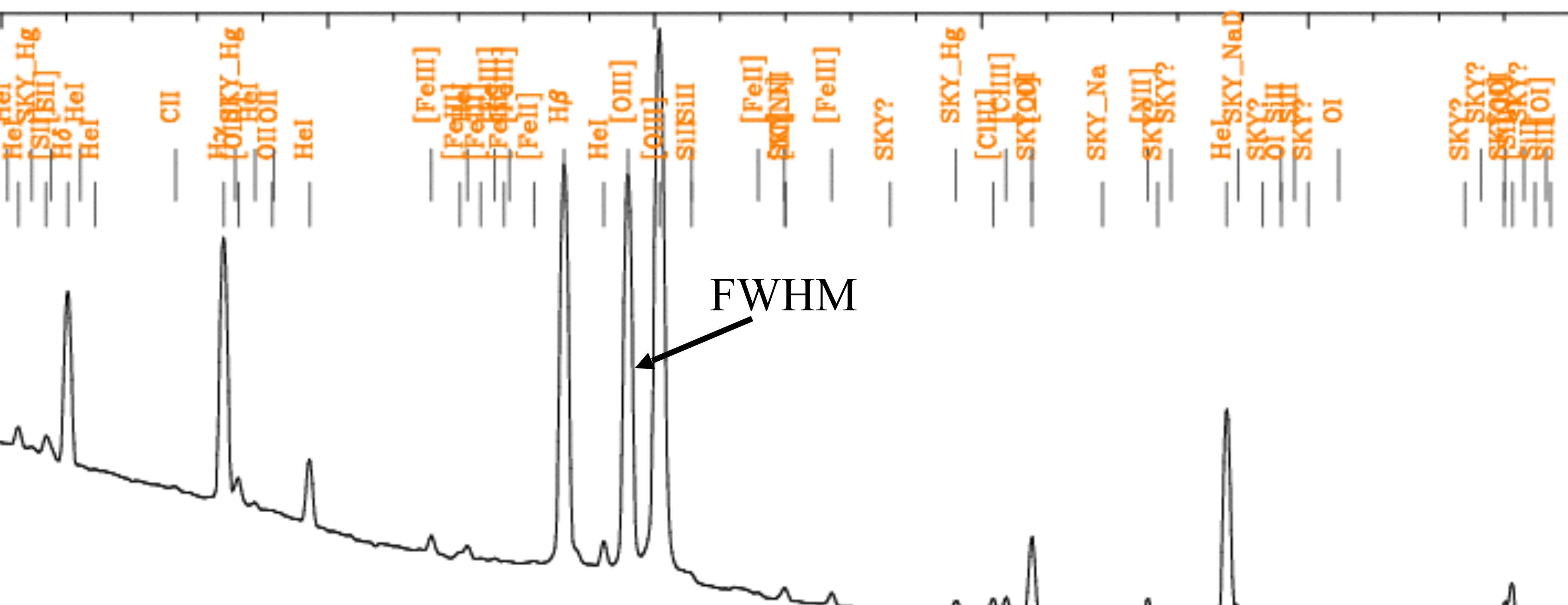

Data reductions: spectroscopy

- Reductions in 2D
  - Correct for CCD bias (and dark current)
  - Correct for detector non-uniformity (and fringes!) – flat fielding
  - Subtract background emission (from sky, host galaxy etc.)
  - Extract the spectrum
- Reductions in 1D
  - Wavelength calibration
    - Use a standard emission line source (arc lamp)
  - Spectrophotometric calibration
    - Use a well-characterised spectrophotometric standard star

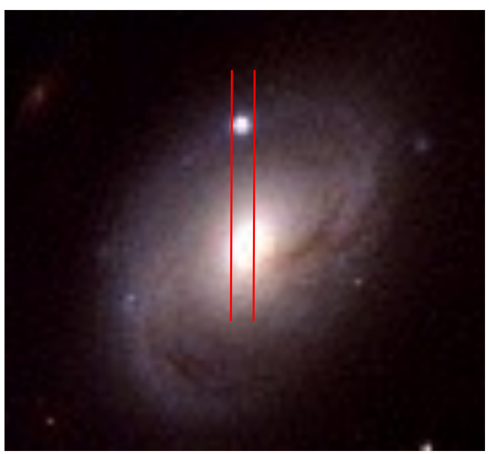

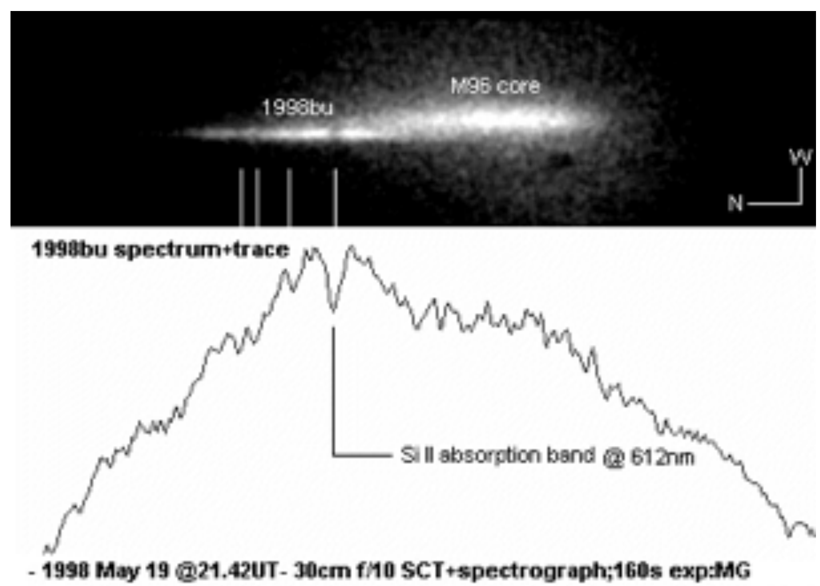

Spectroscopic data

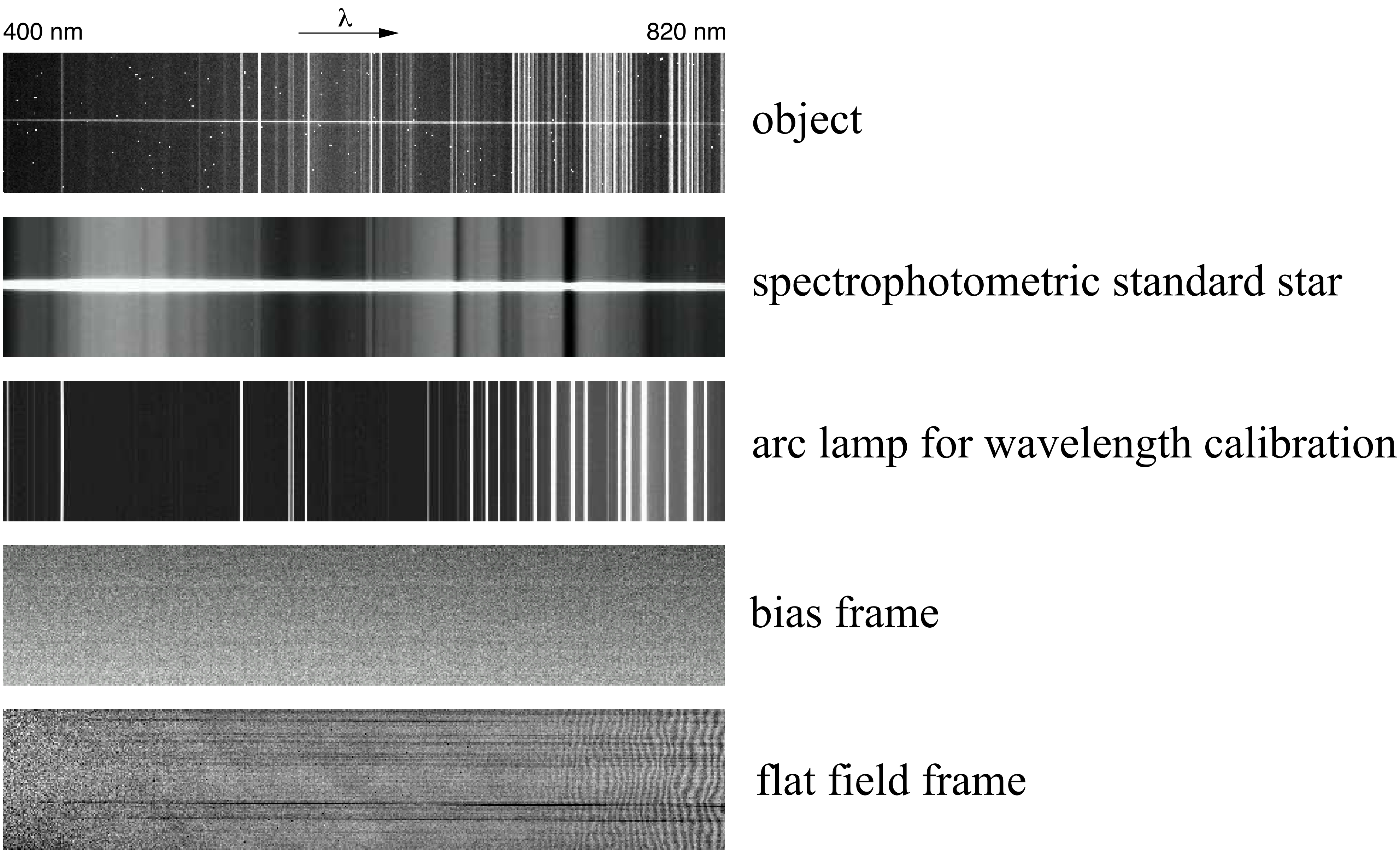

Spectroscopic data

raw object

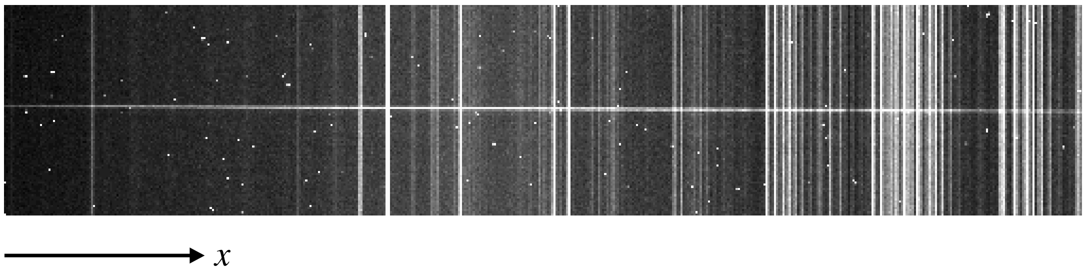

after subtraction of sky background

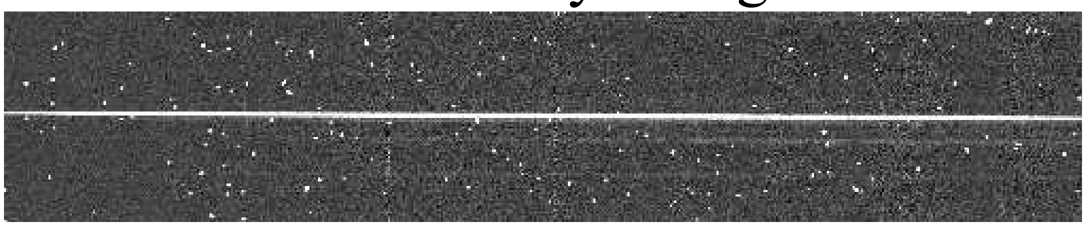

after extraction

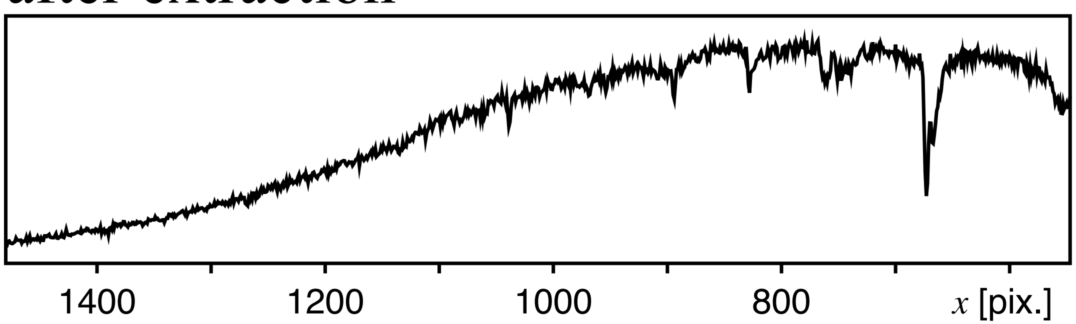

extracted background sky spectrum

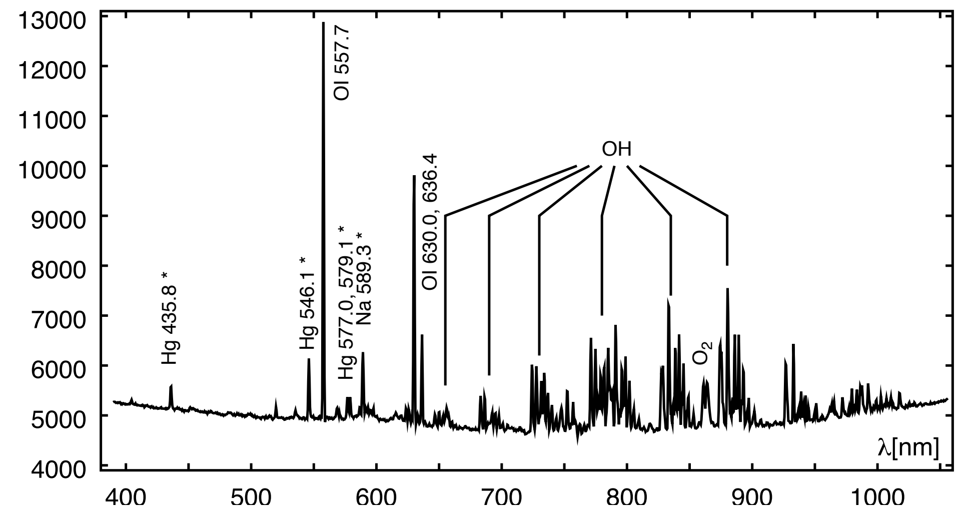

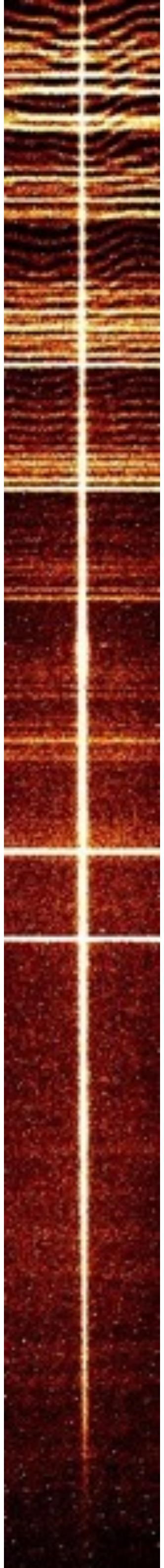

Extraction of the spectrum

- Selecting your extraction aperture
- Fitting the trace of the spectrum
- Fitting the background on both sides of your target
- Extracting the spectrum

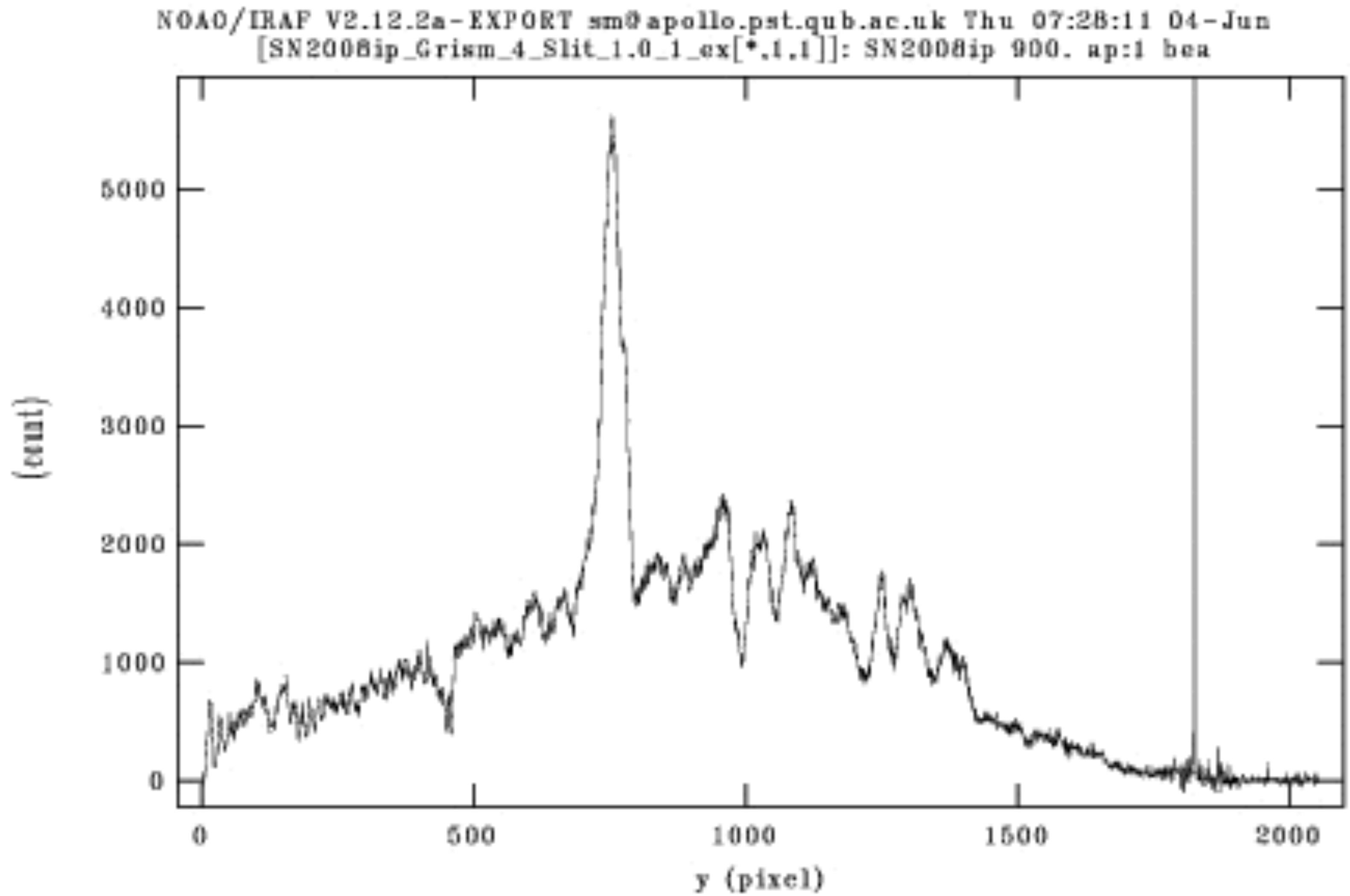

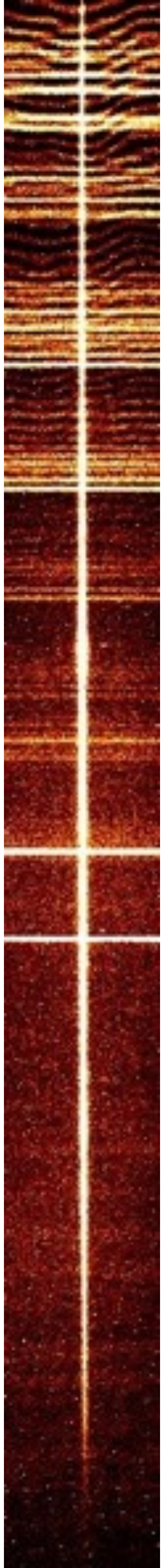

Wavelength calibration

- Identifying the detected arclamp emission lines in observed spectrum
- Measuring their accurate positions
- Fitting a dispersion solution for the spectrum

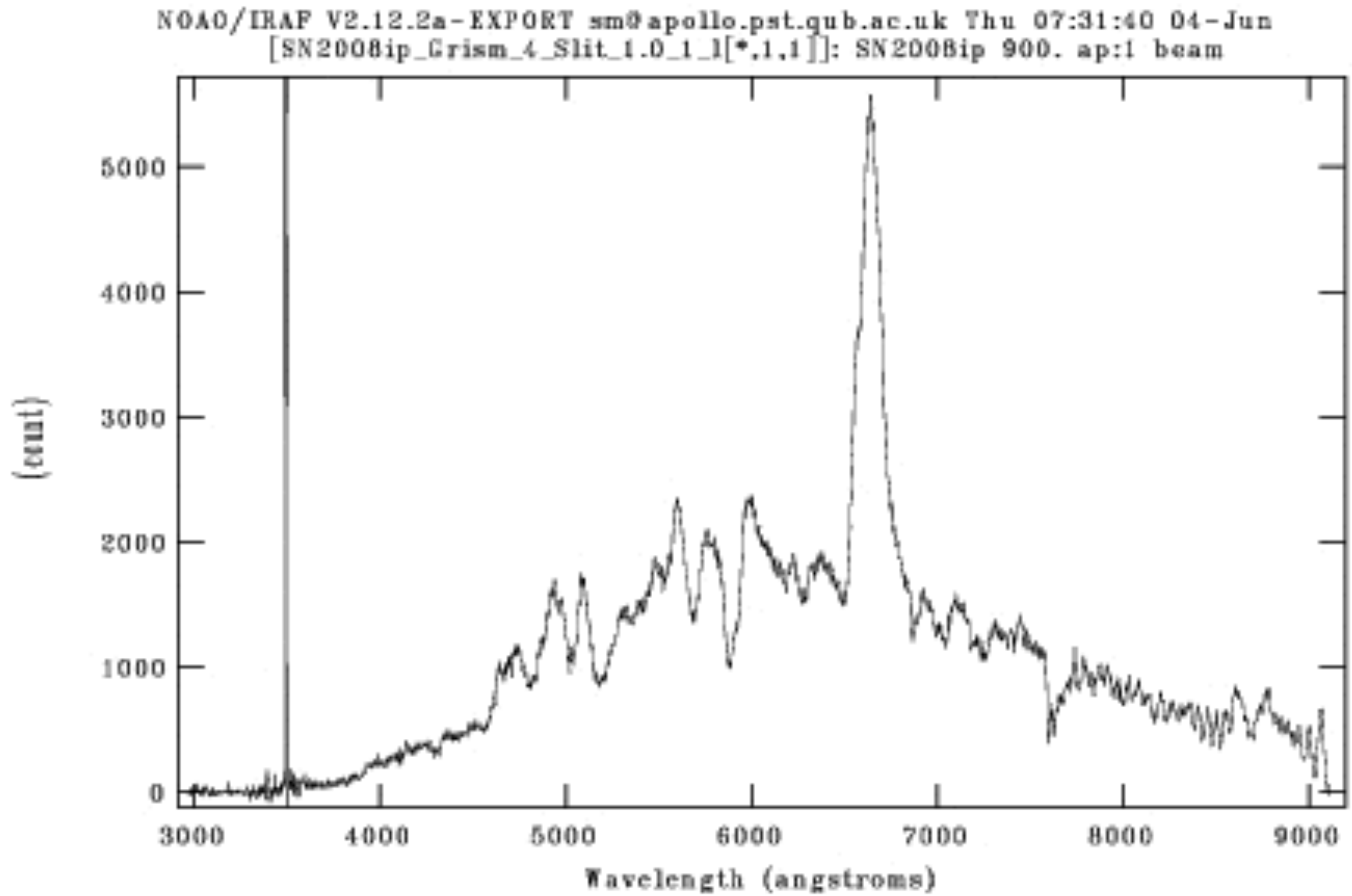

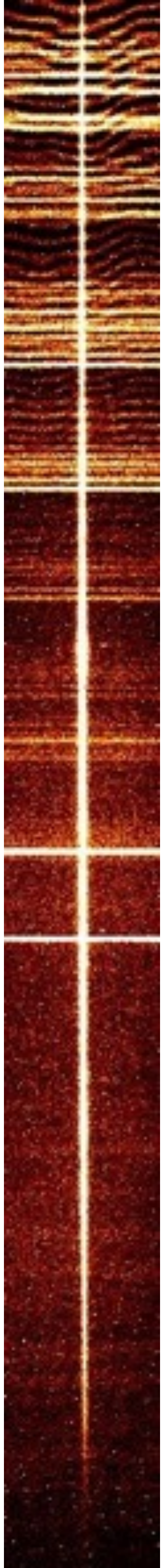

Flux calibration

- Determine the sensitivity function for the observation
- Apply the flux calibration and atmospheric extinction correction for your spectrum

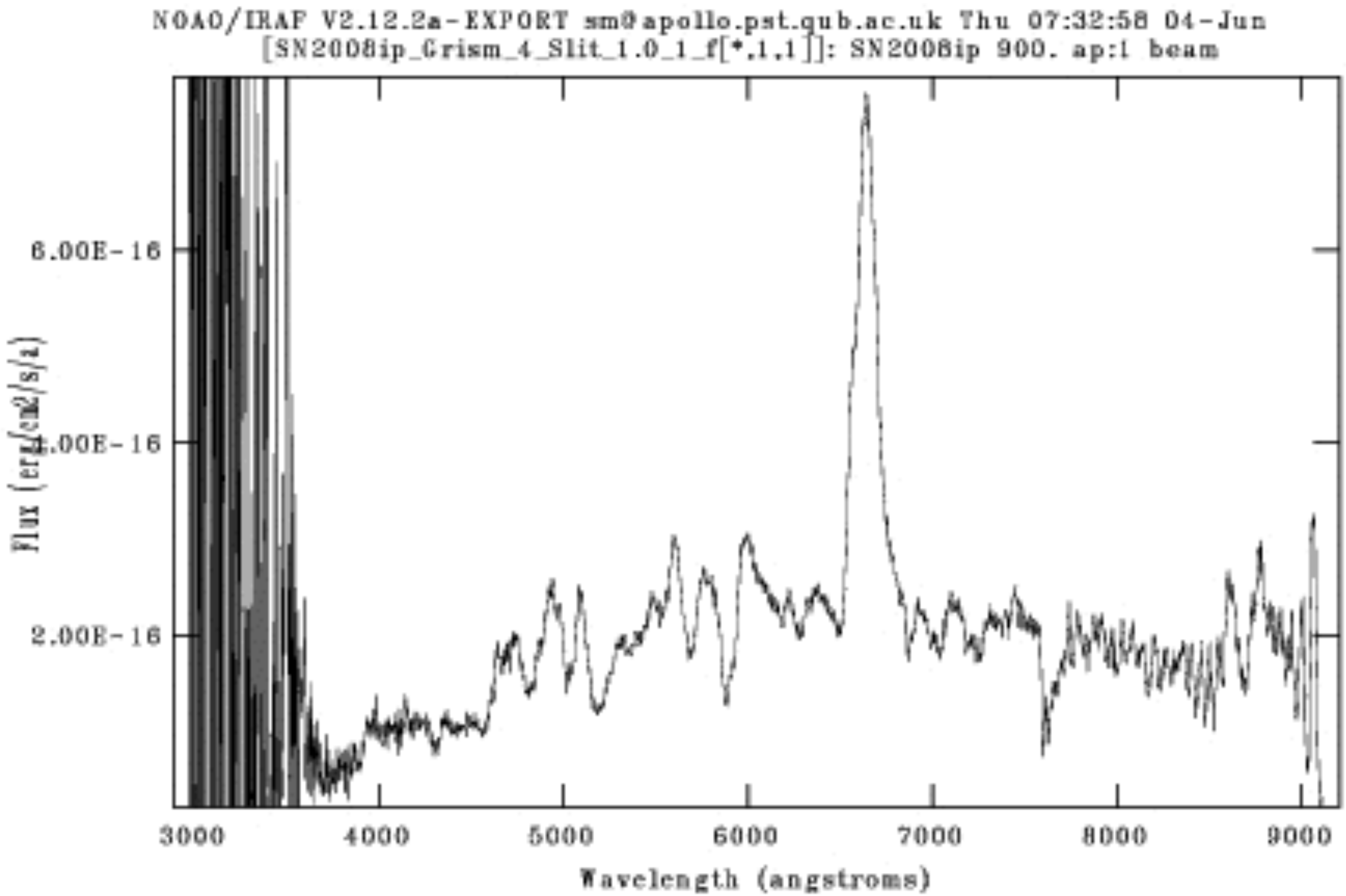

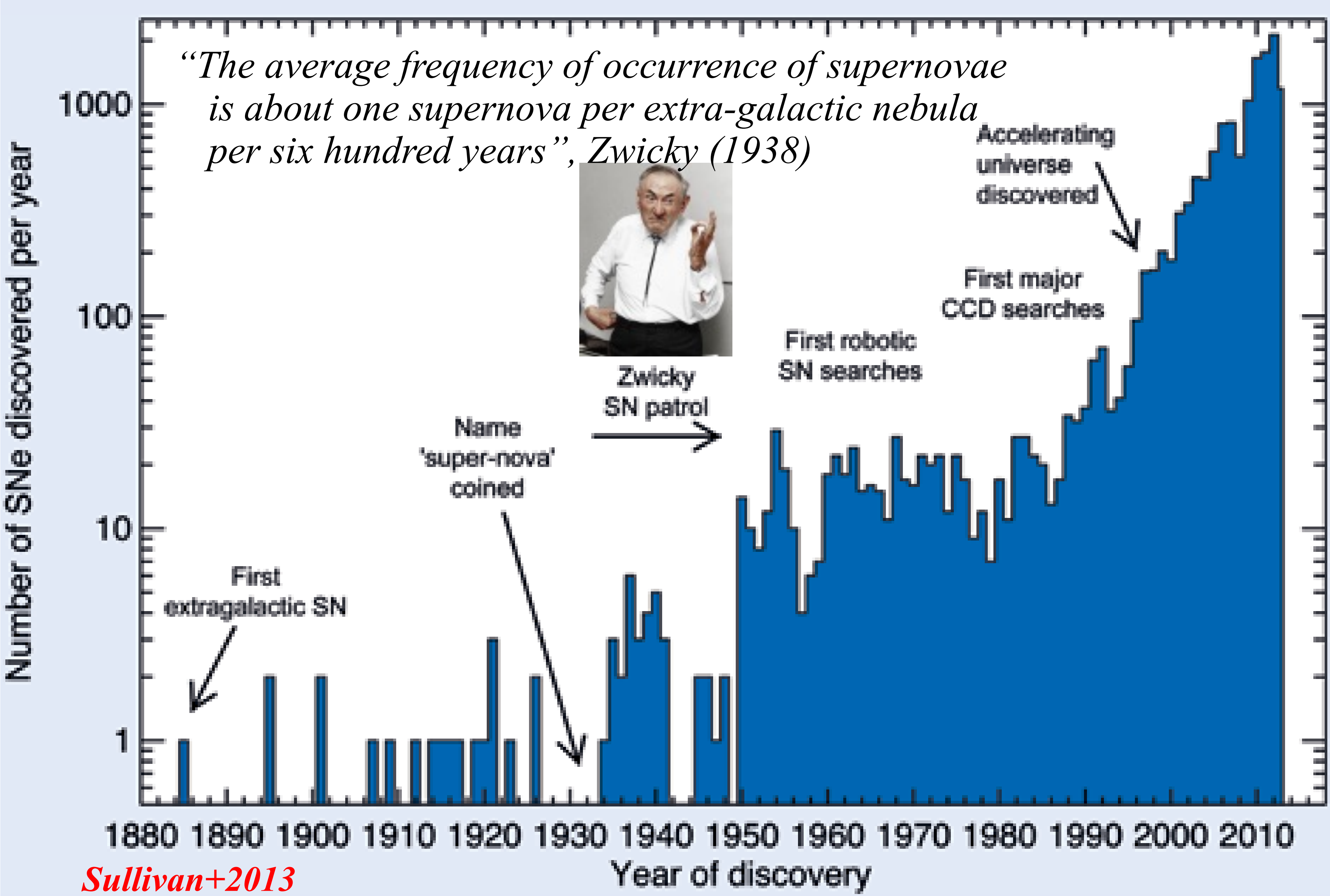

Sullivan+2013

Rudolph Minkowski (1895-197

"Spectroscopic observations indicate at least two types of supernovae. Nine objects form an extremely homogeneous group provisionally called type I"

Rudolph Minkowski (1941)

Supernova types

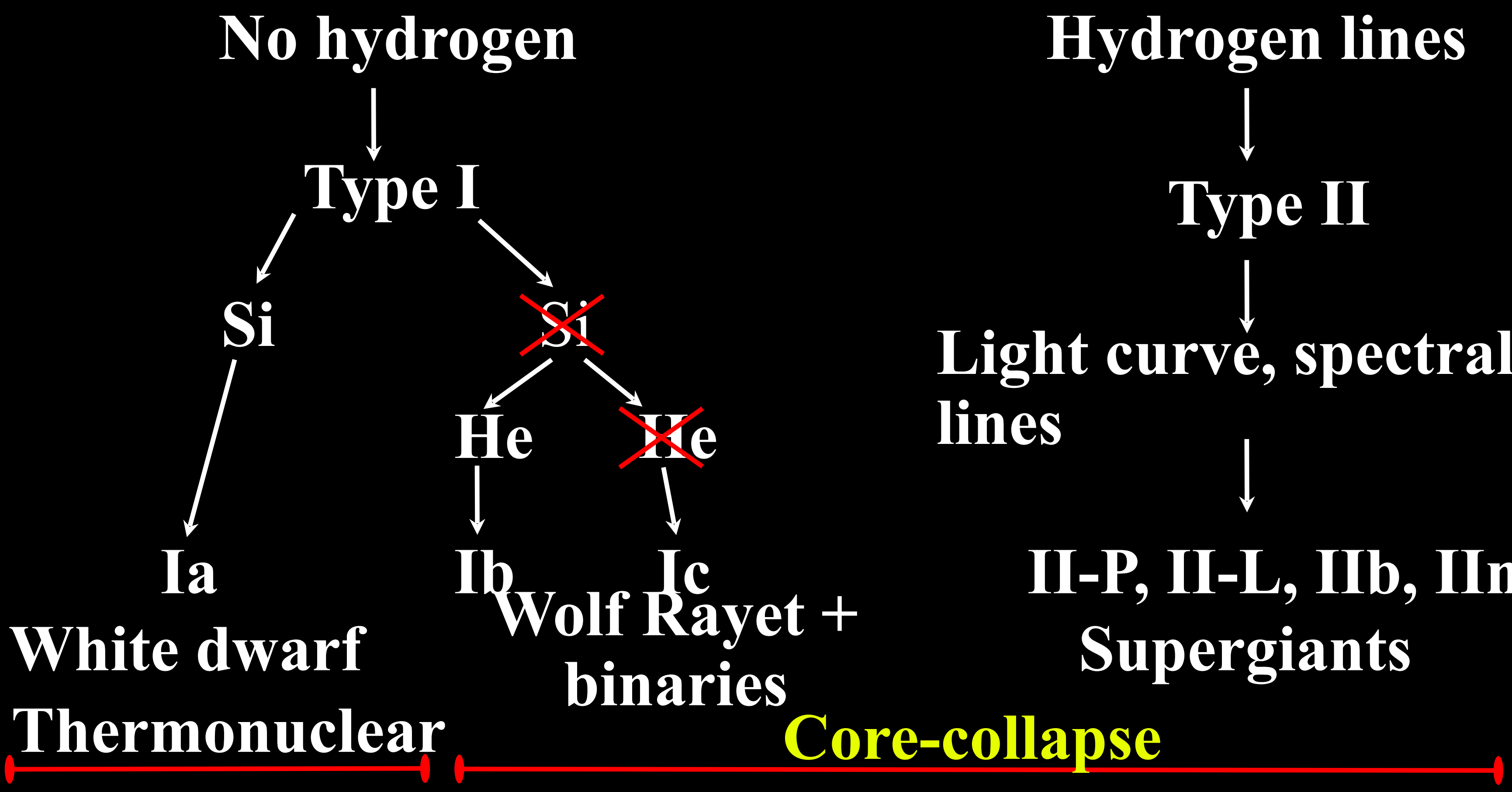

Supernova types

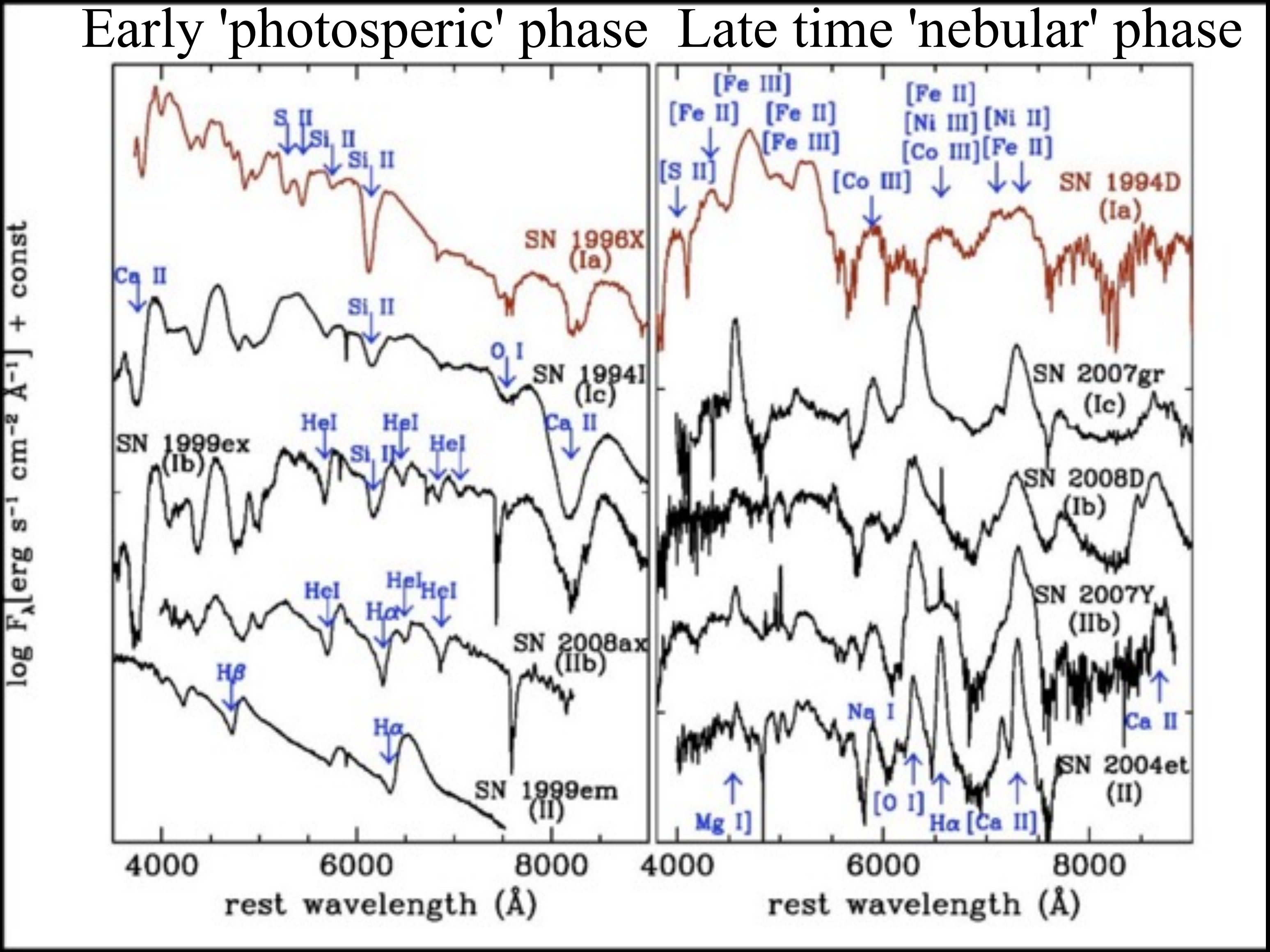

Pastorello+ 2007

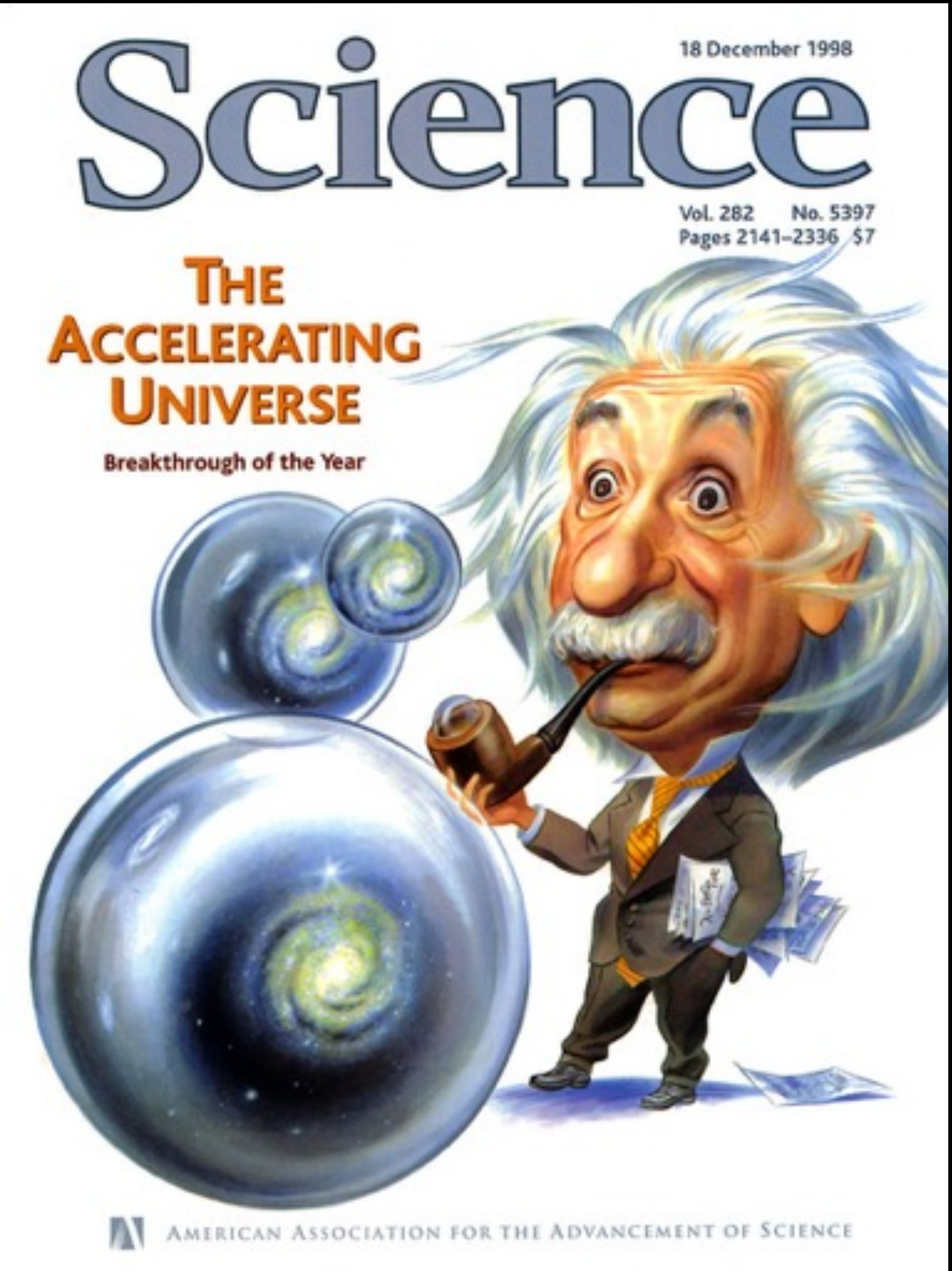
Science
18 December 1998
Vol. 282 No. 5397
Pages 2141–2336 $7
THE ACCELERATING UNIVERSE
Breakthrough of the Year
AMERICAN ASSOCIATION FOR THE ADVANCEMENT OF SCIENCE

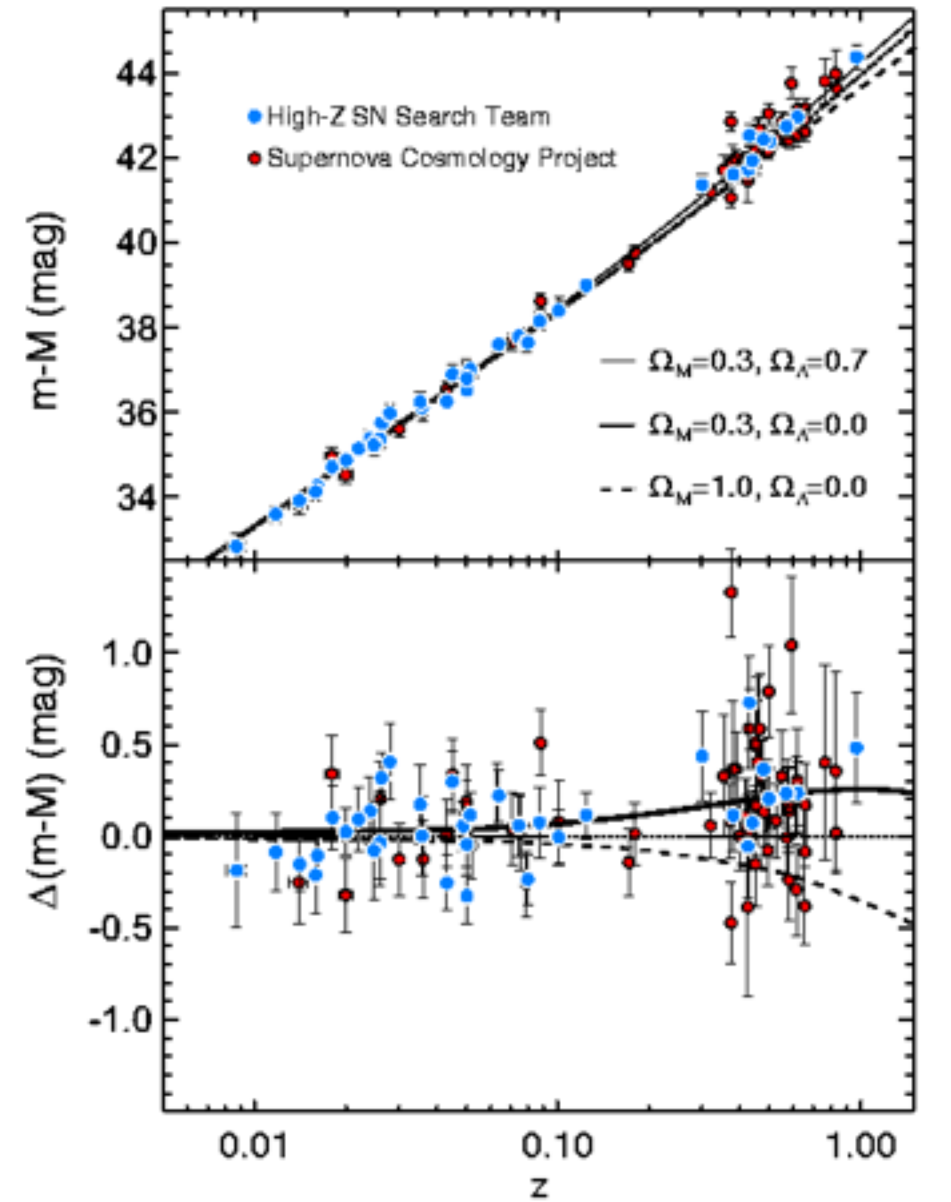
High-Z SN Search Team
Supernova Cosmology Project
m-M (mag)
44
42
40
38
36
34
Ω_M=0.3, Ω_Λ=0.7
Ω_M=0.3, Ω_Λ=0.0
Ω_M=1.0, Ω_Λ=0.0
Δ(m-M) (mag)
1.0
0.5
0.0
-0.5
-1.0
0.01
0.10
1.00
z

Weizmann Interactive Supernova data REPository

public

- Log out

Menu

- Objects
- Spectra
- Instruments
- Telescopes
- Sites
- Programs
- Collaborators
- Object Types
- Filters
- My SQL Query
- IAU SNe List
- Feedbacks
- Spectra Submission for Upload
- Atel RA/DEC List

- PESSTO
  - New Objects
  - New Spectra

Current DB Stat.

No. of Spectra	13330
No. of Objects	4514
Obj. w. Spectra	4219
Public Spectra	7931
IAU SNe	6284
ATels Coords.	4740

Links

WISeREP Reference

- 2012PASP..124..668Y

Internal (WIS)

- Benoziyo Center for Astrophysics
- Experimental Astrophysics Group

External

- IAU SNe
- CBAT TOCP
- ATels

SN Archives

- SUSPECT
- Asiago SN Catalogue
- CfA SN Archive
- NTT/NOT SDSS-II SNe
- UC Berkeley SNDB

Home

Spectra

Submitted by admin on Tue, 12/07/2010 - 17:55

Search: Object: Select Object OR Obj Name like (free text): LSQ13bxv

Obj Type: All Types OR Obj Type like (free text):

Instrument: All Instruments Spec Type: All Types

Program: All Programs Added within the last No limit Public: All

Show additional query fields

Sort by: (1) Observation Date Asc (2) Asc (3) Asc Limit: 100

Show plots: Yes No

1 row(s) returned.

Id	Obj. Name	Type	Spec. Program	Instrument	Obs. Date	Observer	Red. Date	Reducer	Exp. Time	Slit	Public	Ascii File Fits File	Created By	Last Modified	Modified By
15359	LSQ13bxv	SN IIn	PESSTO	ESO-NTT - EFOSC2-NTT	2013-08-28	Kangas,Kankare	2013-08-28	Mattila	1500	1	Y	tLSQ13bxv_20130827_Gr13_Free_slit1.0_1_f.asci tLSQ13bxv_20130827_Gr13_Free_slit1.0_1_f.fits	ilanm-UploadSet	2013-08-28	ilanm-UploadSet

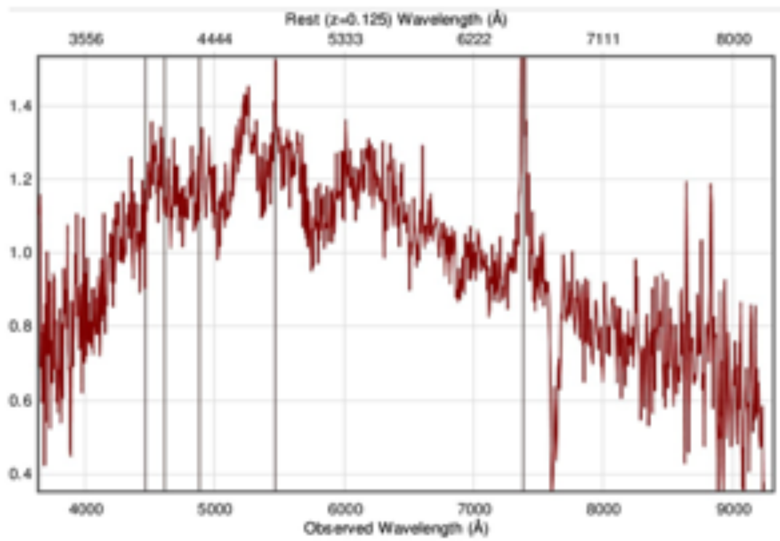

Zoom Full | Auto Zoom | Binning factor: 1 (rounded to nearest integer >1)

Mouse hovers at WL: 9085.76 (observed), 8076.23 (rest)

	z=	Vexp= km/s		z=	Vexp= km/s
Show H at	0.125	0	Show Mg at	0.125	0
Show He at	0.125	0	Show Mg II at	0.125	0
Show He II at	0.125	0	Show Si II at	0.125	0
Show O at	0.125	0	Show S II at	0.125	0
Show O II at	0.125	0	Show Ca II at	0.125	0
Show O III at	0.125	0	Show Fe II at	0.125	0
Show Na at	0.125	0	Show Fe III at	0.125	0
Show Å at	0.125	0	Show Tellurics		
Show Å at	0.125	0	Galaxy lines at	0.125	

PESSTO spectroscopic classification of optical transients

ATel #5335; T. Kangas, E. Kankare, S. Mattila (University of Turku), C. Inserra (QUB), M. Fraser (QUB), R. Scalzo (ANU), M. Nicholl (QUB), A. Gal-Yam, O. Yaron (Weizmann), S. Benetti, A. Pastorello, (INAF - Padova), S. Valenti (LCOGT/UCSB), S. Taubenberger (MPA Garching), S. J. Smartt, K. Smith, D. Young (QUB), M. Sullivan (Uni. of Southampton), C. Knapic, M. Molinaro, R. Smareglia (Trieste), C. Baltay, N. Ellman, E. Hadjiyska, R. McKinnon, D. Rabinowitz, E. S. Walker (Yale University), U. Feindt, M. Kowalski (Universitat Bonn), P. Nugent (LBL Berkeley)
on ***28 Aug 2013; 18:50 UT***
Distributed as an Instant Email Notice Supernovae
Credential Certification: Seppo Mattila (seppo.mattila@utu.fi)

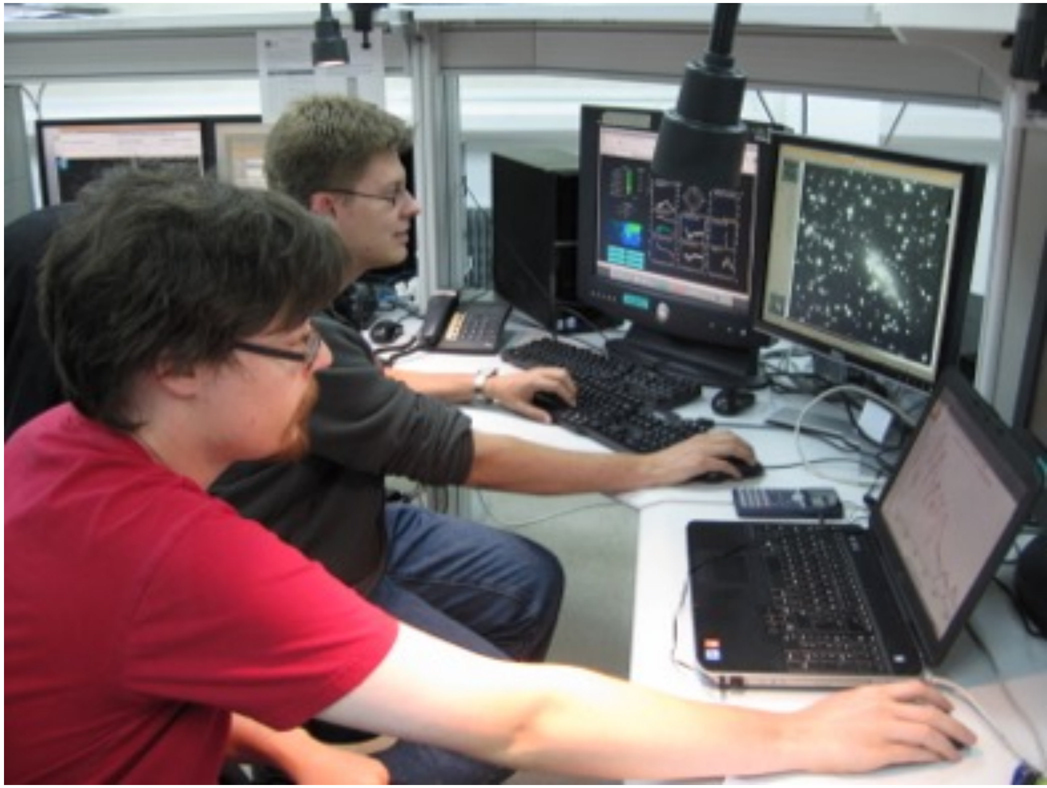

Subjects: Optical, Supernovae

PESSTO, the Public ESO Spectroscopic Survey for Transient Objects (see Valenti et al., ATel #4037; http://www.pessto.org), reports the following supernova classifications. Targets were supplied by the La Silla-Quest survey (see Hadjiyska et al., ATel #3812) and the OGLE-IV Transient Search (see Wyrzykowski et al., ATEL #4495). All observations were performed on the ESO New Technology Telescope at La Silla on 2013 August 27 (UT), using EFOSC2 and Grism 13 (3985-9315A, 18A resolution). Classifications were done with SNID (Blondin & Tonry, 2007, ApJ, 666, 1024) and GELATO (Harutyunyan et al., 2008, A&A, 488, 383). Classification spectra can be obtained from http://www.pessto.org via WISeREP (Yaron & Gal-Yam, 2012, PASP, 124, 668).

Name	RA (J2000)	Dec (J2000)	Disc. Date	Disc. Source	Disc Mag	z	Type	Phase	Notes
LSQ13bor	03:25:49.08	-19:18:10.5	2013-08-11	LSQ	19.9	~0.11	SN Ia	~9d past max	
LSQ13btf	01:39:20.89	-19:49:29.4	2013-08-15	LSQ	20.5	~0.19	SN Ia	~2d pre max	(1)
LSQ13bth	03:44:10.80	-19:51:12.8	2013-08-15	LSQ	20.1	~0.09	SN Ia	~7d past max	
LSQ13bwl	23:33:55.42	+04:31:00.3	2013-08-20	LSQ	18.4	~0.07	SN Ia	~11d past max	
LSQ13bxv	00:39:22.04	-24:05:01.3	2013-08-21	LSQ	19.1	~0.14	IIn	----	(2)
LSQ13byc	04:08:43.69	-21:38:08.9	2013-08-25	LSQ	19.5	~0.04	SN Ibc	----	(3)
LSQ13byn	01:36:41.14	-17:53:59.1	2013-08-25	LSQ	19.4	~0.11	SN Ia	~7d pre max	
OGLE-2013-SN-051	00:32:19.54	-66:25:44.2	2013-08-16	OGLE	18.8	~0.07	SN Ia	~7d past max	

(1) Best match found with SN 2005hk a couple of days before maximum light.

PESSTO spectroscopic classification of optical transients

ATel #5335; *T. Kangas, E. Kankare, S. Mattila (University of Turku), C. Inserra (QUB), M. Fraser (QUB), R. Scalzo (ANU), M. Nicholl (QUB), A. Gal-Yam, O. Yaron (Weizmann), S. Benetti, A. Pastorello, (INAF - Padova), S. Valenti (LCOGT/UCSB), S. Taubenberger (MPA Garching), S. J. Smartt, K. Smith, D. Young (QUB), M. Sullivan (Uni. of Southampton), C. Knapic, M. Molinaro, R. Smareglia (Trieste), C. Baltay, N. Ellman, E. Hadjiyska, R. McKinnon, D. Rabinowitz, E. S. Walker (Yale University), U. Feindt, M. Kowalski (Universitat Bonn), P. Nugent (LBL Berkeley)*
*on **28 Aug 2013; 18:50 UT***
Distributed as an Instant Email Notice Supernovae
Credential Certification: Seppo Mattila (seppo.mattila@utu.fi)

Subjects: Optical, Supernovae

PESSTO, the Public ESO Spectroscopic Survey for Transient Objects (see Valenti et al., ATel #4037; http://www.pessto.org), reports the following supernova classifications. Targets were supplied by the La Silla-Quest survey (see Hadjiyska et al., ATel #3812) and the OGLE-IV Transient Search (see Wyrzykowski et al., ATEL #4495). All observations were performed on the ESO New Technology Telescope at La Silla on 2013 August 27 (UT), using EFOSC2 and Grism 13 (3985-9315A, 18A resolution). Classifications were done with SNID (Blondin & Tonry, 2007, ApJ, 666, 1024) and GELATO (Harutyunyan et al., 2008, A&A, 488, 383). Classification spectra can be obtained from http://www.pessto.org via WISeREP (Yaron & Gal-Yam, 2012, PASP, 124, 668).

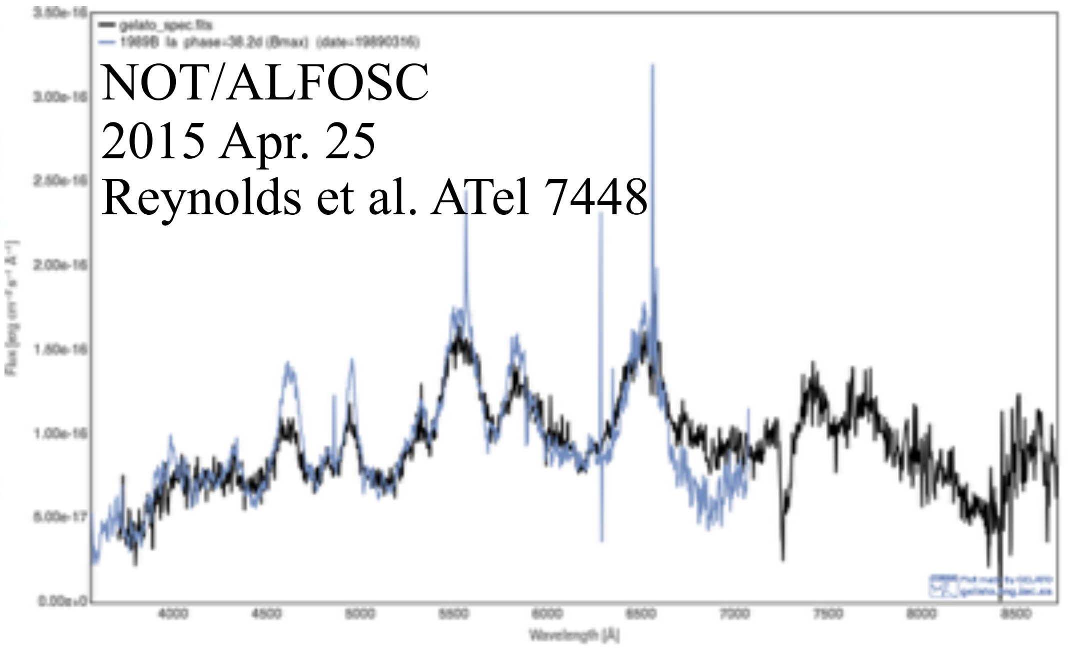

Name	RA (J2000)	Dec (J2000)	Disc. Date	Disc. Source	Disc Mag	z	Type	Phase	Notes
LSQ13bor	03:25:49.08	-19:18:10.5	2013-08-11	LSQ	19.9	~0.11	SN Ia	~9d past max	
LSQ13btf	01:39:20.89	-19:49:29.4	2013-08-15	LSQ	20.5	~0.19	SN Ia	~2d pre max	(1)
LSQ13bth	03:44:10.80	-19:51:12.8	2013-08-15	LSQ	20.1	~0.09	SN Ia	~7d past max	
LSQ13bwl	23:33:55.42	+04:31:00.3	2013-08-20	LSQ	18.4	~0.07	SN Ia	~11d past max	
LSQ13bxv	00:39:22.04	-24:05:01.3	2013-08-21	LSQ	19.1	~0.14	IIn	----	(2)
LSQ13byc	04:08:43.69	-21:38:08.9	2013-08-25	LSQ	19.5	~0.04	SN Ibc	----	(3)
LSQ13byn	01:36:41.14	-17:53:59.1	2013-08-25	LSQ	19.4	~0.11	SN Ia	~7d pre max	
OGLE-2013-SN-051	00:32:19.54	-66:25:44.2	2013-08-16	OGLE	18.8	~0.07	SN Ia	~7d past max	

(1) Best match found with SN 2005hk a couple of days before maximum light.

Circumnuclear SN optical follow-up:

SN2013fc - a luminous type IIL in the circumnuclear ring of a LIRG

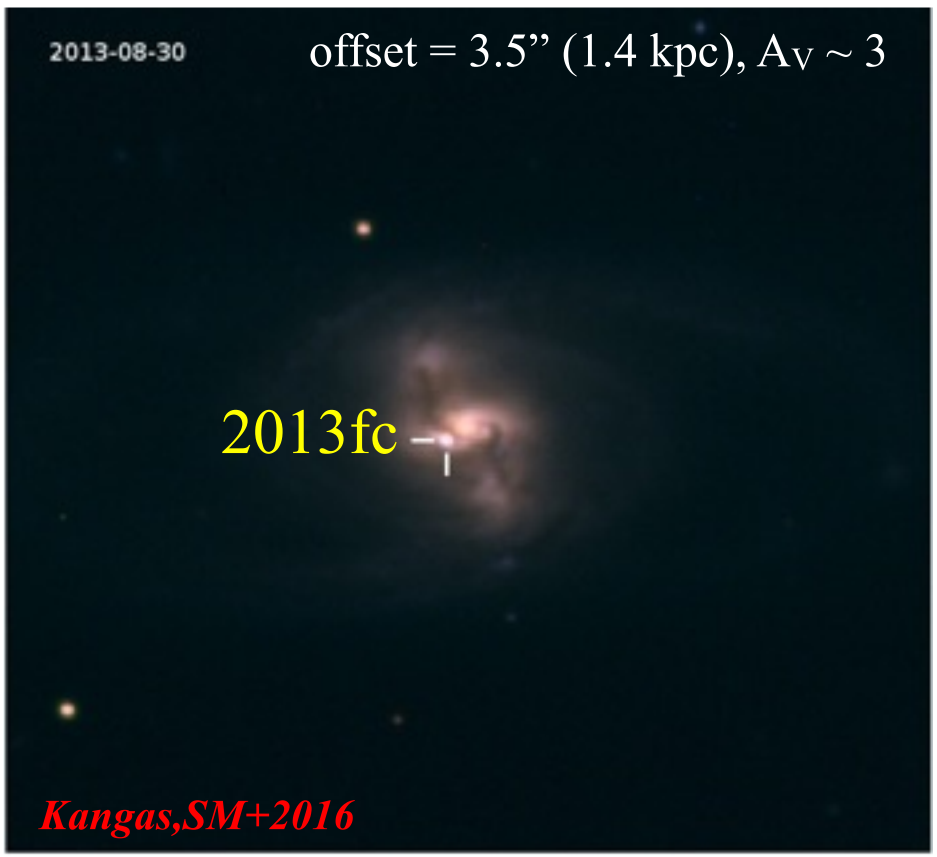

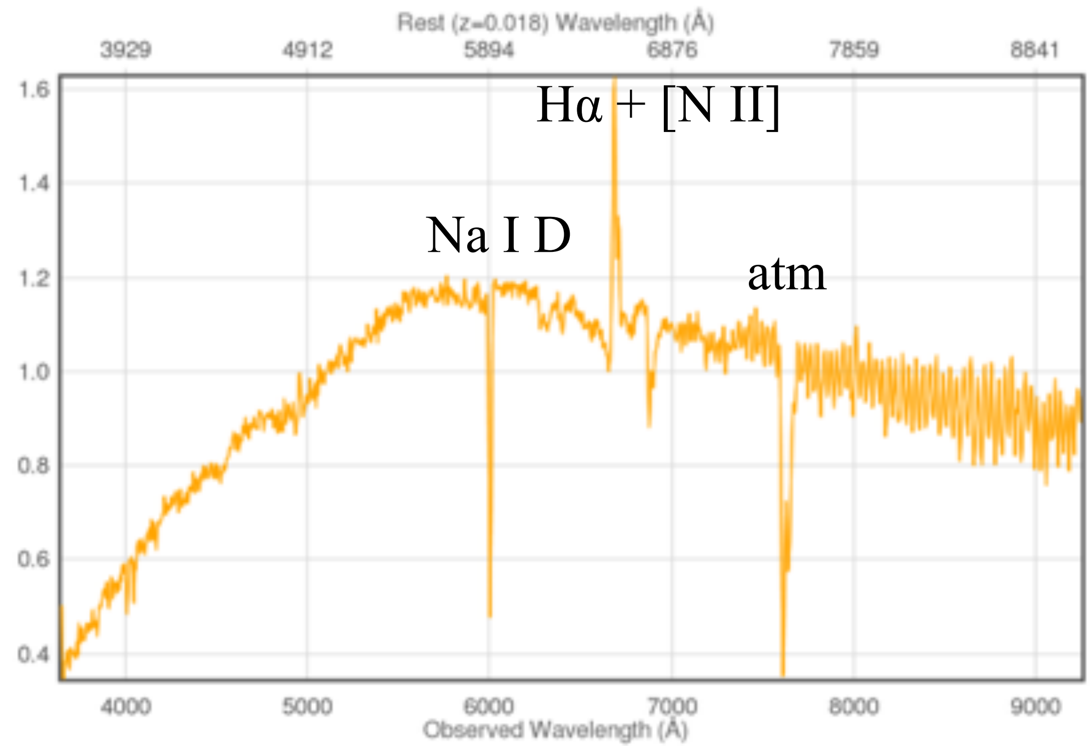

Classified by PESSTO (ESO NTT) at ~17 days post explosion (Kangas et al. 2013)

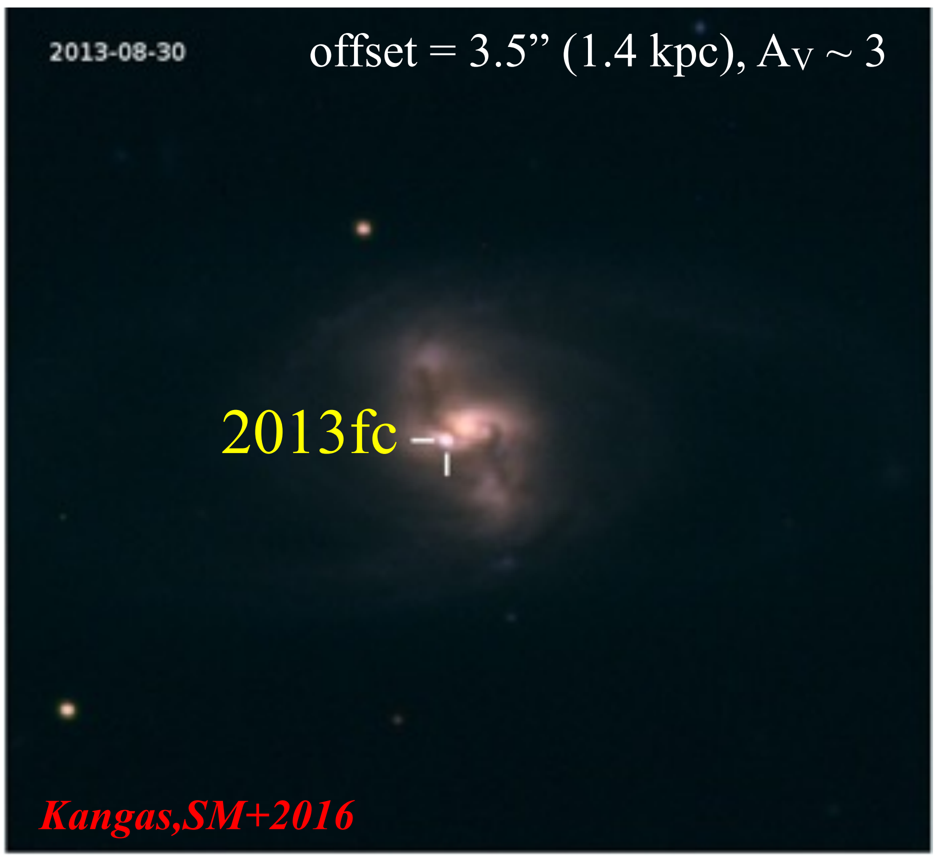

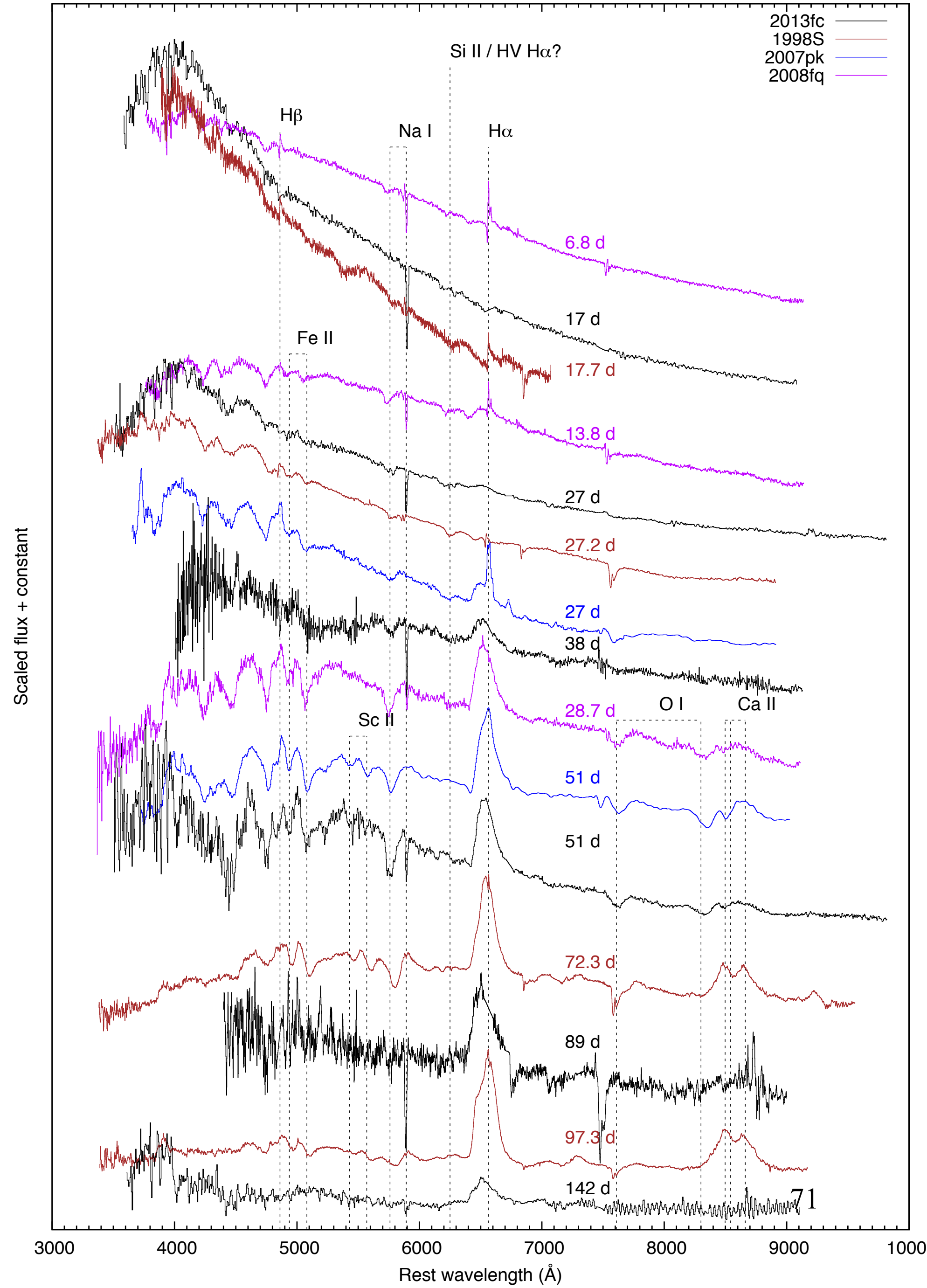

Spectra from ESO NTT, ANU 2.3, SALT/RSS

Surveys for astrophysical transients going all-sky !

- Traditional pointed SN searches (e.g. LOSS) taken over by new wide field surveys
- Pan-STARRS Survey for Transients (PSST)
  - ~6000 sq degrees per night from Haleakala, Hawaii
- Catalina Real-time Transient Survey (CRTS)
  - Observes 33 000 sq degrees from Arizona and Siding Spring, Australia
- All-Sky Automated Survey for SuperNovae (ASAS-SN)
  - Observes 20 000 sq degrees from Haleakala, Hawaii and Cerro Tololo, Chile

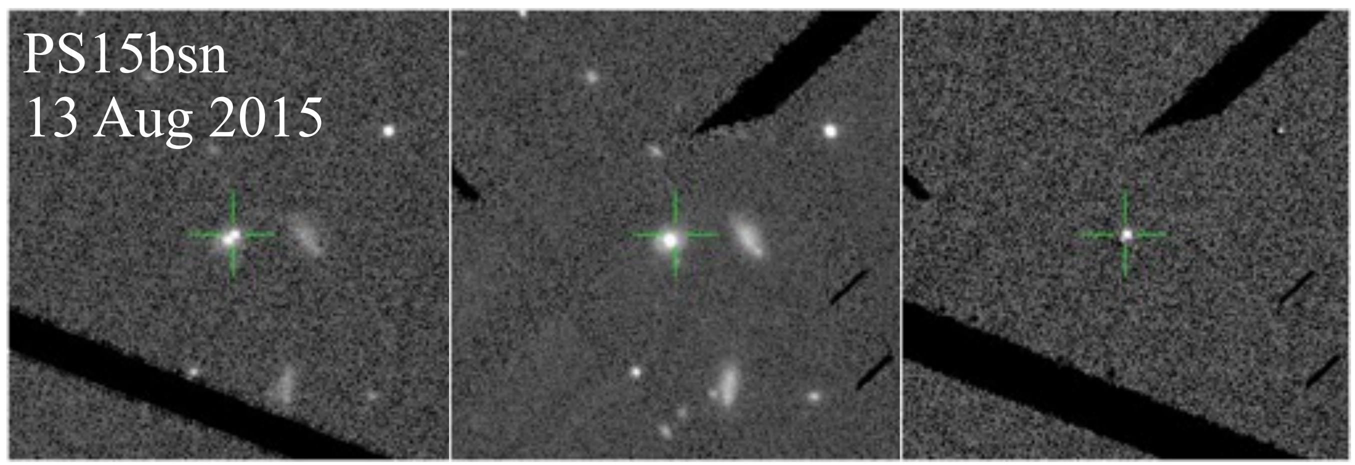

GOTO

GRAVITATIONAL-WAVE OPTICAL TRANSIENT OBSERVER

GOTO concept

WARWICK

Core GW-EM science

•Robotic, rapid-response system

•Deep enough to probe EM signatures of NS mergers within ~150 Mpc

•Wide enough to cover localisation uncertainty and have recent observations of visible sky

•Scalable and flexible design by deploying arrays of small (40cm) telescopes, each with a ~5 deg^2 FoV

•Adaptable survey speed, depth, FoV footprint and filter coverage as GW detectors evolve as well as our understanding of EM counterparts

The primary GW-EM sky survey mode will have multiple secondary science gains…

GW-EM hunters (North)

WARWICK

ZTF(2018-)
- 47 deg^2 FoV
- ~121cm telescope
- 20.5 mag
- Palomar

ATLAS (2015-)
- 2 x 30 deg^2 FoV
- 2 x 50cm telescopes
- ~20.2-20.5
- Hawaii

Pan-STARRS (2014-)
- 7 deg^2 FoV
- 180cm telescope
- ~21 mag
- Hawaii

ASAS-SN (2013-)
- Set of small, wide-field commercial lenses
- ~17 mag

GOTO
GRAVITATIONAL-WAVE OPTICAL TRANSIENT OBSERVER

GOTO Phase II
- 40 deg^2 FoV
- 8 x 40cm telescopes
- 19.5-20.5 mag
- La Palma

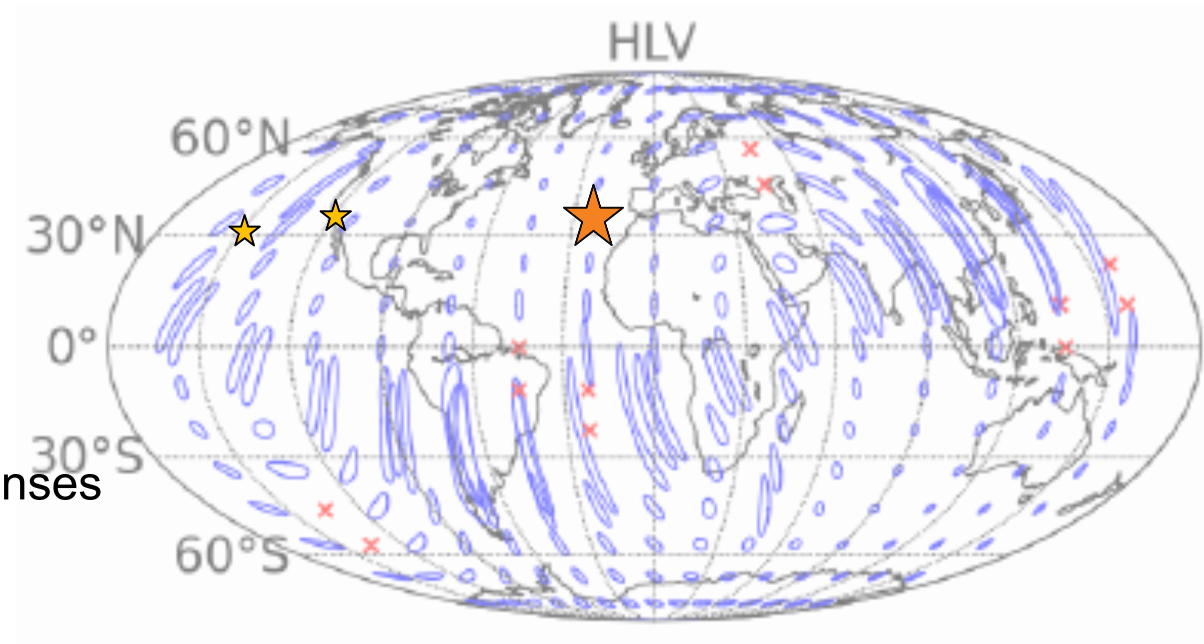

Large Synoptic Survey Telescope
Opening a Window of Discovery on the Dynamic Universe

- 8.4 m primary mirror
- 3.2 Gpixel camera (3.5 deg FOV)
- 1000 images per night - 9600 deg^2 (41 250 deg^2 in the whole celestial sphere)
- ~450 calibration exposures
- ~20 TB of raw data per 24 hr
- 10^7 "alerts" per night
- Final data: 0.5 Exabytes
- Final database: 15 PB

Petabyte = 1000 TB
Exabyte = 1000 PB

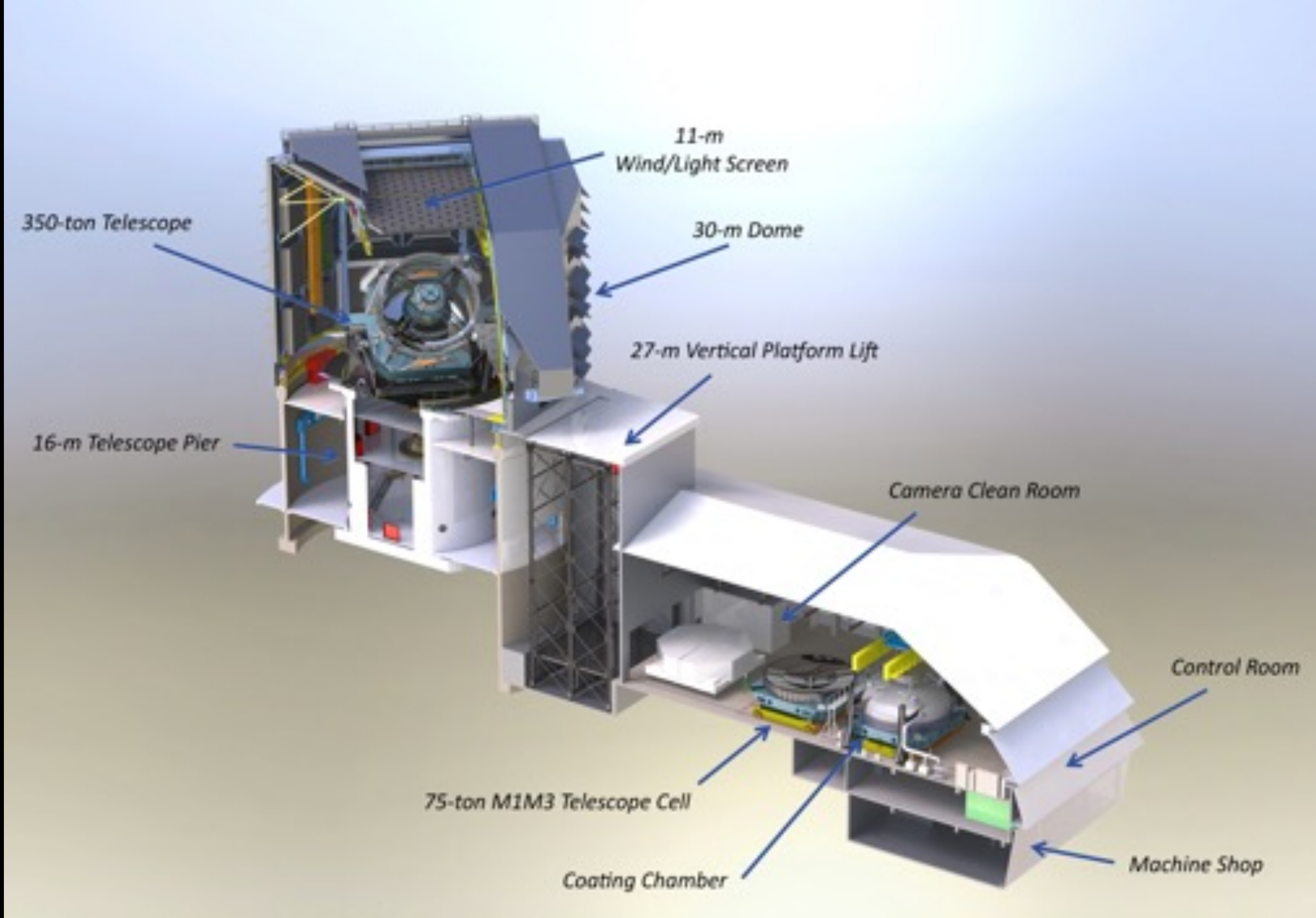

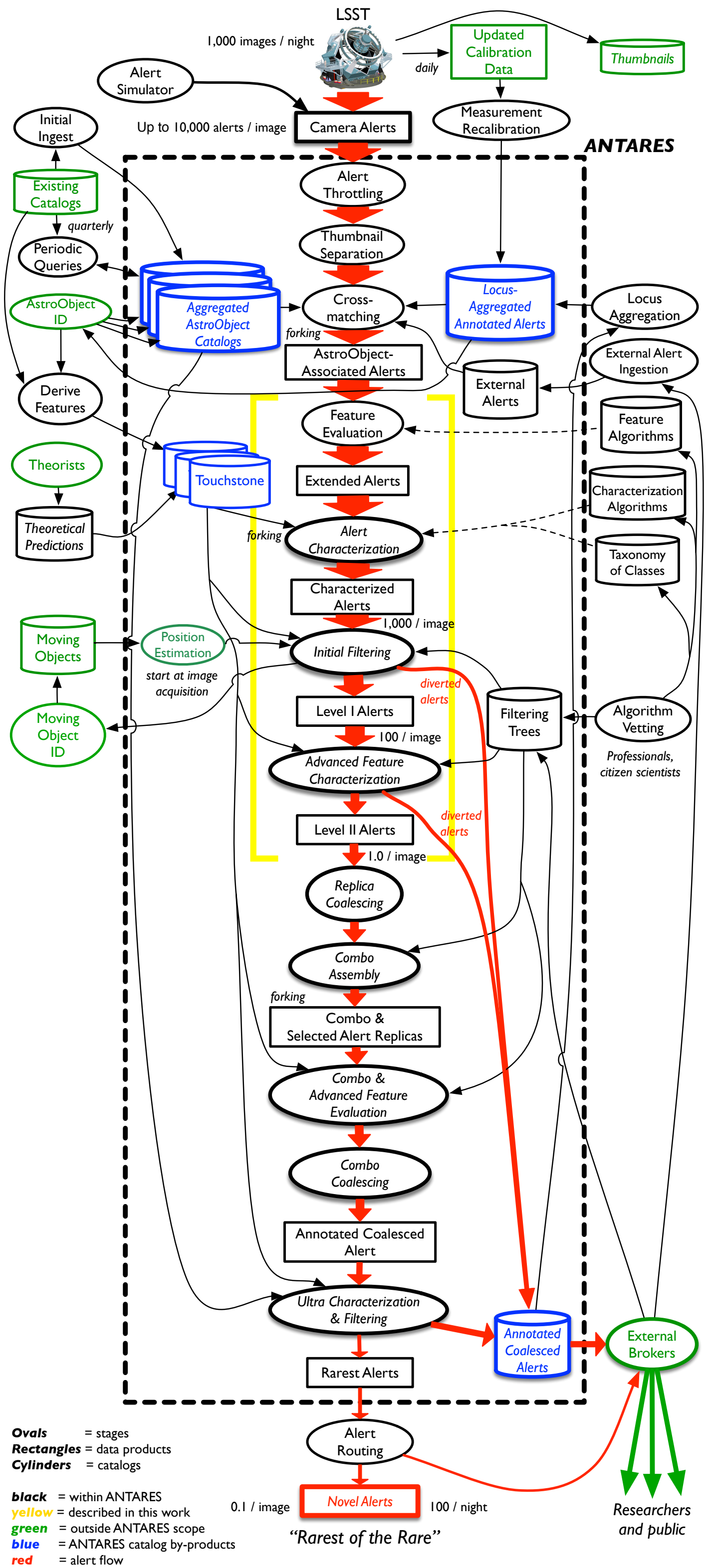

1000 images (~20 terabytes of raw data) / night

$\sim 10^7$ alerts per night

$\sim 10^6$ alerts per night

$\sim 10^3$ alerts per night

$\sim 10^2$ alerts per night

What do we observe?

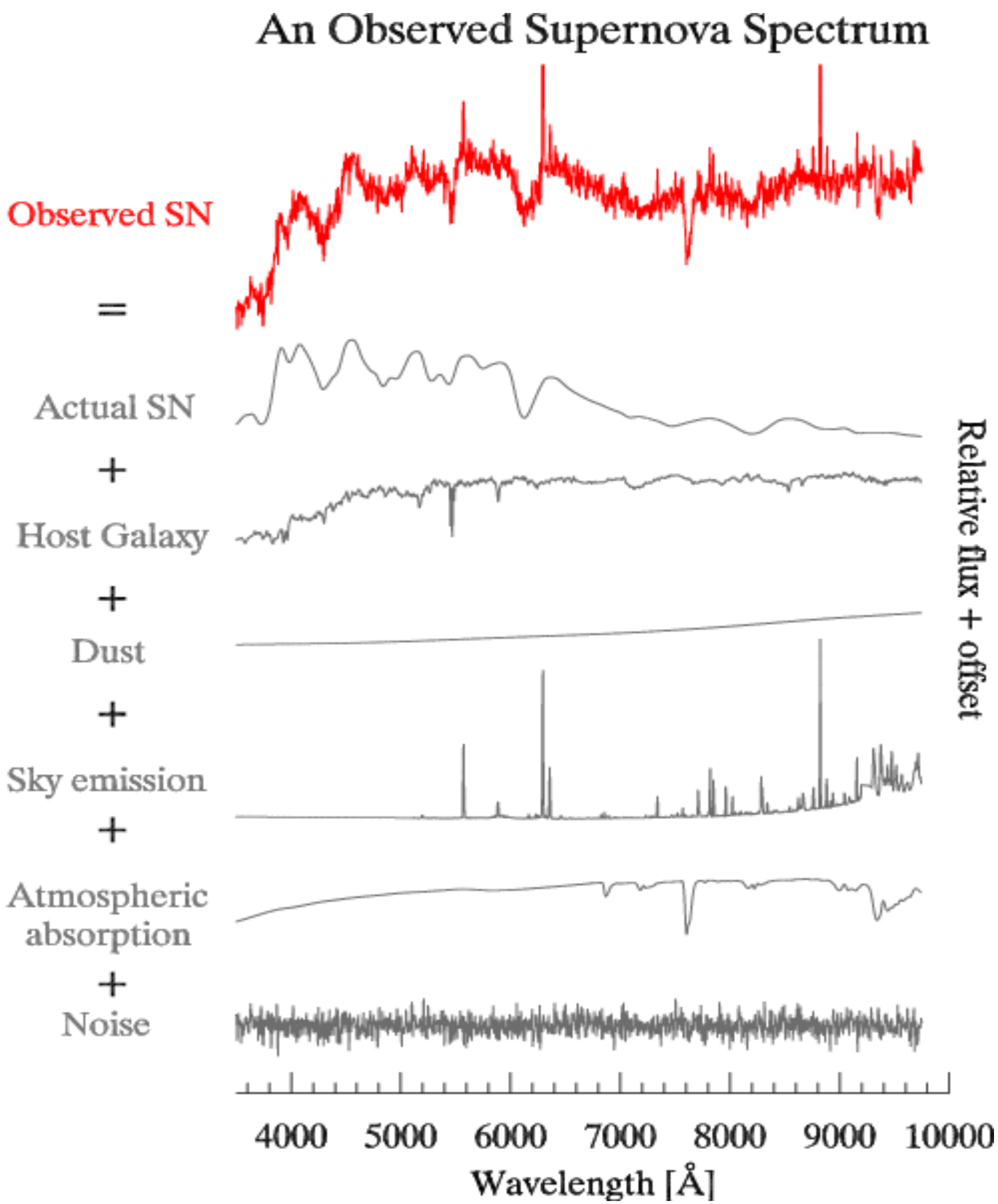

Previous classification methods

- Currently classification is slow, labour-intensive, and can take tens of minutes for a single supernova spectrum
- SNID – Stephane Blondin (Fortran)
  - Uses a cross-correlation of input with templates
  - Fast
  - Inaccurate with signals that are intermixed with host galaxy light
- Superfit – Andy Howell (IDL)
  - Uses a minimisation of chi-squared
  - Very slow, labour-intensive
  - Can deal with intermixed host galaxy light

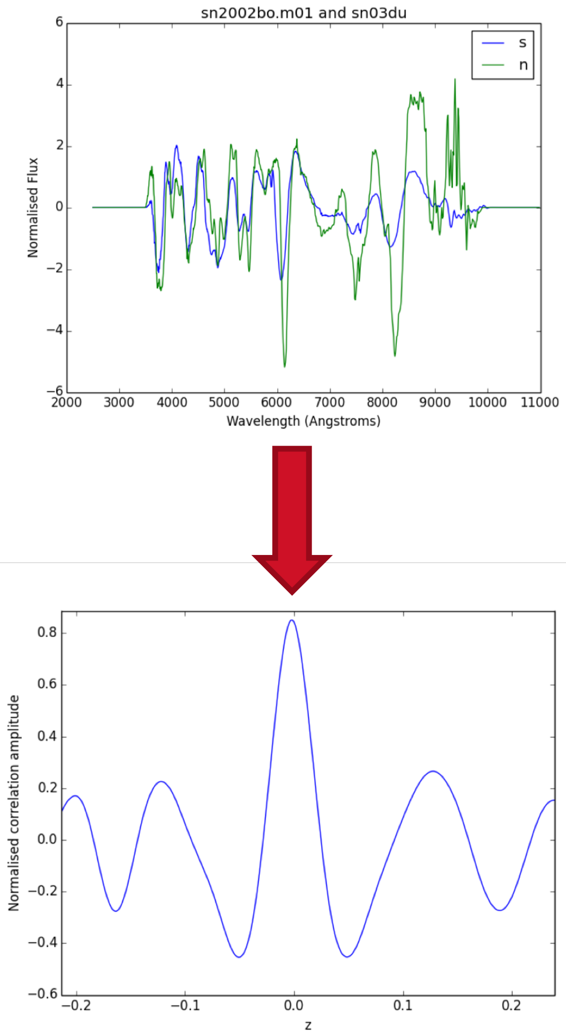

Problems with current methods

- All rely on iterative template matching processes
  - Computation time increases linearly with the number of templates
  - Can only compare to one template at a time (rather than the aggregate set of each SN type)
- Chi-squared minimisations are slow
- Not autonomous: requires a lot of human-input

How DASH improves

- Speed
  - Autonomously classify several spectra at once
  - Significantly faster (example: 250 classified spectra in 18 seconds)
- Accuracy
  - DASH classifies based on *features* instead of templates
    - Uses aggregate set of templates rather than a single template
  - Softmax regression probabilities
- Precision
  - More specific classification including age and specific type

How DASH improves

- Speed
  - Autonomously classify several spectra at once
  - Significantly faster (example: 250 classified spectra in 18 seconds)
- Accuracy
  - DASH classifies based on *features* instead of templates
    - Uses aggregate set of templates rathe
  - Softmax regression probabilities
- Precision
  - More specific classification including ag

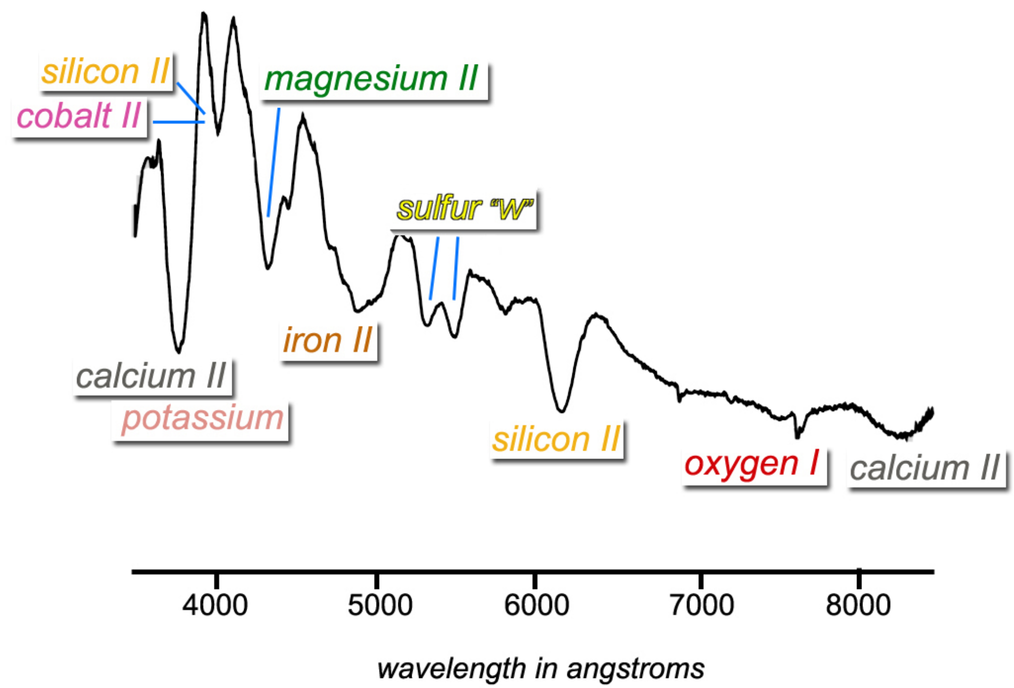

Why Deep Learning?

- Deep Learning has had success in a range of new Big Data problems:
  - Image, speech, language recognition.
- Accuracy improves with number of template (does not affect computation time)
- Training process is separate to testing
- Only need to train once. Then only need the trained model instead of the entire template set.
- Train based on the aggregate set of all templates in a particular SN bin
- Disadvantages
  - Deep learning is often position invariant, which makes redshifting difficult.
  - Softmax probabilities are relative, not absolute measures

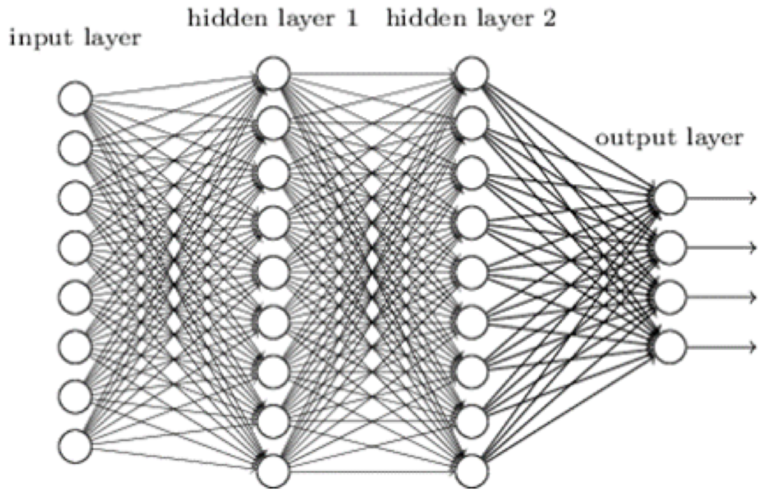

Convolutional Neural Network

- Two convolutional layers with Tensorflow
  - 2 layers was over 10-30% better than a single layer
  - 3 layers provided no significant improvement

- 4831 spectra across 403 different supernovae
  - Training set – 80%
  - Validation set – 20%

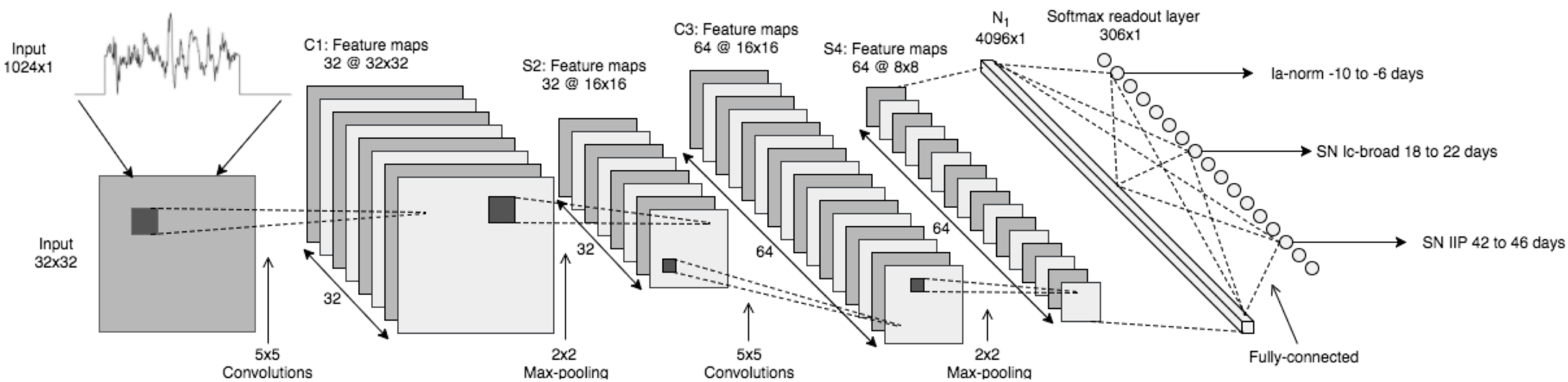

Why Deep Learning?

	Deep Learning	Cross-correlation matching	Chi-squared matching
Classification technique	Matches based on the combined 'features' of all templates	Iteratively compares to templates	Iteratively compares to templates
Speed	Very Fast (no change in speed with templates)	Fast (but increases linearly with number of templates)	Slow (increases linearly with number of templates)
Noise	Can train with noise	Cannot classify low S/N	OK with low S/N
Redshifting	Redshifting is unreliable	Very good at redshifting	OK redshifting
Goodness of Fit	Relative	Absolute	Absolute